1-1-2007

Assessment of Uncertainty in Flow Model Parameters, Channel Hydraulic Properties, and Rainfall Data of a Lumped Watershed Model

Jairo Nelvedir Diazamirez

Follow this and additional works at: https://scholarsjunction.msstate.edu/td

ASSESSMENT OF UNCERTAINTY IN FLOW MODEL PARAMETERS,

CHANNEL HYDRAULIC PROPERTIES, AND RAINFALL DATA

OF A LUMPED WATERSHED MODEL

By

Jairo Nelvedir Diaz-Ramirez

A Dissertation
Submitted to the Faculty of
Mississippi State University
in Partial Fulfillment of the Requirements
for the Degree of Doctor of Philosophy
in Environmental and Water Resources
in the Department of Civil and Environmental Engineering

Mississippi State, Mississippi

August 2007

ASSESSMENT OF UNCERTAINTY IN FLOW MODEL PARAMETERS,

CHANNEL HYDRAULIC PROPERTIES, AND RAINFALL DATA

OF A LUMPED WATERSHED MODEL

By

Jairo Nelvedir Diaz-Ramirez

Approved

_____
James L. Martin
Professor and Kelly Gene Cook, Sr.
Chair of Civil and Environmental
Engineering
(Co-Director of Dissertation)

_____
William H. McAnally
Associate Professor
of Civil and Environmental
Engineering
(Co-Director of Dissertation)

_____
Billy E. Johnson
Adjunct Professor
of Civil and Environmental
Engineering
(Committee Member)

_____
Mary Love Tagert
Assistant Research Professor
of Forestry
(Committee Member)

_____
James L. Martin
Professor and Kelly Gene Cook, Sr.
Chair of Civil and Environmental
Engineering
Graduate Coordinator in the
Civil and Environmental
Engineering Department

_____
Kirk H. Schulz
Dean of the College of
Engineering

Name: Jairo Nelvedir Diaz-Ramirez

Date of Degree: August 11, 2007

Institution: Mississippi State University

Major Field: Environmental and Water Resources Engineering

Major Professor: Drs. James L. Martin and William H. McAnally

Title of Study: ASSESSMENT OF UNCERTAINTY IN FLOW MODEL PARAMETERS, CHANNEL HYDRAULIC PROPERTIES, AND RAINFALL DATA OF A LUMPED WATERSHED MODEL

Pages in Study: 128

Candidate for Degree of Doctor of Philosophy

Among other sources of uncertainties in hydrologic modeling, spatial rainfall variability, channel hydraulic variability, and model parameter uncertainty were evaluated. The Monte Carlo and Harr methods were used to assess 90% certainty bounds on simulated flows. The lumped watershed model, Hydrologic Simulation Program FORTRAN – HSPF, was used to simulate streamflow at the outlet of the Luxapallila Creek watershed in Mississippi and Alabama. Analysis of parameter uncertainty propagation on streamflow simulations from 12 HSPF parameters was accomplished using 5,000 Monte Carlo random samples and 24 Harr selected points for each selected parameter. Spatial rainfall variability propagation on simulated flows was studied using six random grid point sets of Next Generation Weather Radar (NEXRAD) rainfall data (i.e., 109, 86, 58, 29, 6, and 2 grid points) from the baseline scenario (115 NEXRAD grid points).

Uncertainty in channel hydraulic properties was assessed comparing the baseline scenario (USGS FTABLE) versus the EPA RF1 FTABLE scenario. The difference between the baseline scenario and the remaining scenarios in this study was evaluated using two criteria: the percentage of observed flows within the HSPF 90% certainty bounds (*Reliability*) and the width of the HSPF 90% certainty bounds (*Sharpness*). Daily observed streamflow data were clustered into three groups to assess the model performance by each class: below normal, normal, and above normal flows. The parameter uncertainty propagation results revealed that the higher the model *Sharpness* the lower the model *Reliability*. The model *Sharpness* and *Reliability* results using 2 NEXRAD grid points were markedly different from those results using the remaining NEXRAD data sets. The hydraulic property variability of the main channel affected storm event paths at the watershed outlet, especially the time to peak flow and recessing limbs of storm events. The comparison showed that Harr's method could be an appropriate initial indicator of parameter uncertainty propagation on streamflow simulations, in particular for hydrology models with several parameters. Parameter uncertainty was still more important than those sources of uncertainty accomplished in this study because all of the median relative errors of model *Reliability* and *Sharpness* were lower than +/- 100%.

Key words: HSPF, parameter uncertainty, rainfall spatial variability, hydraulic property variability, Monte Carlo simulation, Harr method, certainty bounds of streamflow simulations.

DEDICATION

To God and my family. Especially, my parents, Jose and Amparo; my wife, Germania; my sons, Santiago and Juan Esteban; my brothers, Jorge and Carlos; and my Aunt Estella. Thanks for your majestic love, fidelity, spiritual and economic support.

ACKNOWLEDGEMENTS

First and overall, I wish to thank God for giving me this wonderful life full of health, prosperity, and great people. From the bottom of my heart, I would like to thank my parents, Jose and Amparo, for motivating, supporting, and encouraging me to pursue my academic goals. Additionally, since I left Colombia, six and half years ago, my parents have been the support and parents again of my lovely son Santiago. I would also like to thank my wife Germania, for her patients and fidelity all of these six and half years we have been separated from each other. Thanks to my relatives, especially, my Aunt Estella; you always have supported my academic goals (BS, MS, and Ph.D.). Therefore, I am eternally grateful and forever indebted to my family for their unparallel love and help.

I wish to express my sincere gratitude to my advisors, Dr. James L. Martin and Dr. William "Bill" H. McAnally, for their dedicated instruction, guidance, encouragement, and full support during my Ph.D. studies. Their have been tutors not only for academic education but also life experiences. I enjoyed each course and meeting done on these wonderful years in the "Waterworld" at Mississippi State University. Thanks for giving me the time to reach my dreams of wedding and visiting my family in those days as a Ph.D. student. Thanks for your vote of confidence to reach my goals at MSU and because the family's future will be

better. I also appreciate the funds provided by NASA, NOAA, the Civil and Environmental Engineering Department (CEE), and the Kelly Gene Cook, Sr. foundation. I would also like to thank my committee members, Dr. Billy Johnson and Dr. Mary Love Tagert, for their suggestions and supports.

I like to express thanks to all my teachers from elementary throughout graduate school (*i.e.,* Colegio Gimnasio de Cristo, Colegio Santa Juana de Lestona, Colegio Gimnasio Central del Valle, Universidad del Valle, Universidad Nacional de Colombia, University of Puerto Rico, and Mississippi State University). They introduced me into the amazing world of reading, writing, and research. Additionally, all of my teachers have always given me excellent advice and encourage me to play hard, be constant, and honest during life.

I wish to thank the CEE's staff including Charlsie Halford, Mary Box, and Joe Ivy for their excellent support service. I would also like to thank the tutors of the Shackouls Technical Communication Program, College of Engineering, Mississippi State University, for their time and effort in reviewing the technical English of this Dissertation.

I would like to express my appreciation to all of my friends in Starkville and long distance friends for their spiritual and financial support. Especially, my roommates, Mario Alpuche (*orale mi cuate!*) and Eduardo Arias (*carajo* roomate! thanks for your friendship); my church family, Reverend Olin McBride (thanks for your spiritual support, friendship, and financial support to help people in Honduras), Jim McBride (thanks for your friendship and warm greetings), Janice Kinard (thanks for the first welcome to the church), Jack and Klancie Smith

iv

TABLE OF CONTENTS

viii

LIST OF TABLES

LIST OF FIGURES

xiv

CHAPTER I

INTRODUCTION

1.1 Motivation

Advances in gathering hydrology data using remote sensing, increased computer data storage capability, and faster processing speeds allow researchers to develop and apply increasingly complex hydrologic models (physics-based, 3-dimensional, and distributed models). The more recent availability of high-resolution hydrologic data from modern radar networks provides further potential for advancements in watershed modeling. However, when analyzing model results, hydrologists are faced with various uncertainties in input and output data, model parameters, and model structure. These uncertainties may negatively affect the usefulness of hydrologic models. Error analysis propagation throughout different components of a hydrologic model are one of the major challenges in evaluating a model (Singh and Frevert, 2002b). Thus far, research has focused on determining the magnitude of uncertainties of input data or model parameters. Few researchers have considered the combined effects of uncertainties on model results (Souid, 1999).

Hydrologic models are represented by a series of input data (e.g., precipitation and evaporation), parameters (e.g., soil, land use, and channel

1

properties), and structure (e.g., black-box, conceptual, physically based, grid, and lumped models). Generally, every component of hydrologic models depicts uncertainty due to the lack of knowledge about real systems. Uncertainty in input data is due to natural variability, measurement inaccuracy, and errors in handling and processing data (Melching, 1995). Model parameters and structure show uncertainty due to model assumptions/approximations, scale effects, and variability of inputs and parameters in time and space (Gupta et al., 2005; Tung, 1996). The uncertainty of input data on model results have been studied separately from model parameter uncertainty (Souid, 1999). Georgakakos et al. (2004) pointed out that few have researched model structure uncertainty. Butts et al. (2004) declared that uncertainty evaluation is compensated among components (input data, model parameters, and model structure) because they are strongly interlinked.

Numerous real world hydrologic models exist, e.g., continuous or event based, distributed or lumped parameters, and empirical or physical equations (Singh, 1995; Singh and Woolhiser, 2002; Singh and Frevert, 2002a). The Hydrological Simulation Program - FORTRAN (HSPF), a continuous lumped model supported by the U.S. Environmental Protection Agency (EPA), is extensive and has been successful in evaluating different regions around the world since 1980; however, little work has been done to quantify the combined effect of input data (e.g., rainfall and channel hydraulic properties) and parameter uncertainty on model simulations. EPA's 2002 guideline on modeling recommended

"*best practices to help to determine when a model, despite its uncertainties, can be appropriately used to inform a decision. Specifically, it recommends that model developers and users: (a) subject their model to credible, objective peer review; (b) assess the quality of the data they use; (c) corroborate their model by evaluating the degree to which it corresponds to the system being modeled; and (d) perform sensitivity and uncertainty analysis… A model's quality to support a decision becomes known when information is available to assess these factors*.*"

Researchers believe spatial and temporal variability of precipitation data is the main source of input data uncertainty when rainfall-runoff models are applied (Vieux, 2002; Butts et al., 2004; Neary et al., 2004; Lopez et al., 2005). In addition, model parameter estimation is affected by a poor knowledge of precipitation input data (Andreassian et al., 2001). Indeed, rainfall distribution must be a main feature when a hydrologic model is developed and evaluated (Hromadka II and McCuen, 1989). Osborn and Lane (1982) said

"*for small watersheds, the input with greatest variability is rainfall. Therefore, the accuracy of streamflow simulation depends primarily on how well this variability can be defined in a specific case*."

Aronica et al. (2005) pointed out that model structure and sensitivity of model parameters make a model more or less sensitive to rainfall temporal resolution. Assessments of rainfall input data uncertainty in hydrologic simulation have been done by various authors, e.g., Anagnostou and Krajewski (1999), Bronster and Bardossy (2003), Sharif et al. (2004), and Aronica et al. (2005).

Precipitation is measured/calculated using gage, radar, and satellite data. Point precipitation is directly measured using gages. Both radar and satellite precipitation values are indirect estimates of rainfall. Errors in measuring rain

3

gage data are possibly due to mistakes in reading the scale of the gage, instrumental errors, the malfunctioning of instruments due to biological and human interference, and wind effects (Linsley et al., 1988; Steiner et al., 1999). Data from rain gage networks are used to calculate the average precipitation over an area. Linsley et al. (1988) said that average precipitation errors are greater for storms than for monthly or seasonal rainfall. Dense precipitation networks are expensive to maintain and operate. On the other hand, radar-derived precipitation is now a better alternative for estimating the spatial variability of precipitation (Vieux, 2002; Neary et al., 2004); however, radar rainfall estimations show uncertainty due to radar reflectivity-precipitation rate transformation and radar range (Sharif et al., 2004). Satellite devices provide global information on rainfall frequency and intensity, but depend on the properties of the cloud top, cloud liquid, and ice content to calculate precipitation values.

Model parameters are another component of hydrologic models that propagate uncertainty through model results. Watershed models are complex and highly parameterized. For instance, the HSPF model uses 26 parameters to simulate flow in a pervious land segment without snow simulation (Bicknell et al., 2001). So, more than one calibrated parameter set may be obtained with equal streamflow simulations (Doherty and Johnston, 2003; Jia, 2004) and high correlation between parameters would be expected. Both problems mean that the model and/or measured data may not be appropriate to represent the physical values (Draper and Smith, 1998). In addition to the non-uniqueness and

4

correlation in model parameter sets, watershed models are simplifications of the physical world. Therefore, parameters and structure of watershed models produce uncertainty. Research on model parameter uncertainty in watershed models has been done by several authors, e.g., Dawdy and O'Donnell (1965), Wood (1976), Garen and Burges (1981), Beven and Binley (1992), Farajalla (1995), Senarath (2000), Beven and Freer (2001), Melching and Bauwens (2001), Benaman and Shoemaker (2004), Carpenter and Georgakakos (2004), and Sieber and Uhlenbrook (2005). Some approaches to calculate structural uncertainty have been done by Draper (1995), Wagener et al. (2003), and Butts et al. (2004); however, separation between structural and parametric uncertainty has not yet been understood (Wagener, 2003).

Little research considers the combined effects of input data and parameter uncertainties on model results (Souid, 1999). Assessments of combined uncertainty in both input data and model parameters have been done by Souid (1999), Butts et al. (2004), and Carpenter and Georgakakos (2004). Souid (1999) concluded that "*the main source of the flood forecast uncertainty is due to uncertainties in rainfall model and not those in the catchment model.*" Carpenter and Georgakakos (2004) found an inverse correlation between watershed area and model uncertainty in streamflow simulations. Butts et al. (2004) believe rainfall uncertainty values are less than parametric and structural uncertainties.

Techniques applicable for evaluating error propagation from different sources on hydrology model results can be arranged in three groups:

- first-order methods,

5

- probabilistic point estimate methods (e.g., Harr's method and Rosenblueth's method), and

- Monte Carlo simulation and re-sampling methods.

Applications and comparisons of these techniques on hydrology models can be found in Rogers et al. (1985), Binley et al. (1991), Melching (1995), and Yu et al. (2001). In general, these studies assumed that the results of the Monte Carlo method were most reliable when estimations from other uncertainty methods were compared. The Monte Carlo simulation is the best known and simplest way of sampling the entire range of likely observations of the system being studied (Morgan and Henrion, 1990). Most of the first-order and probabilistic point estimate methods are more computationally efficient than the Monte Carlo method. Melching (1995) pointed out that "*research is needed to define strengths and weaknesses of applying these methods to computer models of watershed hydrology.*"

Uncertainty analysis of computer-based models is a valuable tool to do the following (Morgan and Henrion, 1990; Tung, 1996; Tung and Yen, 2005):

- understand the inability of a model to accurately and precisely depict the real world;

- enhance the value of information reported;

- distinguish between bias and precision error;

- calculate the precision limit of results;

- identify which components are most and least important;

6

- determine where to place more effort/resources to decrease the total uncertainty of the output;

- re-build a model;

- understand model limitations and strengths;

- calculate statistical properties of a model output;

- determine reliability analysis; and

- compare and choose between models.

1.2 Research Goals and Questions

The main goals of this study were to 1) evaluate two uncertainty methods, the Monte Carlo method and Harr's probabilistic point estimate method, and 2) evaluate the effects of rainfall spatial variability, hydraulic channel variability, and parameter uncertainty on HSPF streamflow results. Physical data from the Luxapallila Creek watershed were used to set up the HSPF model. This watershed is located in Alabama and Mississippi. U.S. Geological Survey (USGS) data collected at the watershed outlet from 01/01/2002 to 12/31/2005 were used to evaluate model results. The three basic research questions were stated below:

- How does uncertainty in model parameters, rainfall spatial data, and channel hydraulic properties propagate through flow simulations of a lumped watershed model?

- How consistent is the Harr method (i.e., probabilistic point estimate method) to estimate the 90% certainty bounds of streamflow simulations?

7

- Where do researchers need to put resources in terms of data collection so uncertainty in streamflow simulations may be lowered?

1.3 Research Hypothesis

Uncertainty in rainfall input data, channel hydraulic data, and model parameters introduce significant uncertainty on HSPF streamflow results. This uncertainty can be reliably quantified using either the Monte Carlo or Harr methods.

8

CHAPTER II

LITERATURE REVIEW

2.1 Hydrologic Models

2.1.1 Overview

The U.S. Environmental Protection Agency - EPA (2002) defined a model as "*a representation of the behavior of an object or process, often in mathematical or statistical terms*." Hydrologic modeling is a representation of rainfall and runoff processes. Numerous real world watershed models exist, for instance, continuous or event based, distributed or lumped, and empirical or physical (Singh, 1995; Singh and Woolhiser, 2002; Singh and Frevert, 2002a). Watershed models such as the Hydrological Simulation Program – FORTRAN (HSPF) (Bicknell et al*.,* 2001) and the Soil and Water Assessment Tool (SWAT) (Neitsch et al., 2005) are popular continuous models. The EPA has recently developed the Better Assessment Science Integrating Point and Nonpoint Sources (BASINS) software (USEPA, 2001), which links HSPF, SWAT and other models with a Geographic Information System (GIS) software. Also, BASINS incorporates an extensive U.S. data base (i.e., land use, climatological and water

9

quality data for most regions in the nation), graphical and statistical analysis and reporting tools.

Singh and Woolhiser (2002) and Todini (2007) who give a historical review of hydrological watershed modeling, believe that the Rational Method developed in 1850 was the first hydrological modeling approach. Singh and Woolhiser (2002) pointed out that "*the Stanford Watershed Model – SWM (now HSPF) by Crawford and Linsley (1966), was probably the first attempt to model virtually the entire hydrologic cycle.*" Table 1 shows information on some popular hydrologic models used in North America. The U.S. Bureau of Reclamation developed a hydrologic modeling inventory of 83 models (http://www.usbr.gov/pmts/rivers /hmi/index.html). The inventory is structured by 19 key questionnaire topics. Singh et al. (2006) believe that "*This inventory is among the first of its kind and is useful not only for modelers but water resource planners and managers*." Hydrology models are applied for many reasons (Wagener et al., 2004; Singh and Woolhiser, 2002):

- for water resources assessment (e.g., reservoir system operations);
- to quantify the impacts of watershed management strategies (e.g., development of Total Maximum Daily Loads - TMDLs);
- as load models linked to instream/estuary models;
- to understand dynamic interactions between climate and land surface hydrology; or
- to provide boundary conditions for atmospheric circulation models;

10

- *"to inform decisions that are important for human health and the environment"* (USEPA, 2002), (e.g., real time flood forecasting).

Table 1.   Selected hydrologic models used in North America

Model name/acronym	Source	Author	Characteristics
Hydrological Simulation program – FORTRAN (HSPF)	USEPA and USGS. http://www.epa.gov/ceampubl/swater/hspf/index.htm. http://water.usgs.gov/software/hspf.html	Bicknell et al., 2001	Continuous, processes based, lumped model of hydrology cycle and water quality processes
Soil and Water Assessment Tool (SWAT)	U.S. Department of Agriculture (USDA) .http://www.brc.tamus.edu/swat/	Neitsch et al., 2005	Continuous simulation of hydrology, erosion, sediment transport, and water quality
Hydrologic Engineering Center – Hydrologic Modeling System (HEC-HMS)	U.S. Army Corps of Engineers (USACE). http://www.hec.usace.army.mil/software/hec-hms/	USACE, 2001	Designed to simulate the precipitation-runoff processes of dendritic watershed systems
Storm Water Management Model (SWMM)	USEPA. http://www.epa.gov/ednnrmrl/models/swmm/index.htm	Rossman, 2005	Event or continuous model of water processes in urban areas
Sacramento Soil Moisture Accounting (SAC-SMA) Model	U.S. National Weather System (NWS)	Burnash, R.J.C., 1995	Conceptually based rainfall runoff model with spatially lumped parameters
MIKE SHE	Danish Hydraulic Institute (DHI). http://www.dhi.dk/www.-d-,dhigroup,-d-,com/Software/WaterResources/MIKESHE.aspx	DHI, 1998	Physically based processes of 2-D overland flow, 1-D river flow, and 2-D or 3-D groundwater flow
Annualized Agricultural Non -Point Source (AGNPS) model	USDA. http://www.ars.usda.gov/Research/docs.htm?docid=5199	Bingner et al., 2001	Continuous model developed to predict surface runoff and non point source pollutant loadings within agricultural watersheds.

2.1.2 Hydrology Modeling Using Radar Precipitation

Hydrologic models are represented by a series of input data (e.g., precipitation and evaporation), parameters (e.g., soil, land use, and channel properties), and structure (e.g., black-box, conceptual, physically based, distributed, and lumped models). Researchers believe spatial and temporal variability of precipitation data is the main source of input data uncertainty when rainfall-runoff models are applied (Vieux, 2002; Butts et al., 2004; Neary et al., 2004; Lopez et al., 2005). Precipitation is measured/calculated using gage, radar,

11

or satellite data. Point precipitation is directly measured using gages. Both radar and satellite precipitation values are indirect estimates of rainfall. Dense rain gage networks are expensive to maintain and operate. On the other hand, radar-derived precipitation is now a better alternative to estimate the spatial variability of precipitation (Vieux, 2002; Neary et al., 2004); however, radar rainfall estimations show uncertainty due to radar reflectivity-precipitation rate transformation and radar range (Sharif et al., 2004).

The National Weather Service (NWS), Air Force Weather Agency (AFWA), and Federal Aviation Administration (FAA) control approximately 159 Weather Surveillance Radar-1988 Doppler (WSR-88D) sites throughout the U.S. and selected overseas locations (NOAA/NCDC, 2007). This network is named the Next Generation Weather Radar system (NEXRAD). In general, the range of each radar installation is around 230 km. NEXRAD data are acquired and processed in two levels (i.e., levels II and III). Level II consists of raw data - unprocessed reflectivity, mean radial velocity, and spectrum width data. Level III includes processing raw radar data using computer algorithms to yield 41 products (e.g., 1-hour precipitation total, 3-hour precipitation total, and storm total accumulation). The precipitation products are aggregated at various resolutions and time intervals called Stage I, II, III, and IV. Stage I data are hourly precipitation accumulations without adjustment to rain gage data. Stage II data include gage-radar bias corrections and local adjustments to a multisensor precipitation field. Stage III data use Stage II products from multiple radars to

12

create a mosaic of coverages. The national Stage IV product is based on Stage III data. Stage IV data are archived since January 2002.

Researchers have found differences between rain gage and radar-derived values of mean aerial precipitation (Johnson et al., 1999). Johnson et al. (1999) found a general underestimation between 5% and 10% of mean aerial precipitation derived by stage III radar compared with that derived from a rain gage network in the southern plains region of U.S. In streamflow simulations, they identified large monthly biases, but inconsistent results were found when storm events were evaluated.

Lopez et al. (2005) calibrated an event model using radar and rain gage data in Italy. They found that flow simulations using radar precipitation data performed better than flow simulations using rain gage data. Neary et al. (2004) simulated streamflow in a Tennessee watershed using two rainfall inputs, Stage III NEXRAD data and rain gage data. The main conclusions of this work were that the performance of radar at low precipitation intensities was poor; significant precipitation was not detected by both instruments; flow simulations were not reproduced well; water volumes were better predicted by rain gage data than by radar precipitation; and time to peak simulated with both radar-derived and rain gage data were very similar.

Moon et al. (2004) compared flow simulations using the SWAT model with precipitation data from rain gage and radar devices. Stage III NEXRAD data and data from six rain gages were used in a 2,608 km^2 Texas watershed. The daily coefficient of determination values between rain gage data and radar data were

13

greater than 0.65 for five out of the six stations evaluated. Close values of the daily Nash-Sutcliffe coefficient (see section 2.3) for model simulations using rain gage and radar data were calculated, and high flow events were better simulated using radar data. The authors suggested that radar precipitation is a good alternative to rain gage data in watersheds with sparse or no rain gage networks.

2.2 Hydrological Simulation Program – FORTRAN (HSPF)

This section provides a review of the hydrology model evaluated in this study. The HSPF model is a numerical, process-based, lumped, continuous software developed under EPA sponsorship to simulate hydrology and water quality processes in pervious or impervious areas. The first version of HSPF was released in 1980, while version 12 is the most recent (Bicknell et al., 2001). HSPF has its origin in four previously developed models: 1) Hydrocomp Simulation Programming (HSP); 2) NonPoint Source (NPS) Model; 3) Agricultural Runoff Management (ARM) Model; and 4) Sediment and Radionuclides Transport (SERATRA) (Bicknell et al., 2001). Donigian et al. (1995) declared that database input management and algorithms for the stream sediment-nutrient, wetlands capabilities, and best management practices for the HSPF model have been improved over earlier versions.

Extensive and successful applications of HSPF components (hydrology, erosion, sediment transport, and instream water quality) in urban and rural areas around the world have been reported (e.g., Moore et al., 1988; Chew et al., 1991; Laroche et al., 1996; Fontaine and Jacomino, 1997; Jacomino and Fields, 1997;

14

Carrubba, 2000; Zhang, 2001; Al-Abed and Whiteley, 2002; Engelmann et al., 2002; Doherty and Johnston, 2003; Johnson et al*.,* 2003; Paul, 2003; Albek et al., 2004; Diaz, 2004; Hayashi et al., 2004; Im et al., 2004; Jia, 2004; and Wu, 2004). Graphical interfaces for HSPF are used in various computer simulation programs such as the Watershed Modeling System - WMS (EMS-I, 2002) and BASINS (USEPA, 2001).

2.2.1 Hydrological Simulation

This section presents a brief summary of the capabilities of HSPF for modeling hydrology processes. A detailed description of HSPF can be found in the HSPF User's manual (Bicknell et al., 2001).

The HSPF model is divided into three application modules and five utility modules. Application modules simulate runoff and water quality processes in pervious areas (PERLAND), impervious areas (IMPLND), and during routing through reservoir and reaches (RCHRES) (Donigian et al., 1995). Time series (i.e., meteorological and flow observed data) are accessed, manipulated, and analyzed in the utility modules.

Algorithms for hydrological simulation in HSPF originated from the Stanford Watershed Model (Linsley et al., 1988). A flow diagram of the hydrological components of HSPF is shown in Figure 1. This diagram is a reservoir-type model consisting of five storage classes (interception, upper zone, lower zone, baseflow, and deep percolation), each allowing different types of inflow and outflow. Inflows and outflows are simulated in HSPF as water-balance

15

accounting. Each pervious land segment considers the following processes: interception, evapotranspiration, surface detention, surface runoff, infiltration, shallow subsurface flow (interflow), base flow, and deep percolation (Donigian et al., 1995). Surface detention and surface runoff are the only components simulated in impervious areas.
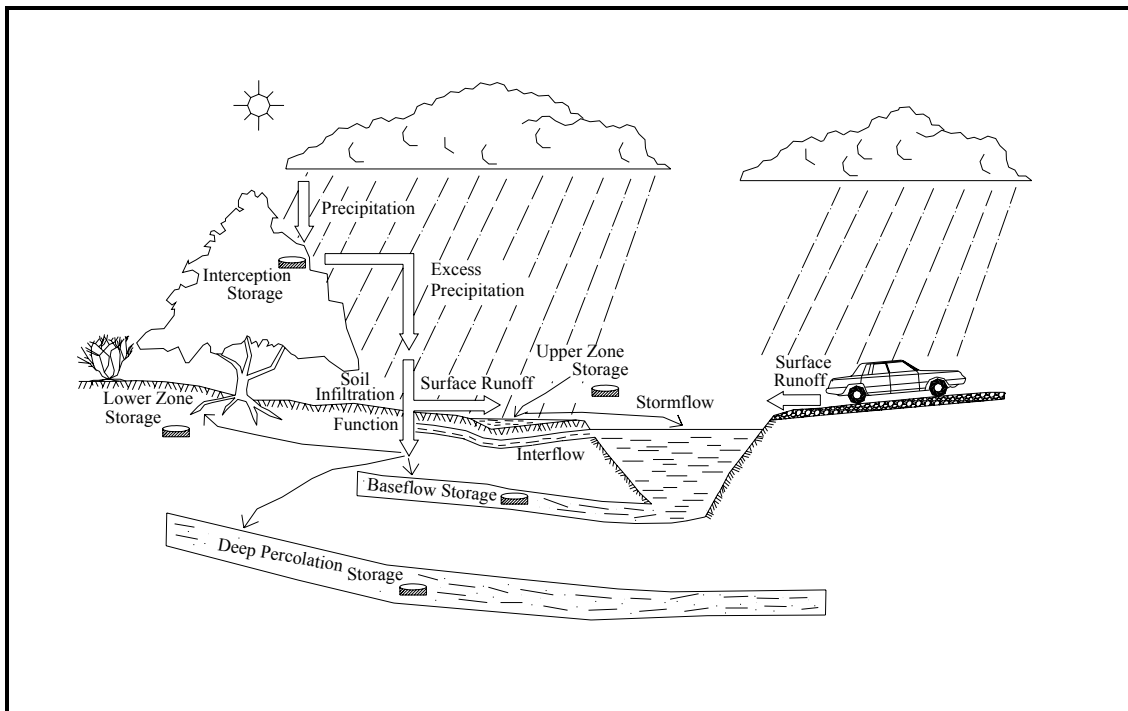
Figure 1.   Hydrological components simulated in HSPF (after Diaz, 2004)

Before running HSPF, the watershed area must be delineated into homogeneous land areas called Hydrologic Response Units (HRUs). For each HRU the combination of weather, soil, land use, topographic and geologic properties is unique, giving rise to its "semi-distributed" model structure. HRUs can be impervious or pervious areas, which are modeled independently. Each

16

HRU requires input data such as rainfall, temperature, potential evapotranspiration, and parameters related to land use, soil characteristics, and agricultural practices to simulate hydrology, sediments, nutrients and pesticides (Donigian et al., 1995). HRU outputs are not connected laterally, but outputs are connected to the nearest channel. This simplification makes the HSPF model implementation/application easy and fast; however, some physical information among HRU processes can be lost.

The HSPF software uses empirical formulations to model the movement of water within each HRU. The model uses 26 parameters (17 constant, 7 initial storage, and 2 monthly parameters) to simulate water budget in a pervious land segment without snow simulation (Bicknell et al., 2001). It uses both conceptual and physical parameters to simulate the water balance in a HRU. Table 2 shows definition and calibration scenarios of 17 HSPF hydrology parameters used to model the water budget in a pervious land segment without snow simulation. This Table shows that most of the HSPF parameters influence only one calibration scenario (LZSN, KVARY, NSUR, and LSUR); however, parameters such as INFILT and LZETP influence more than one calibration scenario. Physical parameters include length and slope of surface flow, LSUR and SLSUR, respectively. Conceptual parameters include storage capacities (upper and lower zones of the soil, UZSN, and LZSN, respectively), interflow parameter (INTFW), infiltration parameter (INFILT), baseflow recession parameter (AGWRC), and evapotranspiration rates from various storage types (LZETP, BASETP, and AGWETP). Interception loss (CEPSC) is simulated by assuming an interception

17

storage capacity according to the type of vegetation on the HRU. Volume of interception storage must be filled before excess precipitation can reach the land surface; intercepted water is subsequently evaporated.

Table 2.   Calibration scenarios (USEPA, 2006b)

Name (unit)	Definition	Calibration Scenarios			
		Water Balance	High/Low Flow Distribution	Storm Flow	Seasonal Discrepancies
LZSN (mm)	Lower zone nominal soil moisture storage	X			
INFILT (mm/hr)	Index to infiltration capacity	X	X	X	
LSUR (m)	Length of overland flow			X	
SLSUR	Slope of overland flow plane			X	
KVARY (1/mm)	Variable groundwater recession				X
AGWRC	Base groundwater recession		X		
INFEXP	Exponent in infiltration equation				
INFILD	Ratio of max/mean infiltration capacity				
DEEPFR	Fraction of groundwater inflow to deep recharge	X	X		
BASETP	Fraction of remaining evapotranspiration from baseflow		X		X
AGWETP	Fraction of remaining evapotranspiration from active groundwater				X
CEPSC (mm)	Interception storage capacity				X
UZSN (mm)	Upper zone nominal soil moisture storage				X
NSUR	Manning's n for overland flow			X	
INTFW	Interflow inflow parameter			X	
IRC	Interflow recession parameter			X	
LZETP	Lower zone evapotranspiration parameter	X			X

18

Infiltration is calculated by means of a negative power relationship. Both Hortonian and saturation excess overland flow can be simulated in HSPF. A portion of surface runoff becomes upper-zone storage, simulating both depression storage and upper-soil storage, and the balance becomes overland flow. Infiltrated water that does not go into interflow or lower-zone storage is finally placed in the active groundwater storage. Active groundwater storage is divided into deep percolation and base flow. Deep percolation is simulated as a sink. Base flow is simulated using linear and power equations.

Actual evapotranspiration is simulated in response to the input value of potential evapotranspiration. Water evaporates first from the riparian vegetation (wetlands). Further actual evapotranspiration is satisfied sequentially by interception storage, upper zone storage, active ground water, and lower-zone storage where each storage type has a different resistance to evaporation. In this way, the maximum potential of each storage type is depleted either when all storage classes have contributed their maximum amount to evapotranspiration or until the potential evapotranspiration has been fully satisfied.

The HSPF program simulates snowmelt as a complex energy balance problem. It is a result of a series of routines that compute net radiation exchange on the snow surface, convection and condensation melt, heat transfer from the earth to the bottom of the snowpack where the soil is not frozen, and melt due to rainfall. Input data used by HSPF for snowmelt are obtained from direct measurements and include: precipitation, dewpoint temperature, wind speed, cloud cover, solar radiation, and evapotranspiration.

19

Flow routing in HSPF takes place in two regimes: on the overland flow plane and in the river channel network. Overland flow is routed using a power equation that relates the Manning friction coefficient, the slope and length of the land surface, and detention storage. HSPF employs the Muskingum method to move water from one reach to the next in the river channel network. This method is based on the principle of mass conservation (Ponce, 1989). Flow is modeled as unidirectional and complete mixing is assumed by the model in streams and lakes. For each reach, a fixed relationship is assumed between water level, surface area, volume, and discharge (components of the FTABLE database). These physical data are specified by the user. HSPF calculates hydraulic variables such as hydraulic radius, shear stress, and velocity, assuming that the cross-section of the reach is constant throughout the reach (Bicknell et al., 2001).

Simplification of the real world with conceptual parameters avoids the need to give physical dimensions of the flow system (Bicknell et al., 2001). This approach is advantages for reducing input requirements and, more importantly, gives the model its generality (Linsley et al., 1988). Parameters such as percentage of impervious area, average length of overland flow, and average slope of overland flow are determined from maps. Other parameters pertaining to infiltration, for instance, soil-moisture zones and interflow are determined by calibration or comparison with observed hydrographs (Linsley et al., 1988).

In summary, the HSPF model uses physical concepts (water balance), empirical equations (linear and power relationships), physical data (rainfall, evaporation, slope and length of land surface, and hydraulic characteristics of the

20

channel network), and parameters (interflow, infiltration) to simulate the flow of water in pervious/impervious areas and channels. Most of the parameters are conceptual and usually must be calibrated against flow measured at the outlet of the watershed. Due to the extensive use of HSPF, a parameter range database (HSPFParm) is available to help in the calibration process (USEPA, 2006a). Additionally, the BASINS EPA website gives guidelines to calibrate HSPF hydrology parameters.

2.3 Evaluation of Hydrologic Model Results

Any computer modeler needs to measure how well the model emulates the real world. James and Burges (1982) defined model evaluation as "*judge of the model adequacy for decision-making.*" This section reviews two approaches to evaluate model outputs: deterministic and probabilistic evaluation.

2.3.1 Deterministic Evaluation

In a deterministic evaluation, it is assumed that all input variables are known with perfect accuracy. For instance, when a hydrologic model is evaluated at the watershed outlet, it is assumed that the simulated and observed streamflows are known with perfect accuracy.

Deterministic evaluation of models requires graphical and statistical tests (James and Burges, 1982; Thomann, 1982; Legates and McCabe, 1999). James and Burges (1982) recommended graphical comparisons such as a continuous time series plot of simulated and observed data, a continuous time series plot of

21

the difference between recorded and simulated values (residuals), and a scatter-gram of recorded data plotted against simulated values. Graphical analyses are clearly visual but quite subjective (Thomann, 1982). On the other hand, statistics such as coefficient of determination (R^2) and Nash-Sutcliffe coefficient (NS) have been developed to better describe the degree of association between the observed and simulated data. Additionally, Legates and McCabe (1999) recommended the use of residual analyses such as mean absolute error (MAE) and root mean square error ($RMSE$).

The coefficient of determination (R^2), which is the square of Pearson's product-moment correlation coefficient, represents the fraction of variability in y that can be explained by the variability in x. It ranges from zero to one, with higher values indicating better agreement, and is given by the following:

$$R^2 = \left\{ \frac{\sum_{j=1}^{n}(O_j - \overline{O})(S_j - \overline{S})}{\left[\sum_{j=1}^{n}(O_j - \overline{O})^2\right]^{0.5}\left[\sum_{j=1}^{n}(S_j - \overline{S})^2\right]^{0.5}} \right\}^2 \tag{1}$$

where O_j is the observed value at time step j; $\overline{O}$ is the average observed value during evaluation period; S_j is the model simulated valued at time step j; and $\overline{S}$ is the average simulated value at time step j.

The NS coefficient (Nash and Sutcliffe, 1970) represents the fraction of the variance in the measured data explained by the model. The NS ranges from minus infinity to one. A value of one in NS represents perfect fit. The NS coefficient has been used by many researchers and is considered as one of the

22

best statistics for evaluation of continuous-hydrograph simulation programs (Bergman et al., 2002; Engelmann et al., 2002; Carrubba, 2000; Legates and McCabe, 1999; Laroche et al., 1996; ASCE, 1993; James and Burges, 1982). The NS is given by the following equation:

$$NS = 1 - \frac{\sum_{j=1}^{n} (O_j - S_j)^2}{\sum_{j=1}^{n} (O_j - \overline{O_j})^2} \tag{2}$$

The mean absolute error (MAE) and root mean square error (*RMSE*) are dimensioned measures of average model-performance error:

$$MAE = \frac{\sum_{j=1}^{n} |O_j - S_j|}{n} \tag{3}$$

$$RMSE = \left[\frac{\sum_{j=1}^{n} |O_j - S_j|^2}{n} \right]^{\frac{1}{2}} \tag{4}$$

Advantages and disadvantages of these statistical criteria are shown in Table 3. Legates and McCabe (1999) pointed out that "*one of the biggest problems associated with all relative error or "Goodness-of-Fit" measures is one of interpretation*."

23

Table 3.   Advantages and disadvantages of selected statistical criteria

Criteria	Advantages	Disadvantages
R^2	Measure of the usefulness of a linear regression equation	Data are normally distributed "*Insensitive to additive and proportional differences between the model simulations and observation; large values can be obtained even when the model simulated values differ considerably in magnitude and variability; more sensitive to outliers than to observations near the mean, because of the squared differences*" (Legates and McCabe, 1999)
NS	"*it is sensitive to differences in the observed and model-simulated means and variances*" (Legates and McCabe, 1999)	"*is more sensitive to extreme values, as is R^2*"(Legates and McCabe., 1999)
RMSE	Evaluation of the error in the units of the variable	"*it tends to become increasingly larger than MAE (but not necessarily in a monotonic fashion) as the distribution of error magnitudes becomes more variable*" (Willmott and Matsuura, 2005)
MAE	Same as RMSE and, *"(unlike RMSE) it is an unambiguous measure of average error magnitude*" (Willmott and Matsuura, 2005)	"*interpretation*" (Legates and McCabe, 1999)

Criteria for evaluating model performance depend on the process simulated (flow, sediments, pesticide or water quality). To date, modeling professionals (developers and users) have not reached a consensus about which criteria is best for evaluating model performance (Beach et al., 2000; Bergman et al., 2002). Donigian (2000), a developer of HSPF for the last 20 years, provides

24

guidelines for evaluation of the HSPF simulation results (Tables 4 and 5). Table 4 shows the relative percentages of error between observed constituent and simulated data by HSPF. This Table applies to monthly and annual errors rather than daily differences. Table 5 shows typical R^2 values for daily and monthly time series to evaluate model performance.

Tabla 4.   General guidelines for evaluation of HSPF performance (Donigian, 2000)

Constituent	% Difference between simulated and recorded values		
	Very good	Good	Fair
Hydrology/flow	< 10	10 - 15	15 - 25
Sediment	< 20	20 - 30	30 - 45
Water temperature	< 7	8 – 12	13 - 18
Water quality/nutrients	< 15	15 - 25	25 - 35
Pesticides/toxics	< 20	20 - 30	30 - 40

Table 5.   Typical values of coefficient of determination (R^2), for daily and monthly time series when evaluating model performance (Donigian, 2000)

Statistic	Poor	Fair	Good	Very good
R^2 (daily)	0.52-0.61	0.62-0.72	0.73-0.81	0.82-1.0
R^2 (monthly)	0.52-0.64	0.65-0.76	0.77-0.85	0.86-1.0

2.3.2 Probabilistic Evaluation

Probability is used to describe variability, including the lack of knowledge or lack of certainty about something. Probability is used as a tool in many areas of modeling. For instance, a hydrologic modeler uses probability to learn how a model parameter propagates uncertainty on model results. In order to analyze

25

uncertainties, a probabilistic evaluation is required. This section provides an introduction to the main terms used in probabilistic evaluation. Further discussion of probabilistic evaluation is found in this study in Section 2.4, Uncertainty Analysis in Hydrologic Modeling.

Haan et al. (1995) described a probabilistic procedure for evaluating hydrologic models. The following steps were declared: "*generate probability distributions on input parameters; generate probability distributions on model outputs; and use the output probability distribution to assess the model.*" Tung (1996) pointed out that

> "*the most complete and ideal description of uncertainty is the probability density function of the quantity subject to uncertainty… Another measure of the uncertainty of a quantity is to express it in terms of a confidence interval…A useful alternative is to use the statistical moments associated with a quantity subject to uncertainty. In particular, the second-order moment.*"

Ponce (1989) defined a probability distribution as "*a function that expresses in mathematical terms the relative chance of occurrence of each of all possible outcomes of the random variable.*" An example of a random variable and probability distribution is shown in Figure 2. The random variable is an HSPF parameter called INTFW (see Table 2 for definition). The possible outcomes have been separated into nine classes. The sum of probabilities of all possible outcomes is equal to one. In Figure 2, the probability that INTFW is in the class 2.5-3.5 is 0.18. Additionally, Figure 2 suggests a curve like the dotted one sketched over the nine classes. This curve is the graph of some function, which is called a continuous probability density function (PDF). Some of the

26

PDFs of model parameters used in hydrology simulation are (Paul, 2003; Binley et al., 1991; Manache and Melching, 2004; Melching and Bauwens, 2001; and Yu et al., 2001): beta, normal, lognormal, triangular, exponential, and uniform. Further discussion on PDFs is found in Haan (2002).
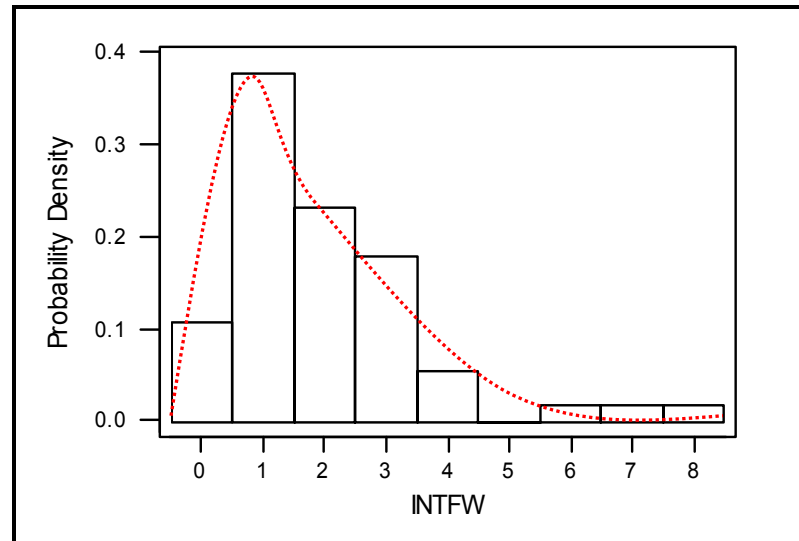
Figure 2.   Probability distribution and PDF of INTFW

Another term used in probabilistic evaluation is the confidence interval, which is a measure of uncertainty that may be illustrated in two forms: using percentiles or calculating statistical moments (mean and standard deviation) of a selected variable. Percentile is defined by USGS as "*a value on a scale of one hundred that indicates the percent of a distribution that is equal to or below it*" (http://water.usgs.gov/waterwatch/ptile.html). For instance, the 90% confidence interval on model simulations is calculated using the difference between the 95th and 5th flow percentiles. Confidence intervals may be calculated using the mean

and standard deviation of a selected variable. For instance, Yu et al. (2001) calculated hourly confidence intervals using the mean +/- two standard deviations of streamflow simulations. Two questions arise when continuous confidence intervals are calculated:

- how many of the observed data are within the confidence intervals? (*Reliability*); and,

- how wide are the confidence intervals? (*Sharpness*).

2.4 Uncertainty Analysis in Hydrologic Modeling

This section reviews topics related to uncertainty analysis in hydrologic modeling. Five topics are illustrated: sources of uncertainty; uncertainty methods; comparisons of uncertainty analysis methods; evaluation of combined effects of uncertainties on model results; and, sensitivity/uncertainty studies of the HSPF model.

2.4.1 Sources of Uncertainty

Generally, every component of hydrologic models (input data, parameters, and structure) introduces uncertainty due to the lack of knowledge about real systems. Uncertainty in input data is due to natural variability, measurement inaccuracy, and errors in handling and processing data (Melching, 1995). Model parameters and structure show uncertainty from model assumptions/approximations, scale effects, and variability of inputs and parameters in time and space (Gupta et al., 2005; Tung, 1996). The uncertainty

28

of input data on model results have been studied isolated from model parameter uncertainty (Souid, 1999). Georgakakos et al. (2004) pointed out that few have researched model structure uncertainty. Butts et al. (2004) declared that uncertainty evaluation is compensated among components (input data, model parameters, and model structure) because they are strongly interlinked.

Many researchers believe spatial and temporal variability of precipitation data is the main source of input data uncertainty when rainfall-runoff models are applied (Vieux, 2002; Butts et al., 2004; Neary et al., 2004; Lopez et al., 2005). In addition, model parameter estimation is affected by a poor knowledge of precipitation input data (Andreassian et al., 2001). Indeed, rainfall distribution must be a main feature when a hydrologic model is developed and evaluated (Hromadka II and McCuen, 1989). Osborn and Lane (1982) said that "*for small watersheds, the input with greatest variability is rainfall. Therefore, the accuracy of streamflow simulation depends primarily on how well this variability can be defined in a specific case.*" Aronica et al. (2005) pointed out that model structure and sensitivity of model parameters make a model more or less sensitive to rainfall temporal resolution. Assessments of rainfall input data uncertainty in hydrologic simulation have been done by various authors, Anagnostou and Krajewski (1999), Bronster and Bardossy (2003), Sharif et al. (2004), and Aronica et al. (2005).

Model parameters are another component of hydrologic models that propagate uncertainty through model results. Watershed models are complex and highly parameterized. For instance, the HSPF model uses 26 parameters to

29

simulate flow in a pervious land segment without snow simulation (Bicknell et al., 2001). So, more than one calibrated parameter set may be obtained with equal streamflow simulations (Doherty and Johnston, 2003; Jia, 2004) and high correlation between parameters would be expected. Both problems mean that the model and/or measured data may not be appropriate to represent the physical values (Draper and Smith, 1998). In addition to the non-uniqueness and correlation in model parameter sets, watershed models are simplifications of the physical world. Therefore, parameters and structure of watershed models produce uncertainty. Research on model parameter uncertainty in watershed models has been done by several authors, Dawdy and O'Donnell (1965), Wood (1976), Garen and Burges (1981), Beven and Binley (1992), Farajalla (1995), Senarath (2000), Beven and Freer (2001), Melching and Bauwens (2001), Benaman and Shoemaker (2004), Carpenter and Georgakakos (2004), and Sieber and Uhlenbrook (2005). Some approaches to calculate structural uncertainty have been developed by Draper (1995), Wagener et al. (2003), and Butts et al. (2004); however, separation between structural and parametric uncertainty is not well understood (Wagener, 2003).

Little research has examined the combined effects of input data and parameter uncertainties on model results (Souid, 1999). Assessments of combined uncertainty in both input data and model parameters have been done by Souid (1999), Butts et al. (2004), and Carpenter and Georgakakos (2004). Souid (1999) concluded that "*the main source of the flood forecast uncertainty is due to uncertainties in rainfall model and not those in the catchment model.*"

30

Carpenter and Georgakakos (2004) found an inverse correlation between watershed area and model uncertainty in streamflow simulations. Butts et al. (2004) believe rainfall uncertainty values are less than parametric and structural uncertainties.

2.4.2 Uncertainty Methods

Uncertainty analysis methods used in hydrology simulation can be arranged in three groups: first-order methods, probabilistic point estimation methods, and Monte Carlo simulation and re-sampling methods. The following sections describe each of these methods.

2.4.2.1 First-order Methods

Methods of uncertainty propagation that use Taylor series expansions are explained in this section. The first (mean) and second (variance) moments of the probability distributions are used to propagate and analyze uncertainty in first-order methods (Morgan and Henrion, 1990). The mean-value first-order second-moment (MFOSM) method and advanced first-order second-moment (AFOSM) method have been applied to rainfall-runoff models (Melching, 1995).

MFOSM uses a Taylor series expansion of the model output that is truncated after the first order term (Melching 1995), making the uncertainty function become linear (Morgan and Henrion, 1990). Melching (1995) shows some applications of MFOSM in evaluating uncertainty of hydrology simulations. Advantages and disadvantages in using this method are shown in Table 6. The

31

application of the MFOSM method is simple and computationally efficient (Melching 1995). The main disadvantage is the poor calculation of the first and second moments of the probability distributions in nonlinear uncertainty functions (Melching, 1995). In rainfall-runoff models, the nonlinear assumption is difficult to justify because this kind of system is usually nonlinear (Gupta et al., 2005).

The approach used in the AFOSM method comes from the work of Hasofer and Lind (1974). The AFOSM method uses a "likely" point in the parameter space, instead of the mean used in the MFOSM method (Gupta et al., 2005). The mean and variance of the uncertainty function are approximated using a Taylor series truncated after the first order term at the "likely" point on the failure surface (Melching, 1992). The AFOSM method is applied to nonlinear functions and maintains the simplicity of the MFOSM method (Tung, 1996). Advantages and disadvantages of this method are shown in Table 6. An application of the AFOSM method in assessing rainfall-runoff uncertainty can be found in Melching (1992).

Table 6.   Advantages and disadvantages of uncertainty analyses methods (Morgan and Henrion, 1990; Melching, 1995; Tung, 1996; Christiaens and Feyen, 2002; Haan, 2002)

Method	Advantages	Disadvantages
MFOSM	Simple numerical calculations; does not require knowledge of the PDF of stochastic variables	Restricted to linear models with small uncertainties; input parameters are statistically independent; tails of output distribution are not characterized; non-invariability of the performance function
AFOSM	Calculations are simple and straightforward; can be applied to non-normal and correlated random variables; can be applied to non-linear functions	Determination of the "likely" point is usually hard
Rosenblueth	Calculations are simple and direct	Restricted to linear models; computationally impractical for large number of uncertain variables; inadequate for evaluating extreme percentiles; restricted to low coefficient of variation
Harr	More computationally efficient than the Rosenblueth method	Same disadvantages as the Rosenblueth method; limited to symmetrical distributions; sometimes the uncorrelated and standardized coordinates are calculated out of the parameter bounds
MCS	Simple structure of the computation algorithm; used in complex/nonlinear models; computational complexity is linear	Time consuming at high levels of accuracy; results are not in analytical form
LHS	Number of runs can be fewer than MCS	Results are not in analytical form

33

2.4.2.2 Probabilistic Point Estimate Methods (PPEMs)

The concept of PPEMs was originated by Rosenblueth (1975). A PPEM propagates the parameter uncertainty by performing point estimations of the function without calculating the derivatives of the function (MFOSM and AFOSM methods). Selected point estimations of the function are calculated using statistical moments (mean, variance) of the function instead of computing the entire PDF of the function (Monte Carlo simulation).

Rosenblueth (1975) proposed a PPEM for handling symmetric and correlated stochastic input variables. In 1981 Rosenblueth extended the previous method to deal with non-symmetrical random variables. The Rosenblueth method approximates a random variable with probability distribution function by two points, determined by the first three moments of the random variable. Using N random variables, a total of 2^N possible solutions are produced in the parameter space. This exponential equation of possible solutions makes the method computationally impractical for large N random variables (Haan, 2002). Advantages and disadvantages of using the Rosenblueth method are shown in Table 6. Applications of this method in watershed hydrology are found in Yu et al. (2001), Binley et al. (1991), and Rogers et al. (1985).

The Rosenblueth method was modified by Harr (1989) to reduce the number of evaluations from 2^N to $2N$. Harr (1989) developed a PPEM using the principal component matrix theory. This method considers the mean, standard deviation, and correlation of the parameters evaluated. Figure 3 shows a schematic of the Harr method.

34
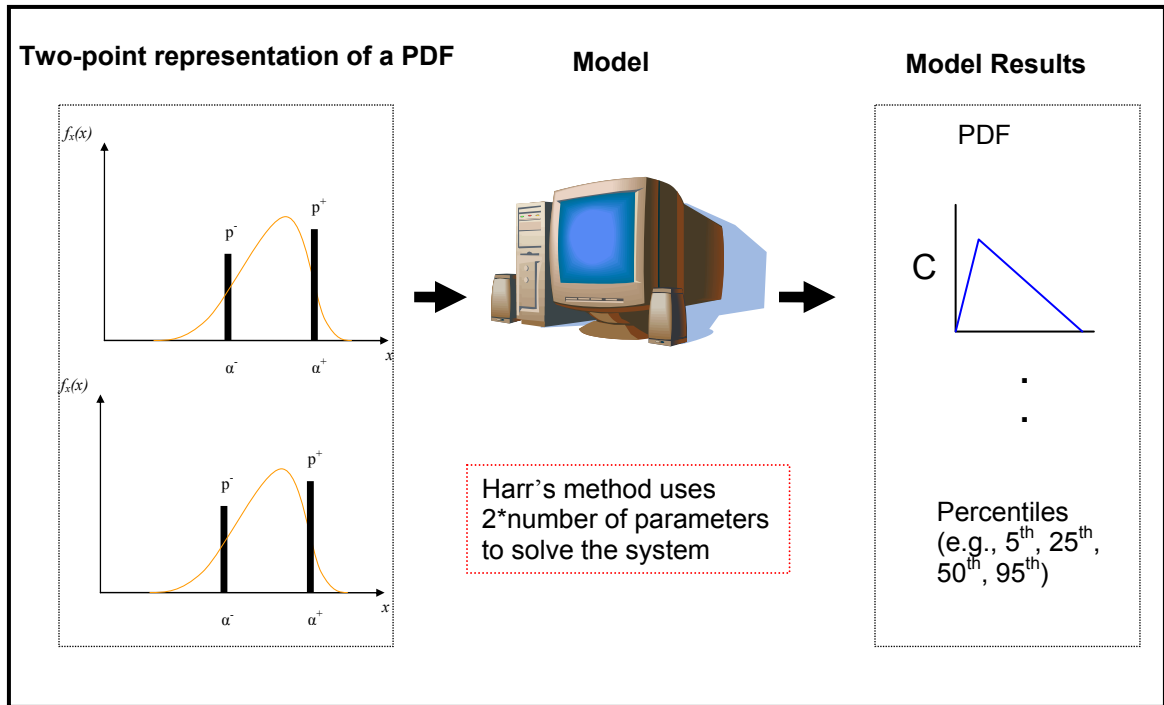
Figure 3.   Schematic of the Harr method

The Harr method propagates the parameter uncertainty through model outputs by performing two point estimations of the parameter space. The correlation matrix of parameters, *C*, is decomposed as

$$C = e\lambda e^{T}$$

(5)

where *e* = eigenvector matrix; *λ* = diagonal eigenvalue matrix; e^{T} = transpose of eigenvector matrix;. Thus, someone using Harr's method must generate the correlation matrix of selected parameters and then compute, using mathematical programs such as Matlab, the eigenvector matrix and the diagonal eigenvalue matrix. The uncorrelated and standardized coordinates can be calculated by

$$x_i^{+} = \mu + \sqrt{n} * \sigma * e_i$$

(6a)

35

$$x^- = \mu - \sqrt{n} * \sigma * e_i \qquad\qquad (6b)$$

where μ = vector of the expected values of the parameter; n = number of parameters; σ = diagonal matrix of the standard deviation of the parameters; and e_i = eigenvector for the eigenvalue λ_i. Finally, based on the two coordinates selected along each eigenvector (equations 6a and 6b), the user must compute the corresponding model output values. For instance, this research used 12 HSPF parameters; thus 24 coordinates were calculated and 24 model outputs were generated for each simulated day. Then, the 95th and 5th percentiles of these 24 model outputs were calculated to generate the 90% certainty bounds of model outputs.

A drawback of the Harr method is that the uncorrelated and standardized coordinates may fall outside the parameter bounds (Christian and Baecher, 2002). In this study, when a coordinate was outside the pre-established HSPF parameter range, the closest parameter limit was used in instead of the outside value. Table 6 shows the advantages and the disadvantages of the Harr method. An application of this method in simulating watershed hydrology is found in Yu et al. (2001).

2.4.2.3 Monte Carlo Simulation and Re-sampling Methods

The origination of the Monte Carlo method is credited to Metropolis and Ulam, who wrote a paper entitled "The Monte Carlo Method" in 1949. The idea of the method is to compute an empirical probability distribution of the model output using random values for the input variables sampled from their probability

36

distribution. Detailed information on Monte Carlo simulation is found in Ronen (1988), Morgan and Henrion (1990), and Sobol' (1994). The Monte Carlo simulation is the best known uncertainty method, and simplest way of sampling the entire range of likely observations of the system being studied (Morgan and Henrion, 1990). Melching (1995) declared that the Monte Carlo method "*it may be the only method that can estimate the CDF and PDF of Z for cases with highly nonlinear and/or complex system relationships.*" The Monte Carlo simulation involves five steps:

1. generate probability distributions of selected model parameters (e.g., normal, triangular, beta, etc);

2. calculate a random value from the parameter's distributions;

3. evaluate the model using the random value calculated in step 2;

4. repeat steps 2 and 3 many times; and

5. analyze the model outputs (e.g., cumulative distribution function - CDF, percentiles, mean, standard deviation, etc).

The Monte Carlo simulation has been applied to study the uncertainty of forcing input data and model parameters in computer models of watershed hydrology (Melching, 1995; Carpenter and Georgakakos, 2004). Table 6 shows the advantages and the disadvantages of the Monte Carlo method. Melching (1995) pointed out that "*for complex, nonlinear models with many uncertainty basic variables, however, the number of simulations (thus the computer time) necessary to achieve an accurate estimate may become prohibitive.*" Increasing of computer processing speeds makes computations more tractable. Monte

37

Carlo method results have been used as a baseline when comparisons with other uncertainty methods have been done (Binley et al., 1991; Melching, 1992; Melching, 1995; Yu et al., 2001).

An alternative to selecting the values of input variables is the Latin Hypercube Sampling, LHS (McKay et al., 1979). The LHS method is a stratified sampling approach similar to the Monte Carlo simulation (Manache and Melching, 2004). The advantage of this approach is that random samples are represented from all the ranges of possible values in a fully stratified manner, thus giving insight into the tails of the probability distributions (McKay et al., 1979). Table 6 shows the advantages and the disadvantages of the LHS. Melching (1995) reported results of an application of LHS to the HEC-1 model. Chu (2003) analyzed the parameter uncertainty of the Soil and Water Assessment Tool (SWAT) model using the Monte Carlo simulation based on an LHS scheme. Manache and Melching (2004) applied the LHS to a water quality model called DUFLOW. Melching and Bauwens (2001) evaluated the LHS in coupled nonpoint source and stream water-quality models, which were used to simulate dissolved oxygen. Yu et al. (2001) examined the uncertainty of model output from a distributed rainfall-runoff model using LHS.

2.4.3 Comparisons of Uncertainty Analysis Methods

This section reviews comparisons of uncertainty analysis methods on hydrologic modeling. Garen and Burges (1981) evaluated parameter uncertainty for a modified version of the Stanford Watershed Model (predecessor of HSPF)

38

using the Monte Carlo simulation and the MFOSM method. Mean and standard deviations were computed in both methods. Values of mean and standard deviations were underestimated by MFOSM. For extreme conditions (storms), the model responded in a high nonlinear fashion, and the MFOSM method gave poor results.

Binley et al. (1991) assessed the parameter uncertainty in the Institute of Hydrology distributed model (IHDM) using the Rosenblueth and Monte Carlo simulation methods. The Rosenblueth method required fewer simulation runs to calculate uncertainty bounds than in the Monte Carlo method due to the non-linearity of the response function considered by the Rosenblueth method. The Monte Carlo method was recommended if the probability distribution is expected to be highly skewed.

Melching (1992) evaluated the AFOSM, the MFOSM, and Monte Carlo approaches for two rainfall-runoff event models, the Flood Hydrograph Package (HEC-1) and the Australian Runoff Routing Program (RORB). The AFOSM approach overcomes the problems of non-linear systems and extreme failure events shown by MFOSM. In addition, AFOSM is simpler than the Monte Carlo simulation and similar results were achieved by both the AFOSM and Monte Carlo simulations.

Melching and Bauwens (2001) employed the LHS and the MFOSM methods to calculate parameter uncertainty of coupled nonpoint source and stream water quality models. They found that only six out of 53 parameters considerably affected the uncertainty in simulated dissolved oxygen

39

concentrations. The LHS and MFOSM approaches identified the same key parameters. Haan and Skaggs (2003) used the first-order approximation analysis (FOA) and the Monte Carlo simulation to evaluate parameter uncertainty on the DRAINMOD model, and both methods yielded similar results.

Yu et al. (2001) compared four methods - the Monte Carlo simulation, LHS, Rosenblueth's point estimation method (RPEM), and Harr's point estimation method (HPEM) - to estimate uncertainty of model output for a distributed rainfall-runoff model. Monte Carlo simulation and LHS showed similar results. The LHS approach used a relatively small number of simulations compared to the Monte Carlo simulation. The RPEM and HPEM approaches demonstrated different results than the Monte Carlo simulation, due to the small number of model parameters analyzed (three).

2.4.4 Evaluation of Combined Effects of Uncertainties on Model Results

Few researchers have considered the combined effects of uncertainties on model results (Souid, 1999). Souid (1999) evaluated uncertainties of a rainfall model and runoff model using the Monte Carlo method, and found that "*the main source of the flood forecast uncertainty is due to uncertainties in the rainfall model and not those in the catchment model.*"

Gourley and Vieux (2003) evaluated the impact of uncertainties in input radar-rainfall data on streamflow simulations in an Oklahoma watershed. They studied the model performance with different precipitation inputs (50%, 75%, 100%, 133%, and 200% of observed values) and model parameter uncertainty

40

using the Generalized Likelihood Uncertainty Estimation (GLUE) method. The authors recommended separation of the error associated with rainfall data and model parameters to determine the statistical significance of each component.

2.4.5 Sensitivity/Uncertainty Studies of the HSPF Model

This section discusses a reviewing of sensitivity and/or uncertainty studies of the HSPF model (see Table 2 for HSPF parameter definition). While the HSPF model has been extensively and successfully tested in different countries since 1980, little work has been done to quantify the effect of land cover datasets, evapotranspiration bias, rainfall spatial variability, channel hydraulic variability (FTABLE database), and parameter uncertainty on streamflow simulations.

Garen and Burges (1981) evaluated parameter error propagation of the SWM, which is the hydrology predecessor to the HSPF model. They assessed error bounds of channel inflow hydrographs for several storm events using two uncertainty approaches, first-order uncertainty analysis and Monte Carlo analysis. The most sensitive parameters were the raingage scaling factor (K1) and the upper zone storage nominal capacity (UZSN). The authors pointed out that the first-order uncertainty analysis did not perform satisfactorily under extreme conditions (a highly nonlinear response of the model) or coefficients of variation greater than 0.25 for most sensitivity parameters.

Jacomino and Fields (1997) performed a sensitivity analysis of thirteen HSPF hydrologic parameters. The AGWRC and AGWS parameters showed the greatest sensitivity. The degree of saturation in the lower zone soil moisture

41

(LZSN, LZS), the volume of the upper soil moisture zone (UZSN, UZS) and the rate infiltration (INFILT) were less significant. The remaining parameters had no detectable effect on model results.

Fontaine and Jacomino (1997) evaluated the sensitivity of HSPF parameters for simulating flow and sediments at the hillslope and watershed levels. In addition, HSPF parameters were evaluated for normal and flood flow scenarios. Table 7 shows the most sensitive HSPF parameters for streamflow simulation found by the authors.

Table 7.   The most sensitive HSPF parameters for streamflow simulation (Fontaine and Jacomino, 1997)

Flow Scenario	Hillslope Level	Watershed Level
Normal	AGWRC	AGWRC
Flood	LZS, AGWRC, LZSN, and UZSN	LZS, AGWRC, and LZSN

Young (2000) tested the effect of rainfall spatial resolution on the HSPF model using radar and raingage data in the Little Washita River experimental watershed, Oklahoma. In addition, the author evaluated the error variance in radar precipitation data, finding high uncertainty for both hydrology and water quality simulations. He concluded that the hydrology simulation for this 600-km^2 watershed with a high density of quality raingages was insensitive to rainfall spatial resolution; however, the use of raingage data showed high uncertainty when sediments and other water quality constituents were simulated. He

42

recommended evaluating the error propagation of rainfall through the model and the variability of other spatial properties (soils, land use).

Al-Abed and Whiteley (2002) tested the HSPF model in a Canadian watershed and a sensitivity-index approach showed that the LZSN parameter was the most sensitive. Doherty and Johnston (2003) performed an uncertainty analysis of nine HSPF parameters (LZSN, UZSN, INFILT, BASETP, AGWETP, LZETP, INTFW, IRC, and AGWRC) using the parameter estimation (PEST) software. The most sensitive parameters were AGWRC and INFILT at the watershed outlet. In addition, the authors found a number of different parameter sets with the same fit between simulated and observed streamflows.

Paul (2003) evaluated the effect of parameter uncertainty on the HSPF model to predict in-stream bacterial concentrations using Monte Carlo and First Order Analysis techniques. He pointed out that hydrologic parameters drive most of the parameter uncertainty in simulated in-stream bacterial concentrations. In addition, he concluded that the simulation of hydrologic processes must be accurate to make a reliable total maximum daily load.

Jia (2004) investigated parameter uncertainties in the HSPF model applying the GLUE approach. An LHS technique was used to generate random multiple parameter sets. Seven hydrologic parameters were evaluated in this project (i.e., LZSN, INFILT, AGWRC, DEEPFR, UZSN, INTFW, and IRC) at the watershed level. After 50,000 HSPF runs, many acceptable parameter sets were identified by the GLUE approach. Information on the total runoff distribution was not available, and wide variations of the total runoff (surface runoff, interflow, and

43

baseflow) were considered acceptable. The author pointed out that many combinations in model parameter sets were equally acceptable (this is called "equifinality" by Beven, 2001) due to the accumulative effects of model structure errors, flow measure errors, and a lack of sufficient data (lack of runoff distribution data at hillslope level).

Wu (2004) assessed the propagation of parameter uncertainty in both HSPF and CE-QUAL-W2 models using First-Order Error Analysis (FOEA). He pointed out that the uncertainty in parameters related to streamflow generation was the main source of variance in simulated nutrient loads. However, when simulated nutrient concentrations were analyzed, some parameters related to hydrologic processes have no significant effect. The author justified this difference by the non-linear relationship between pollutant loads and their concentrations. So, FOEA may not be an appropriate method to analyze propagation of parameter uncertainty in complex models. Wu recommended more analyses between FOEA and Monte Carlo simulation.

Diaz (2004) evaluated the HSPF model in a Caribbean island watershed (Puerto Rico). Based on the results of the sensitivity analysis, the HSPF parameters that most affected the streamflow prediction were AGWRC and INFILT. Diaz et al. (2007) assessed the effect of three land use/land cover datasets on HSPF streamflow simulations. Physical data from the Luxapallila Creek watershed, located in Alabama and Mississippi, were used to set up and evaluate model results. At daily levels, streamflow relative errors between -20.3% and 22.3% were calculated when the three datasets were compared.

44

CHAPTER III

METHODOLOGY

3.1 Study Area

This study used physical data from the Luxapallila Creek watershed (Figure 4). The watershed flows through Fayette, Lamar, Marion, and Pickens counties in Alabama and into Lowndes and Monroe counties in Mississippi. Near the outlet (USGS Station 02443500), the watershed has a drainage area of 1,801 km^2, an average basin slope of 2%, and average annual precipitation (1982 - 2004) of 1,379 mm recorded at the Millport 2E weather station (Figure 5). Seasonal fluctuations in rainfall result in maximum river discharges from January to April and minimum discharges from August to September. Elevation in the study area ranges from 45 to 274 m mean sea level. The USGS Geographic Information Retrieval and Analysis System (GIRAS) land cover developed in the early 1980's is distributed as 73% forest land, 20% agricultural land, 6% wetlands, and 1% other land types (barren, urban, and non-urban), (Figure 6).

45
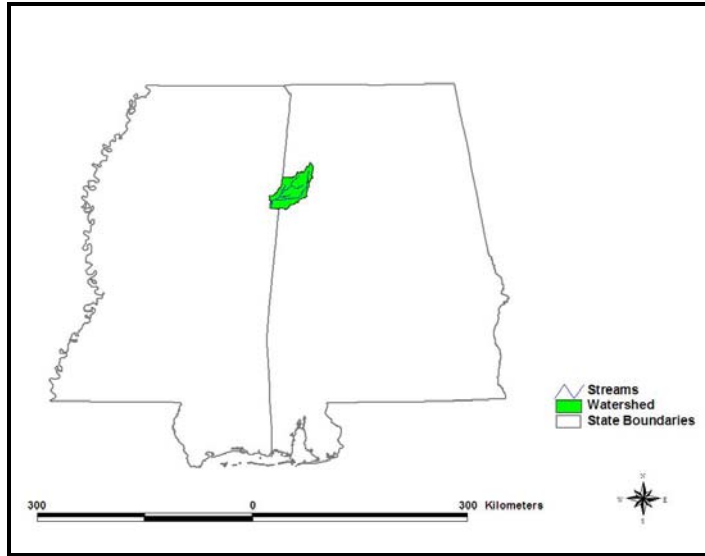
Figure 4.   Location of the Luxapallila Creek watershed
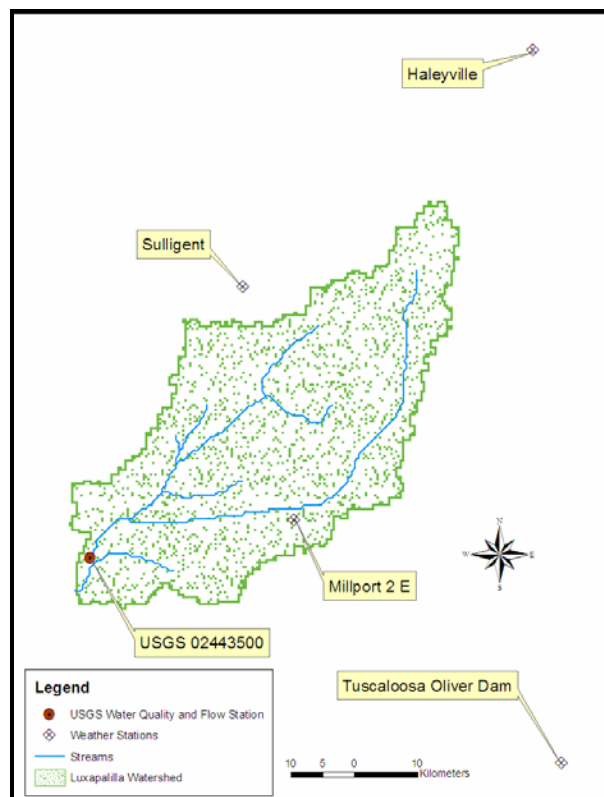
Figure 5.   Location of USGS and weather stations

46
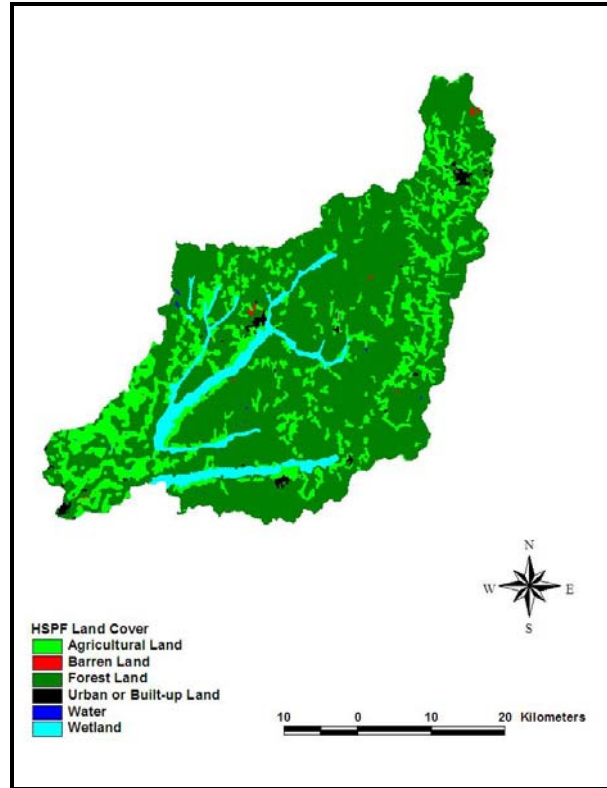
Figure 6.   Land cover distribution

3.2 HSPF Model Setup

The Luxapallila watershed model was set up with a standard set of procedures and data as might be used in any BASINS application to provide a HSPF input data file (uci file). Spatial and climatic time series databases, including land use, overland flow slope and length, reach characteristics, and detailed meteorological data are used as inputs to HSPF.

47

3.2.1 Segmentation of the Model

The model was lumped using one basin area and one main channel because streamflow-gaging station data from only one station were available (USGS 2443500). Topographic data were created from the standard USGS Digital Elevation Models (DEMs), and the DEMs were also used to delineate the watershed boundaries in ArcView. The length and slope of overland flow and reach were calculated and kept constant throughout the simulations. Manning's *n* roughness coefficients for overland flows were determined by literature review and were kept constant throughout the simulations. The watershed was partitioned into six pervious and one impervious land types (Table 8).

Table 8.   Pervious and impervious land types simulated

Land cover	Surface area (km^2)	Surface area (%)
Forest land	1316.9	73.1
Agricultural land	360.0	20.0
Barren land	2.5	0.1
wetlands	104.4	5.8
Urban land (pervious)	8.1	0.4
Urban land (impervious)	8.1	0.4
Water	1.5	0.1

3.2.2 Data Sets Used

Hourly precipitation data were NEXRAD stage IV data from the Earth Observing Laboratory web page (http://data.eol.ucar.edu/codiac/dss/id=21.093). Downloaded rainfall data were uncompressed and incorporated into input files by use of the Watershed Data Management (WDMUtil) software. Hourly potential

48

evapotranspiration, air temperature, dew point, wind speed, solar radiation, evaporation, and cloud cover values were obtained from the Haleyville station (Figure 5). The weather database for the Haleyville station was downloaded from the BASINS web site. The model was run from 01/01/2002 through 12/31/2005. The model time step was hourly, but streamflow data were output daily to compare with observed data (USGS Station 02443500).

3.3 Computational Experiment

This study used a desktop computer with a 3.06GHz Xeon(TM) CPU and 1.00 GB of RAM. A HSPF model of Luxapallila watershed was created using input weather data from 01/01/2002 to 12/31/2005. Input data from 2002 were used to "spin up" the model and limit the effect of initial condition values on the performance of uncertainty methods. This study was focused on developing HSPF certainty bounds under different scenarios. Model performance due to parameter uncertainty was accomplished using 12 HSPF parameters as a lumped modeling approach. Hydraulic property variability of the main channel was done using two different FTABLE databases (USGS versus RF1). Parameter uncertainty and rainfall spatial variability were evaluated using 12 HSPF parameters and seven different sets of NEXRAD data (115, 109, 86, 58, 29, 6, and 2 grid points). Two uncertainty methods were used in this study, the Monte Carlo and Harr methods. The Monte Carlo method using 12 HSPF parameters, USGS FTABLE, and a 115 NEXRAD rainfall grid set was taken as

49

the baseline for comparisons to the rest of the NEXRAD grid sets, RF1 FTABLE,

and Harr method. Four scenarios were explored in this research (Table 9).

Table 9.   Scenarios evaluated

Scenario	Components
Baseline	Monte Carlo method + 12 HSPF parameters + USGS FTABLE + 115 NEXRAD grid points
Hydraulic property variability of the main channel	Monte Carlo method + 12 HSPF parameters + RF1 FTABLE + 115 NEXRAD grid points
Spatial rainfall variability	Monte Carlo method + 12 HSPF parameters + USGS FTABLE + 109/86/58/29/6/2 NEXRAD grid points
Harr method	Harr method + 12 HSPF parameters + USGS FTABLE + 115 NEXRAD grid points

3.3.1 Sources of Uncertainty

This study evaluated three sources of uncertainty propagation on HSPF

model results: hydrologic parameter uncertainty, hydraulic property variability of

the main channel, and rainfall spatial variability.

3.3.1.1 Hydrologic Parameter Uncertainty

Parameter uncertainty was accomplished using 12 HSPF parameters

(Table 10). The range of each HSPF parameter was extracted from the BASINS

Technical Note 6 (USEPA, 2000).

50

Table 10.   HSPF parameter ranges

Parameter (unit)	Definition	Range
LZSN (mm)	Lower zone nominal soil moisture storage	50.8 -381.0
INFILT (mm/hour)	Index to infiltration capacity	0.025 – 12.7
KVARY (1/mm)	Variable groundwater recession	0.0 – 127.0
AGWRC	Base groundwater recession	0.92 - 0.999
DEEPFR	Fraction of groundwater inflow to deep recharge	0.0 - 0.5
BASETP	Fraction of remaining evapotranspiration from baseflow	0.0 - 0.2
AGWETP	Fraction of remaining evapotranspiration from active groundwater	0.0 - 0.2
CEPSC (mm)	Interception storage capacity	0.0 – 10.2
UZSN (mm)	Upper zone nominal soil moisture storage	1.27 – 50.8
INTFW	Interflow inflow parameter	1.0 - 10.0
IRC	Interflow recession parameter	0.3 - 0.85
LZETP	Lower zone evapotranspiration parameter	0.0 - 0.9

3.3.1.2 Hydraulic Property Variability of the Main Channel

The HSPF channel network consisted of one main channel. The HSPF model required a tabular FTABLE with relationships among surface area, volume, and flow in a channel. The hydraulic properties of the main channel were characterized using two approaches: the BASINS reach file (RF1), and USGS cross sectional data at the watershed outlet (USGS station 2443500). Table 11

51

describes the RF1 database. In general, the RF1 dataset is coarse, not updated (data achieved in 1982), and may be used as an initial evaluation on watershed simulation. Table 12 shows the FTABLE results using the RF1 data. This Table was automatically created in the HSPF-BASINS interface.

Table 11.   Description of the RF1 database (USEPA, 2007)

Characteristic	Description
File format	ArcInfo coverage
Source	EPA
Scale	1:500,000
Restrictions	Public domain
Data achieved	1982
Data type	Vector
Map units	Decimal degrees
Projection	Geographic
Remarks	"*Data consist of mean annual flow and 7Q10 low flow estimations made at the downstream ends of more than 60,000 transport reaches coupled to an estimate of the time-of-travel velocity for the full length of those same reaches under each of those two flow regimes… Streamflow data from the USGS Daily Values File for the 4112 gages were used to develop estimates of mean annual flow and 7Q10 flow at the gage sites... EPA has advised users (1983 EPA memo to Regions, States and other RF1 users), that the overall flow estimation methodology used in producing the RF1 flow estimates was not designed to produce accurate results on start reaches or small ungaged tributaries, nor in estuaries or ungaged coastal streams…EPA added that use of these flow values may benefit from an initial evaluation on a basin-wide.*"

52

Table 12.   FTABLE data using the RF1 data

Depth (m)	Surface area (km^2)	Volume (km^3)	Outflow (m^3/s)
0.0	0.0	0.0	0.0
0.3	2.5	6.6	7.6
2.6	2.6	67.2	353.4
3.3	2.7	84.4	512.2
4.1	8.0	149.4	642.6
4.9	8.1	214.9	1170.4
83.9	15.3	9444.2	405438.5
162.9	22.5	24355.5	1503105.3

Table 13 depicts the FTABLE results using the USGS cross sectional data. The USGS has collected 240 surface water measurements (water depth, channel width, and flow) since 1929 to 2006 at station 2443500. All 2140 surface water measurements were clustered by selected percentiles (10th, 20th, 30th, 40th, 50th, 60th, 70th, 80th, 90th, 95th, 98th, 99th and 100th percentiles) and used to calculate the FTABLE columns. Surface area was calculated using the channel width and length. Channel length was calculated as 70 km using the DEMs. Hydraulic properties of the channel at 30.5 m water depth were extrapolated using the previous eight values of the FTABLE in order to ensure that all computed water depths fell within the FTABLE data range.

53

Table 13.   FTABLE data using the USGS cross sectional data

Depth (m)	Surface area (km^2)	Volume (km^3)	Outflow (m^3/s)
0.0	0.0	0.0	0.0
1.9	1.2	22.6	4.2
2.1	1.7	34.9	5.8
2.2	1.9	41.4	9.0
2.3	2.2	51.1	13.9
2.5	2.3	57.0	19.1
2.7	2.8	74.3	27.0
2.8	3.1	86.9	37.5
3.2	3.3	105.1	61.4
4.0	5.3	211.5	213.3
5.4	8.7	464.0	457.0
7.3	14.9	1081.6	667.0
8.5	15.8	1342.6	744.5
9.1	19.4	1733.6	1027.9
30.5	72.8	22200.2	4074.5

Figure 7 depicts water depth versus volume of reach using the USGS data and RF1 data. The curves match relatively closely for values less than 200 km^3. The USGS values were higher than the RF1 data for values larger than 200 km^3. Therefore, the USGS data showed a reservoir type and the RF1 data depicted a channel form. Figure 8 depicts water depth versus outflow at the watershed outlet using the USGS data and RF1 data. Outflow values using the RF1 data were consistently higher than USGS data. In general, use of USGS data resulted in higher water retention times than RF1 data.

54
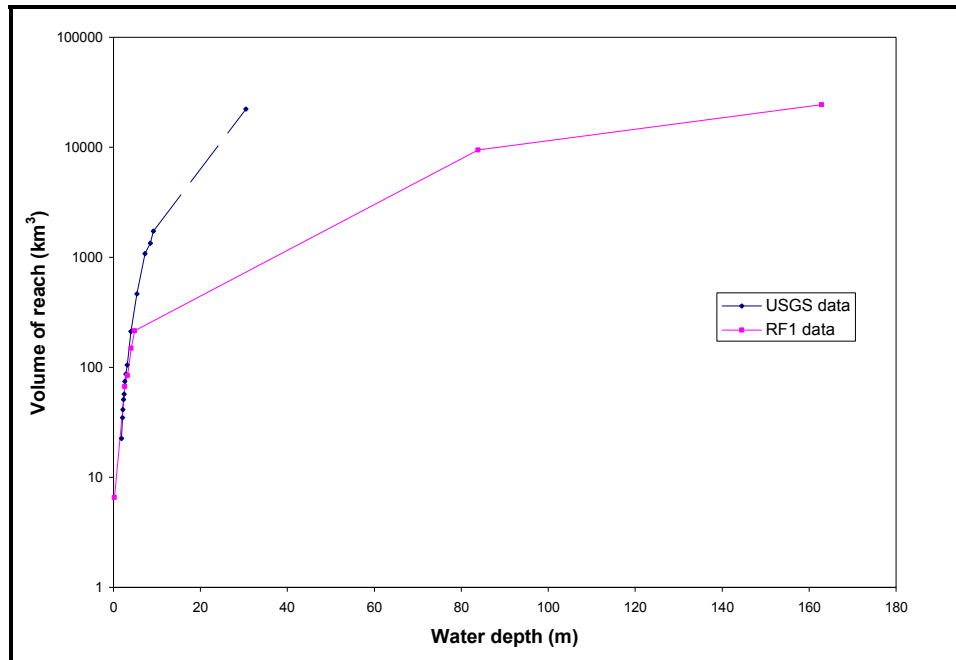
Figure 7.   Water depth versus volume of reach using the USGS data and RF1 data (Y axis on a logarithmic scale)
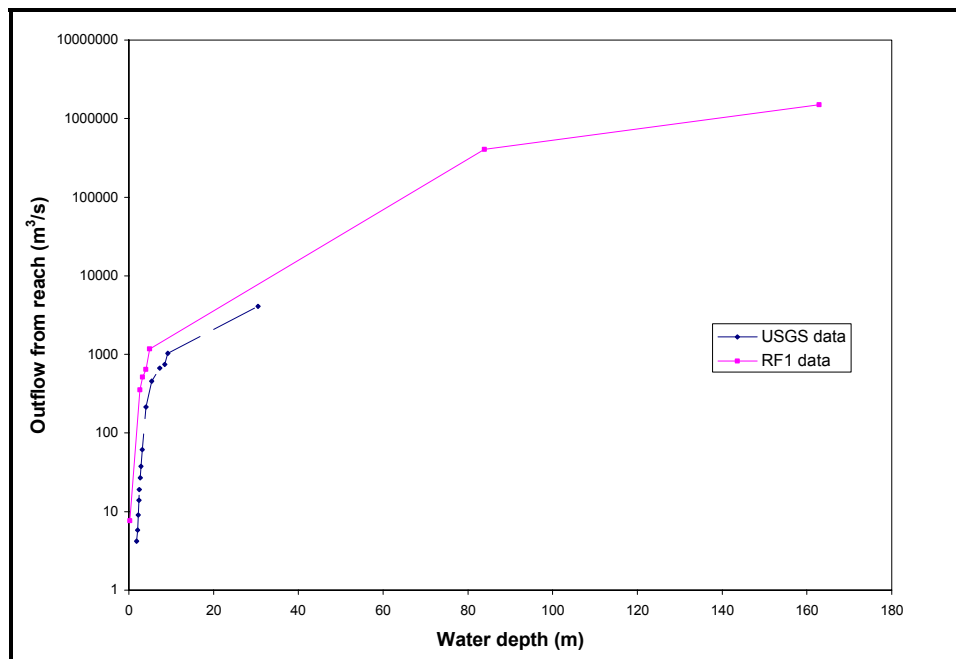
Figure 8.   Water depth versus outflow at the watershed outlet using the USGS data and RF1 data (Y axis on a logarithmic scale)

55

3.3.1.3 Rainfall Spatial Variability

Hourly NEXRAD Stage IV rainfall data at a 4 km resolution were downloaded from the Earth Observing Laboratory web page (http://data.eol.ucar.edu/codiac/dss/id=21.093). The rainfall data period downloaded was from 01/01/2002 to 12/31/2005. Rainfall spatial variability was characterized using seven sets of NEXRAD grid points (115, 109, 86, 58, 29, 6, and 2 grid points). Each grid point of the set had the same weight (1/115, 1/109, 1/86, 1/58, 1/29, 1/6, and 1/2). The time series of 115 radar grid points (4 km x 4 km pixel resolution) were considered as the "ground truth" rainfall pattern (Figure 9). The remaining grid point sets were selected randomly from one to 115 using the Research Randomizer, V3.0 (http://www.randomizer.org/form.htm), with each grid point in a set remaining unique.

Rainfall spatial variability across the seven NEXRAD grid point sets was quantified using the coefficient of variation (*CV*) at daily levels. The *CV* of 115 NEXRAD grid points was used as a baseline to calculate daily relative errors as follows:

$$CV = \frac{\sigma}{\bar{X}} \tag{7}$$

$$RE_{CV} = \frac{CV_{NEXRAD\ set} - CV_{115\ NEXRAD\ set}}{CV_{115\ NEXRAD\ set}} * 100 \tag{8}$$

where σ was the standard deviation of the data, $\bar{X}$ was the mean of the data, RE_{CV} was the relative error, $CV_{NEXRAD\ set}$ was the coefficient of variation of 109,

56

86, 58, 29, 6, or 2 NEXRAD set, $CV_{115\ NEXRAD\ set}$ was the coefficient of variation of 115 NEXRAD set.
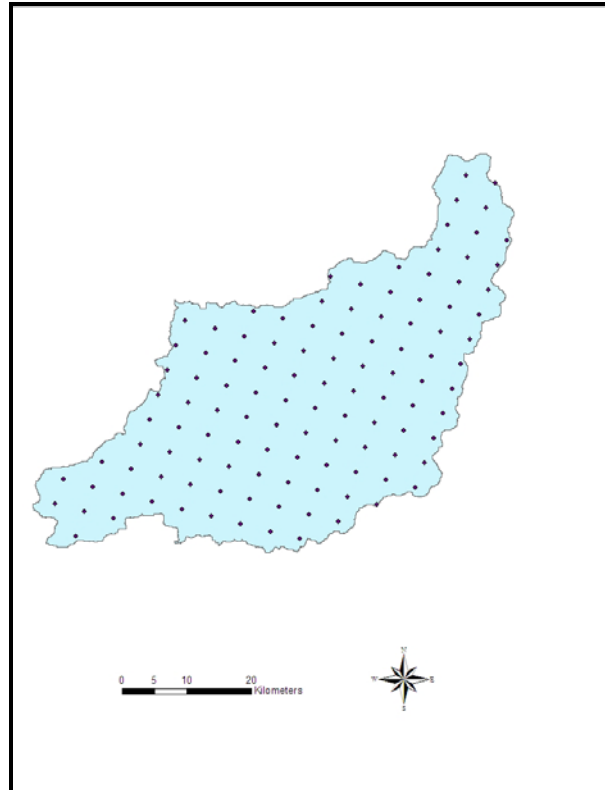
Figure 9.   115 NEXRAD grid points used in Luxapallila Creek HSPF simulations

NEXRAD rainfall data were recorded for 386 days out of 1096 days between 01/01/2003 and 12/31/2005, and the analysis of rainfall spatial variability was focused on these 386 days.

57

3.3.2 Uncertainty Methods

This research explored the performance of two uncertainty methods: the Monte Carlo and Harr methods.

3.3.2.1 Monte Carlo Method

The first step in the Monte Carlo simulation (MCS) was to determine the probability density functions (PDFs) for the input parameters considered in the study. Due to the lack of data to estimate the PDFs, all parameters were assigned a triangular distribution, which is defined by the lowest, most probable, and highest values. Most probable values were extracted from an 18-year model calibration of the Luxapallila Creek watershed (McAnally et al., 2006), (Table 14). Highest and lowest values were assigned based on the EPA BASINS Technical Note 6 (USEPA, 2000), (Table 10).

Table 14.   Most probable values of the HSPF parameters in the Luxapalilla
             Creek model

Parameter (unit)	Most Probable Value
LZSN (mm)	228.6
INFILT (mm/hour)	2.8
KVARY (1/mm)	45.7
AGWRC	0.997
DEEPFR	0.2
BASETP	0.04
AGWETP	0.025
CEPSC (mm)	3.8
UZSN (mm)	27.9
INTFW	3.0
IRC	0.6
LZETP	0.1

58

Five thousand random numbers from the 12 HSPF parameter's distributions (triangular distributions) were generated using the Matlab software. Then, the HSPF program was run using the selected random numbers from 01/01/2002 to 12/31/2005. Finally, evaluation of streamflow simulations was accomplished (stability results, 95th and 5th percentiles) at daily levels with 5,000 streamflow simulations for each simulation day.

To determine the number of realizations (stability results) sufficient to analyze the uncertainty of streamflow simulations, the values of absolute relative errors (*ARE*) of simulated daily flows were calculated as

$$ARE = \sum_{i=1}^{N} \left[\frac{|Q_{i+1} - Q_i|}{Q_i} \right]$$

(9)

where *N* is the number of Monte Carlo simulations; Q_i is the simulated daily flow for run *i*. For instance, in this study, 1,096 daily HSPF streamflows from 01/01/2003 through 12/31/2005 were used; this means that 1,095 *ARE* results were calculated for each Monte Carlo simulation.

3.3.2.2 Harr Method

The first step in the Harr method was to calculate the correlation matrix, mean, and standard deviation of the 12 HSPF parameters evaluated. The USEPA developed a database of HSPF model parameters (USEPA, 2006a). This database was called HSPFParm and contains HSPF parameter values of several model applications in the U.S. Twenty eight sets of parameter values

59

were used to compute the correlation matrix, mean, and standard deviation of selected parameters. Table 15 depicts mean and standard deviation values of selected HSPF parameters. Table 16 shows the correlation matrix of selected HSPF parameters. The eigenvector and eigenvalue matrices from the correlation matrix were calculated using Matlab (Table 17).

Table 15.   Mean and standard deviation values of selected HSPF parameters

Parameter (unit)	Mean	Standard Deviation
LZSN (mm)	146.7	48.0
INFILT (mm/hour)	2.0	1.0
KVARY (1/mm)	24.3	25.4
AGWRC	0.97	0.02
DEEPFR	0.04	0.1
BASETP	0.02	0.02
AGWETP	0.02	0.04
CEPSC (mm)	0.3	0.7
UZSN (mm)	14.8	7.3
INTFW	2.9	1.7
IRC	0.7	0.2
LZETP	0.3	0.3

Table 16.   Correlation matrix of selected HSPF parameters

	LZSN	INFILT	KVARY	AGWRC	DEEPFR	BASETP
LZSN	1.0	0.1	0.6	-0.2	-0.1	0.2
INFILT	0.1	1.0	0.1	0.2	0.5	-0.1
KVARY	0.6	0.1	1.0	-0.3	0.0	0.3
AGWRC	-0.2	0.2	-0.3	1.0	0.1	-0.6
DEEPFR	-0.1	0.5	0.0	0.1	1.0	-0.1
BASETP	0.2	-0.1	0.3	-0.6	-0.1	1.0
AGWETP	0.3	0.1	0.5	-0.2	0.1	0.7
CEPSC	0.0	0.6	-0.3	0.1	0.0	0.2
UZSN	0.4	0.1	0.6	0.0	-0.1	0.0
INTFW	0.1	0.0	0.3	-0.1	-0.3	-0.1
IRC	-0.3	-0.2	-0.2	-0.1	-0.2	-0.2
LZETP	0.4	0.3	0.6	-0.5	0.0	0.2

60

Table 16. Correlation matrix of selected HSPF parameters (continued)

	AGWETP	CEPSC	UZSN	INTFW	IRC	LZETP
LZSN	0.3	0.0	0.4	0.1	-0.3	0.4
INFILT	0.1	0.6	0.1	0.0	-0.2	0.3
KVARY	0.5	-0.3	0.6	0.3	-0.2	0.6
AGWRC	-0.2	0.1	0.0	-0.1	-0.1	-0.5
DEEPFR	0.1	0.0	-0.1	-0.3	-0.2	0.0
BASETP	0.7	0.2	0.0	-0.1	-0.2	0.2
AGWETP	1.0	0.3	0.1	-0.1	-0.5	0.1
CEPSC	0.3	1.0	0.0	-0.1	-0.5	0.0
UZSN	0.1	0.0	1.0	0.4	-0.2	0.4
INTFW	-0.1	-0.1	0.4	1.0	0.2	0.6
IRC	-0.5	-0.5	-0.2	0.2	1.0	0.1
LZETP	0.1	0.0	0.4	0.6	0.1	1.0

Table 17. Matrix of eigenvalues and eigenvectors of selected HSPF parameters

	Eigenvalues					
	3.3	2.3	1.9	1.3	1.1	0.7
Parameter	Eigenvectors					
LZSN	0.4	0.0	0.0	0.3	0.1	-0.7
INFILT	0.1	-0.4	0.5	-0.3	0.0	-0.2
KVARY	0.5	0.1	0.1	0.2	0.3	0.1
AGWRC	-0.3	-0.2	0.4	0.4	0.0	0.1
DEEPFR	0.0	-0.3	0.2	-0.2	0.7	0.2
BASETP	0.3	-0.1	-0.5	-0.2	-0.1	0.1
AGWETP	0.3	-0.3	-0.3	0.1	0.1	0.3
CEPSC	0.1	-0.5	0.1	-0.2	-0.5	-0.1
UZSN	0.3	0.1	0.3	0.4	-0.1	0.2
INTFW	0.2	0.4	0.3	-0.2	-0.4	0.4
IRC	-0.2	0.4	0.0	-0.4	0.1	-0.2
LZETP	0.4	0.2	0.2	-0.4	0.0	-0.1

61

Table 17.   Matrix of eigenvalues and eigenvectors of selected HSPF
            parameters (continued)

	Eigenvalues					
	0.5	0.4	0.3	0.2	0.1	0.0
Parameter	Eigenvectors					
LZSN	0.1	-0.1	-0.4	-0.2	-0.2	0.1
INFILT	0.1	0.1	0.3	0.3	-0.3	0.4
KVARY	0.2	-0.2	0.4	0.3	-0.2	-0.5
AGWRC	0.5	0.0	-0.3	0.3	0.3	-0.1
DEEPFR	-0.2	0.1	-0.4	-0.2	-0.1	-0.2
BASETP	0.0	0.3	-0.4	0.6	0.0	0.0
AGWETP	0.5	0.0	0.1	-0.4	0.0	0.3
CEPSC	0.0	0.1	0.0	-0.3	0.0	-0.6
UZSN	-0.3	0.7	0.1	-0.1	0.1	0.1
INTFW	0.0	-0.3	-0.4	-0.1	-0.4	0.1
IRC	0.5	0.5	0.0	-0.2	-0.1	-0.2
LZETP	0.0	-0.2	0.0	0.0	0.8	0.0

The model runs required to solve the system were 2**number of parameters*. In this study, 12 parameters were evaluated; thus 24 model HSPF runs were required to solve the system. Using Tables 15 and 17, and equations 6a and 6b (see section 2.4.2.2 in methodology), the coordinates of the 24 intersection points by each HSPF parameter were calculated (Table 18). This Table shows that 16% of the data were outside of the pre-established parameter ranges (highlighted). Data out of ranges were changed by the closest limit value (Table 19). Finally, using these 24 sets of parameters to determine the 95th and 5th percentiles of model outputs, the 90% certainty bounds (95th-5th percentiles) were calculated at daily levels from 01/01/2003 to 12/31/2005.

62

Table 18.   Coordinates of the 24 intersection points by each HSPF parameter

Eigenvalue	3.3		2.3		1.9		1.3	
Parameter	X^+	X^-	X^+	X^-	X^+	X^-	X^+	X^-
LZSN	8.171	3.381	5.962	5.591	5.915	5.638	7.794	3.759
INFILT	0.0942	0.0645	0.0326	0.126	0.145	0.0141	0.0366	0.122
KVARY	2.574	-0.659	1.442	0.473	1.183	0.733	1.482	0.434
AGWRC	0.955	0.991	0.961	0.985	0.998	0.948	1.003	0.943
DEEPFR	0.0356	0.0470	-0.0658	0.148	0.124	-0.0410	-0.0394	0.122
BASETP	0.0480	-0.00656	0.00803	0.0334	-0.0223	0.0637	0.00474	0.0367
AGWETP	0.0662	-0.0160	-0.0143	0.0646	-0.0116	0.0619	0.0325	0.0178
CEPSC	0.0202	0.00573	-0.0375	0.0635	0.0228	0.00317	-0.00571	0.0317
UZSN	0.898	0.266	0.686	0.478	0.878	0.286	0.985	0.179
INTFW	4.150	1.692	4.974	0.868	4.637	1.204	2.037	3.805
IRC	0.642	0.849	0.967	0.524	0.753	0.737	0.560	0.931
LZETP	0.627	-0.103	0.430	0.0944	0.470	0.0539	-0.0728	0.597

Table 18.   Coordinates of the 24 intersection points by each HSPF parameter (continued)

Eigenvalue	1.1		0.7		0.5		0.4	
Parameter	X^+	X^-	X^+	X^-	X^+	X^-	X^+	X^-
LZSN	6.205	5.348	1.070	10.483	6.525	5.027	5.074	6.478
INFILT	0.0786	0.0800	0.0551	0.104	0.0970	0.0616	0.0903	0.0684
KVARY	1.931	-0.0160	1.371	0.544	1.528	0.387	0.327	1.589
AGWRC	0.970	0.976	0.983	0.964	1.009	0.938	0.971	0.975
DEEPFR	0.279	-0.197	0.107	-0.0248	-0.0233	0.106	0.0674	0.0152
BASETP	0.0133	0.0281	0.0285	0.0130	0.0234	0.0181	0.0489	-0.008
AGWETP	0.0341	0.0161	0.0661	-0.0159	0.0902	-0.0400	0.0226	0.0276
CEPSC	-0.0405	0.0664	0.00107	0.0249	0.0116	0.0144	0.0244	0.00157
UZSN	0.518	0.646	0.754	0.410	0.315	0.849	1.276	-0.112
INTFW	0.714	5.128	5.425	0.417	3.088	2.754	1.434	4.408
IRC	0.792	0.699	0.659	0.831	1.018	0.473	1.000	0.491
LZETP	0.268	0.256	0.179	0.345	0.288	0.236	0.128	0.397

63

Table 18. Coordinates of the 24 intersection points by each HSPF parameter (continued)

Eigenvalue	0.3		0.2		0.1		0.0	
Parameter	X^+	X^-	X^+	X^-	X^+	X^-	X^+	X^-
LZSN	3.203	8.349	4.748	6.804	4.427	7.126	6.127	5.425
INFILT	0.115	0.0436	0.125	0.0340	0.0429	0.116	0.138	0.0211
KVARY	2.464	-0.548	1.826	0.090	0.198	1.717	-0.880	2.796
AGWRC	0.954	0.993	0.994	0.953	0.992	0.954	0.964	0.983
DEEPFR	-0.104	0.186	-0.025	0.107	0.00841	0.0741	-0.029	0.112
BASETP	-0.013	0.0545	0.0726	-0.031	0.0206	0.0209	0.0174	0.0241
AGWETP	0.0369	0.0134	-0.031	0.0811	0.0280	0.0223	0.0655	-0.015
CEPSC	0.0158	0.0101	-0.015	0.0404	0.0107	0.0152	-0.043	0.0691
UZSN	0.643	0.521	0.459	0.705	0.664	0.500	0.679	0.485
INTFW	0.542	5.299	2.506	3.336	0.613	5.228	3.267	2.575
IRC	0.749	0.742	0.667	0.824	0.680	0.811	0.656	0.834
LZETP	0.218	0.307	0.240	0.285	0.933	-0.409	0.272	0.252

Table 19. Corrected coordinates of the 24 intersection points by each HSPF parameter

Eigenvalue	3.3		2.3		1.9		1.3	
Parameter	X^+	X^-	X^+	X^-	X^+	X^-	X^+	X^-
LZSN	8.171	3.381	5.962	5.591	5.915	5.638	7.794	3.759
INFILT	0.094	0.064	0.033	0.126	0.145	0.014	0.037	0.122
KVARY	2.574	0.000	1.442	0.473	1.183	0.733	1.482	0.434
AGWRC	0.955	0.991	0.961	0.985	0.998	0.948	0.999	0.943
DEEPFR	0.036	0.047	0.000	0.148	0.124	0.000	0.000	0.122
BASETP	0.048	0.000	0.008	0.033	0.000	0.064	0.005	0.037
AGWETP	0.066	0.000	0.000	0.065	0.000	0.062	0.032	0.018
CEPSC	0.020	0.006	0.000	0.063	0.023	0.003	0.000	0.032
UZSN	0.898	0.266	0.686	0.478	0.878	0.286	0.985	0.179
INTFW	4.150	1.692	4.974	1.000	4.637	1.204	2.037	3.805
IRC	0.642	0.849	0.850	0.524	0.753	0.737	0.560	0.850
LZETP	0.627	0.000	0.430	0.094	0.470	0.054	0.000	0.597

64

Table 19.   Corrected coordinates of the 24 intersection points by each HSPF parameter (continued)

Eigenvalue	1.1		0.7		0.5		0.4	
Parameter	X^+	X^-	X^+	X^-	X^+	X^-	X^+	X^-
LZSN	6.205	5.348	1.070	10.483	6.525	5.027	5.074	6.478
INFILT	0.079	0.080	0.055	0.104	0.097	0.062	0.090	0.068
KVARY	1.931	0.000	1.371	0.544	1.528	0.387	0.327	1.589
AGWRC	0.970	0.976	0.983	0.964	0.999	0.938	0.971	0.975
DEEPFR	0.279	0.000	0.107	0.000	0.000	0.106	0.067	0.015
BASETP	0.013	0.028	0.028	0.013	0.023	0.018	0.049	0.000
AGWETP	0.034	0.016	0.066	0.000	0.090	0.000	0.023	0.028
CEPSC	0.000	0.066	0.001	0.025	0.012	0.014	0.024	0.002
UZSN	0.518	0.646	0.754	0.410	0.315	0.849	1.276	0.050
INTFW	1.000	5.128	5.425	1.000	3.088	2.754	1.434	4.408
IRC	0.792	0.699	0.659	0.831	0.850	0.473	0.850	0.491
LZETP	0.268	0.256	0.179	0.345	0.288	0.236	0.128	0.397

Table 19.   Corrected coordinates of the 24 intersection points by each HSPF parameter (continued)

Eigenvalue	0.3		0.2		0.1		0.0	
Parameter	X^+	X^-	X^+	X^-	X^+	X^-	X^+	X^-
LZSN	3.203	8.349	4.748	6.804	4.427	7.126	6.127	5.425
INFILT	0.115	0.044	0.125	0.034	0.043	0.116	0.138	0.021
KVARY	2.464	0.000	1.826	0.090	0.198	1.717	0.000	2.796
AGWRC	0.954	0.993	0.994	0.953	0.992	0.954	0.964	0.983
DEEPFR	0.000	0.186	0.000	0.107	0.008	0.074	0.000	0.112
BASETP	0.000	0.055	0.073	0.000	0.021	0.021	0.017	0.024
AGWETP	0.037	0.013	0.000	0.081	0.028	0.022	0.066	0.000
CEPSC	0.016	0.010	0.000	0.040	0.011	0.015	0.000	0.069
UZSN	0.643	0.521	0.459	0.705	0.664	0.500	0.679	0.485
INTFW	1.000	5.299	2.506	3.336	1.000	5.228	3.267	2.575
IRC	0.749	0.742	0.667	0.824	0.680	0.811	0.656	0.834
LZETP	0.218	0.307	0.240	0.285	0.933	0.000	0.272	0.252

3.3.3 Performance Evaluation

The overall effect of parameter uncertainty, hydraulic property variability of the main channel, and rainfall spatial variability through streamflow simulations was demonstrated calculating the 5th and 95th percentiles (90% certainty

65

bounds) of the Monte Carlo results. Two criteria were used to evaluate the HSPF 90% certainty bounds:

- *Reliability*: the number or percentage of daily observed streamflows within the HSPF 90% certainty bounds;

- *Sharpness*: the width of the HSPF 90% certainty bounds (minimum, median, and maximum values).

The HSPF 90% confidence intervals were evaluated using daily observed flow data from 01/01/2003 to 12/31/2005 at the watershed outlet (USGS station 02443500). Three percentile classes of observed flows developed by the USGS (http://water.usgs.gov/waterwatch/) were calculated to find the effect of model *Reliability* to above normal, normal, and below normal flows (Table 20).

Table 20.   Percentile classes of flow observed data

Percentile classes	Explanation
>75th	Above normal
25th-75th	Normal
<25th	Below normal

In addition to the *Reliability* and *Sharpness* criteria, continuous hydrographs of 90% confidence bounds and observed data were plotted. Scatterplots were drawn of 5th and 95th flow percentiles using the baseline scenario as compared to the remaining scenarios.

66

Evaluation of the Harr method was accomplished in the same form for the remaining scenarios (calculating the 95th and 5th percentiles of model outputs, and *Reliability* and *Sharpness* criteria). To compare the baseline scenario results versus the remaining scenario results (see Table 9 for scenario description), the relative error of *Reliability ($RE_{Reliability}$)* and *Sharpness ($RE_{Sharpness}$)* criteria values was calculated as follows:

$$RE_{\mathrm{Re}\,liability}(\%) = \frac{(\mathrm{Re}\,liability)_{selected\ scenario} - (\mathrm{Re}\,liability)_{baseline}}{(\mathrm{Re}\,liability)_{baseline}} *100 \tag{10}$$

$$RE_{Sharpness}(\%) = \frac{(Sharpness)_{selected\ scenario} - (Sharpness)_{baseline}}{(Sharpness)_{baseline}} *100 \tag{11}$$

CHAPTER IV

RESULTS

4.1 Sources of Uncertainty

This section shows results of three sources of uncertainty propagation on streamflow simulations using the Monte Carlo method: parameter uncertainty, hydraulic property variability of the main channel, and spatial rainfall variability. See Table 9 in methodology for scenario description.

4.1.1 Baseline Scenario

The baseline scenario depicts results of the Monte Carlo simulation using 5,000 random samples from 12 HSPF parameters and 115 NEXRAD rainfall stations.

4.1.1.1 Stability Results of the Monte Carlo Method

Figure 10 shows the relationship between absolute relative errors (*ARE*) of simulated daily flows and number of Monte Carlo simulations - MCS (see equation 9 in methodology). Each line in Figure 10 represents one simulation day between 01/01/2003 and 12/31/2005. This Figure reveals that the *ARE* values

68

were close between runs 2,000 and 5,000. In general, higher MCS yielded lower *ARE* results.
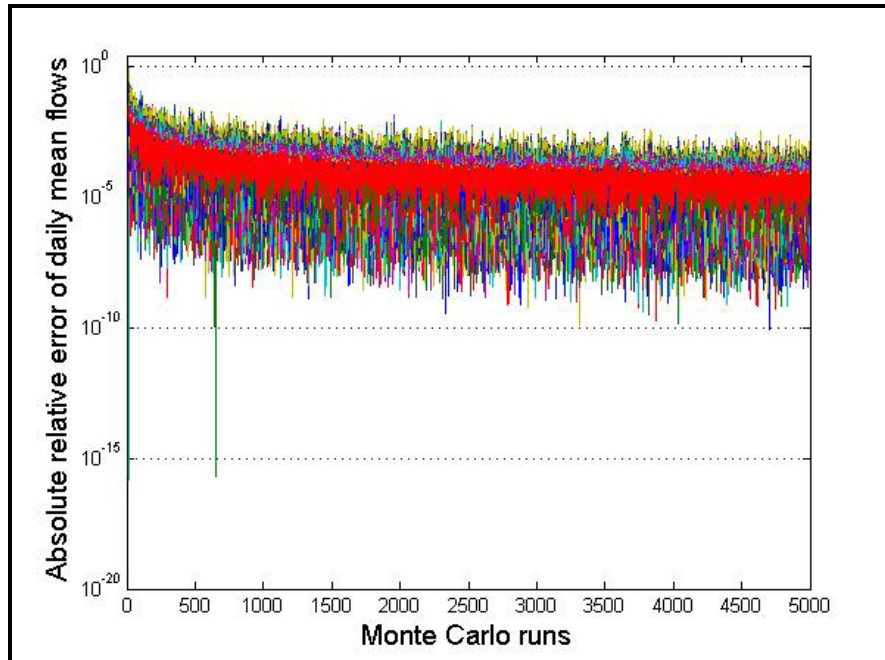
Figure 10.   Stability of results using Monte Carlo method with Y-axis on a logarithmic scale

Table 21 depicts the minimum, median, and maximum values of *ARE* by selected MCS. This Table shows that the median *ARE* values from 3,000 to 5,000 MCS were close. It took approximately 12 hours of CPU time to produce 5,000 simulations of the Luxapallila watershed model (with 115 NEXRAD grid points, one hour time step, and time simulation between 01/01/2002 and 12/31/2005) using a desktop computer with a 3.06GHz Xeon(TM) CPU and 1.00 GB of RAM. The best fit equation describing the relationship between the median *ARE - MARE* and the number of MCS was a power regression (*MARE* = 0.29 x

69

MCS$^{-1.04}$). The resulting power regression depicted a coefficient of determination equal to 0.99, meaning 99% of variability in *MARE* values can be explained by the variability in MCS results. The power regression showed that to decrease the *MARE* by one order of magnitude from 7E^{-05} to 4E^{-06}, 50,000 MCS and 120 hours of CPU time are required. Therefore, 5,000 MCS, a *MARE* value of 7E^{-05}, and 12 hours of CPU time were considered sufficient for the purpose of this research.

Table 21.   Minimum, median, and maximum values of *ARE* by selected Monte Carlo simulations

MCS	Minimum *ARE*	Median *ARE*	Maximum *ARE*
2	4E^{-04}	2E^{-01}	2E^{+00}
10	2E^{-06}	2E^{-02}	9E^{-02}
100	3E^{-06}	2E^{-03}	1E^{-02}
1,000	2E^{-07}	2E^{-04}	1E^{-03}
2,000	5E^{-08}	1E^{-04}	6E^{-04}
3,000	9E^{-08}	5E^{-05}	4E^{-04}
4,000	1E^{-07}	5E^{-05}	3E^{-04}
5,000	5E^{-07}	7E^{-05}	2E^{-04}

4.1.1.2 Parameter Uncertainty

Confidence intervals for HSPF simulated daily streamflows at the watershed outlet were generated using the 5th and 95th percentiles after 5,000 MCS (Table 22). From the bounds constructed for the period 01/01/2003 to 12/31/2005, the *Reliability* and median *Sharpness* of the HSPF streamflow simulations were 65.4% and 16.1 m^3/s, respectively. Thus, 65.4% of the daily observed data within the 90% confidence bounds (*Reliability*), and the median width of the 90% certainty bounds was 16.1 m^3/s (*Sharpness*).

70

Table 22.   Results of the Monte Carlo simulations for daily flows

Year	Observed flows under the 5th percentile (%)	*Reliability* (%)	Observed flows over the 95th percentile (%)
2003	5.2	61.6	33.2
2004	4.1	71.6	24.3
2005	1.1	63.0	35.9
2003-2005	3.5	65.4	31.1

Median annual observed flows at the USGS station 2443500 for 2003, 2004, and 2005 were 27.8 m^3/s, 20.4 m^3/s, and 19.2 m^3/s, respectively. Previous flows compared to the 90% certainty bounds in Table 22 showed that the percentage of model *Reliability* was greater for the two low median annual flows than for the highest median annual flow. Observed streamflow data were 31.1% over the 95th percentile and 3.5% below the 5th percentile. Therefore, uncertainty on model results was higher in the upper level of certainty bounds than the lower level of certainty bounds. The median error of the observed flows over the simulated 95th percentile was 6.8 m^3/s. The median error of the observed flows below the simulated 5th percentile was 2.6 m^3/s. Median errors, 6.8 m^3/s and 2.6 m^3/s, compared to the median observed flow between 2003 and 2005 (i.e., 23.2 m^3/s) were 29.3% and 11.4%, respectively. Therefore, observed flows out of the 90% certainty bounds were near to the bounds, especially for the 5th percentile bound.

Results of the model *Reliability* by observed flow percentiles are shown in Table 23. This table depicts that the greater the observed flow the poorer the HSPF performance. The model had a very good performance for below normal

71

flows (<25th percentile), but the poorest performance was for above normal flows (>75th percentile).

Table 23.   Results of the model *Reliability* by observed flow percentiles (2003-2005)

Observed flow percentiles	Observed flows within 90% certainty bounds (%)
<25th	92.3
25th-75th	60.2
>75th	48.2

The HSPF parameters evaluated in this study and related to storm flows (above normal flows) were as follows: index to infiltration capacity (INFILT), interflow inflow parameter (INTFW), and interflow recession parameter (IRC), (see Table 2 in literature review). The INFILT parameter is related to Soil Conservation Service (SCS) hydrologic soil groups (A, B, C, and D). The physical range of the INFILT parameter is between 0.025 mm/h and 12.7 mm/h (see Table 10 in methodology). Interflow from surface detention storage is controlled by the INTFW parameter, which has a range from 1.0 to 10.0. The IRC is the ratio of the current daily interflow discharge to the interflow discharge on the previous day; it ranges from 0.35 to 0.85. The INFILT parameter showed the highest interval value with the highest variability (three orders of magnitude).

Figures 11, 12, and 13 show the HSPF certainty bounds of the daily hydrograph for 2003, 2004, and 2005, respectively. Observed streamflow variations were closely tracked by the certainty bounds, and most of the

72

observed daily flows were located within or very near the HSPF certainty bounds. Fifth flow percentiles were usually lower than observed flows. Certainty bounds were narrow when rising limbs started (February/2003, May/2003, and December/2004). Peak flows showed the highest uncertainty (wide certainty bounds), for example, February/2003, May/2003, February and December/2004. These certainty bounds incorporated the uncertainty derived from input time series (rainfall and evapotranspiration), model structure (hydraulic routing uses the kinematic wave theory), model conceptualization (one basin, one main channel, seven pervious and impervious areas), and model parameterization (length and slope of overland flow)

Figure 11.   Daily observed hydrographs and certainty bounds estimated by the MCS for 2003

73

Figure 12.   Daily observed hydrographs and certainty bounds estimated by
the MCS for 2004
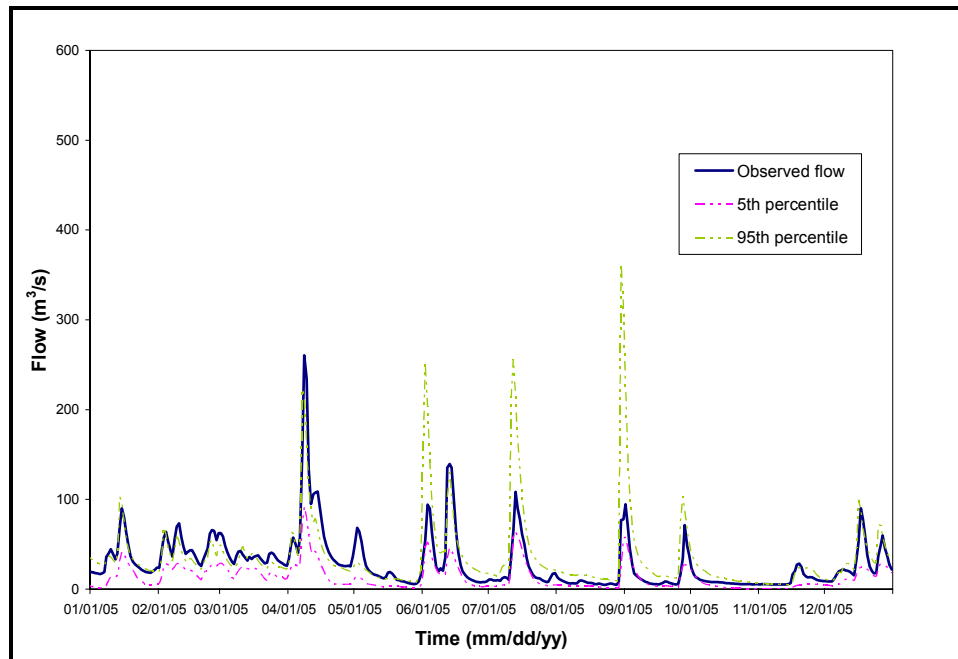
Figure 13.   Daily observed hydrographs and certainty bounds estimated by
the MCS for 2005

74

Selected storm events are shown in Figures 14-19. Figure 14 indicates that most of the observed storm events for February-March of 2003 were within the 90% certainty bounds; however, a few weeks before and after this time period, the observed flows were constantly over the 95th flow percentile. Figure 15 illustrates that most of the observed flows were within the simulated certainty bounds for the summer of 2003. Figure 16 depicts that the peak and recession limbs of the 95th flow percentile were delayed at least one day as compared with the observed flows; however, the rising limb of the highest event was mostly within the 90% certainty bounds. Figure 17 shows fairly well simulated 90% certainty bounds for rising and recession limbs, but the observed peak flow was over the 95th percentile. Figure 18 indicates that the rising limbs of the 90% certainty bounds were fairly well simulated; however, the observed peak flow and recession limb were ahead of the 90% certainty bounds by one day. Figure 19 depicts that the observed data were contained well within the 90% certainty bounds for the period of June to August 2005. In general, most of the observed flow data were close or within the HSPF certainty bounds. However, some observed peaks and recession limbs were ahead of the HSPF certainty bounds, possibly as a consequence of the following: the use of coarse data (only one USGS station) for the calculation of the storage-release relationships of the main channel (FTABLE); rainfall conceptualization (radar data rather than gage data); and/or wetland area conceptualization (simulated as a pervious area instead of a high water table area). Additional analyses of the HSPF certainty bounds, with respect to the conceptualization of the hydrology and hydraulic processes of the

75

Luxapallila Creek watershed, are required to determine the off shift of the model

simulations.
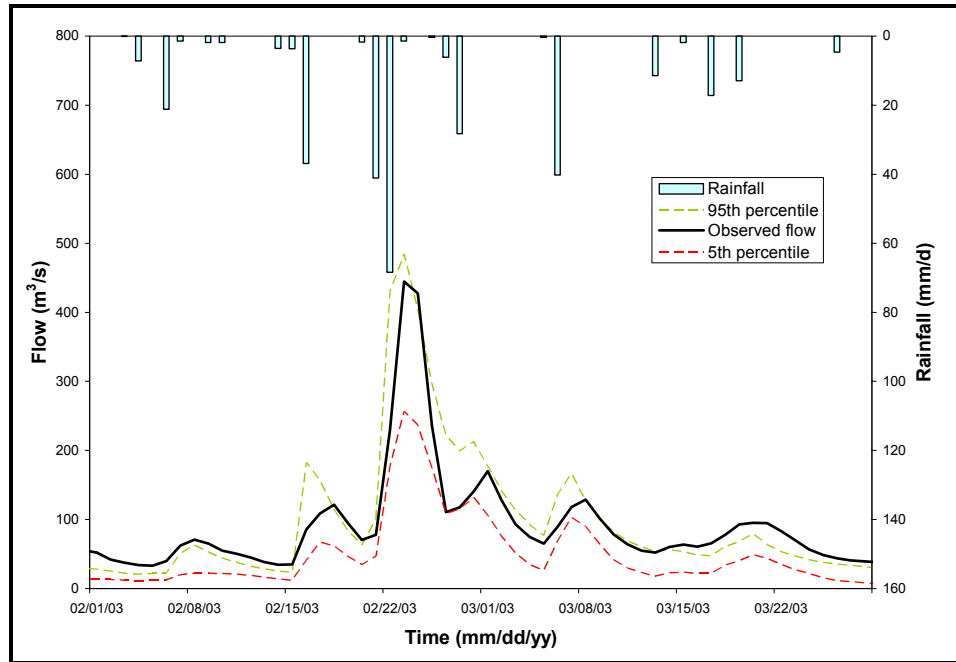
Figure 14.   Daily observed hydrographs and certainty bounds estimated by the
MCS for February-March/2003
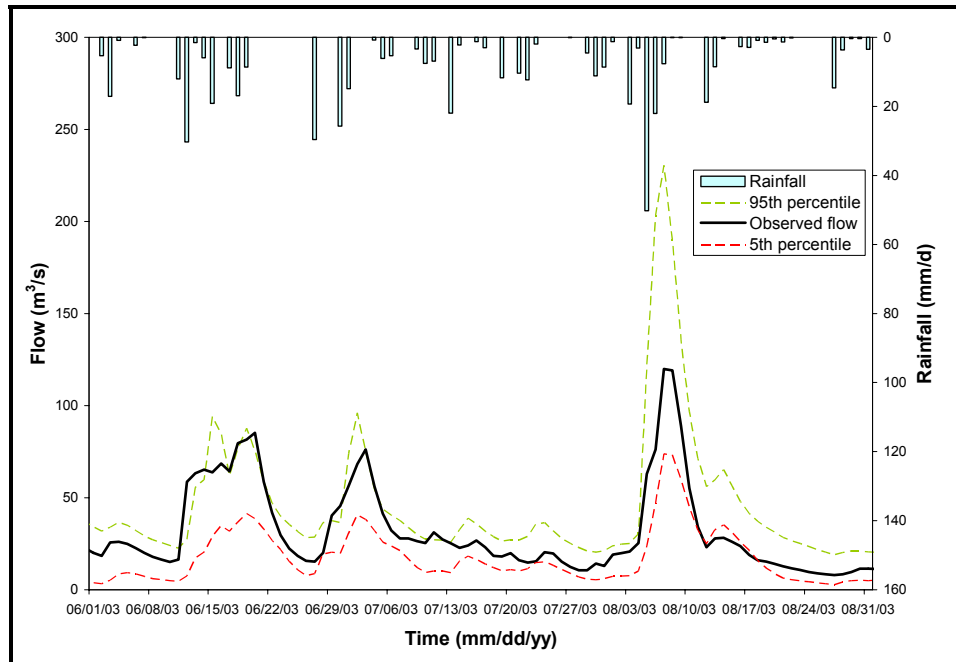
Figure 15.   Daily observed hydrographs and certainty bounds estimated by the MCS for June-August/2003
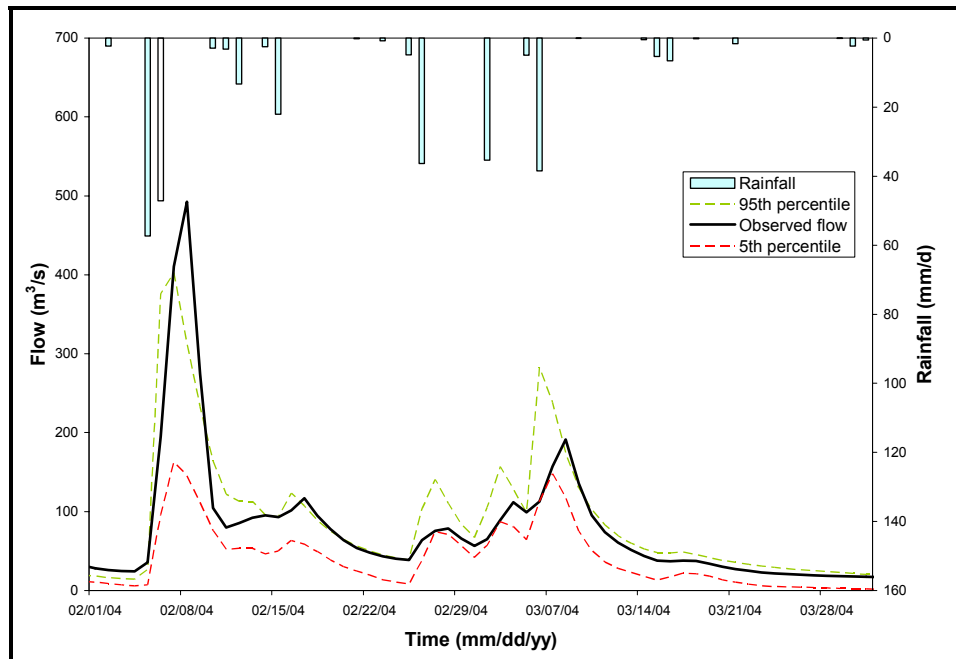
Figure 16.   Daily observed hydrographs and certainty bounds estimated by the MCS for February-March/2004

77
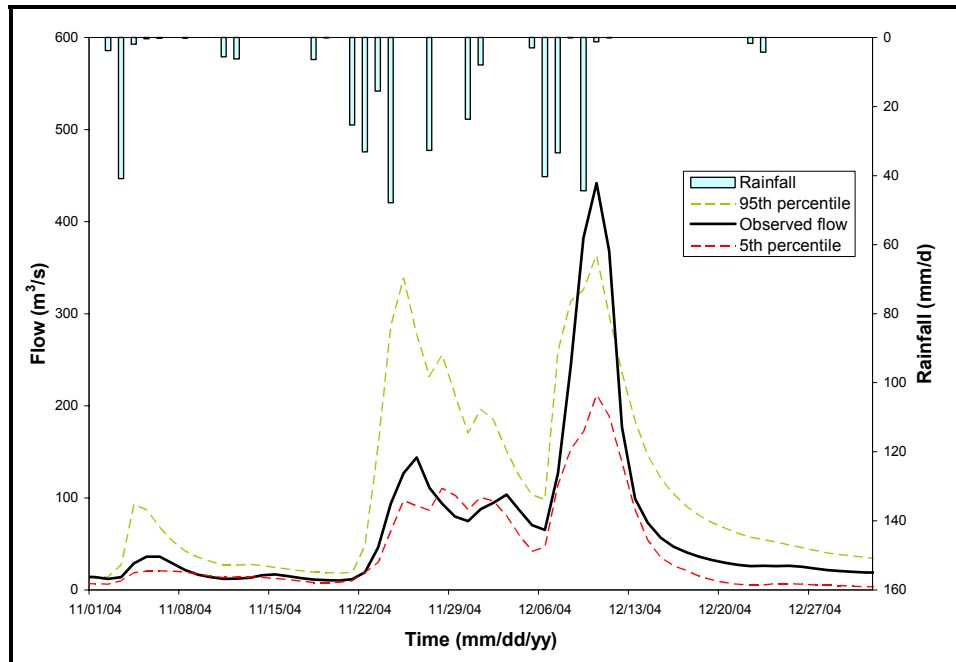
Figure 17.   Daily observed hydrographs and certainty bounds estimated by the MCS for November-December/2004
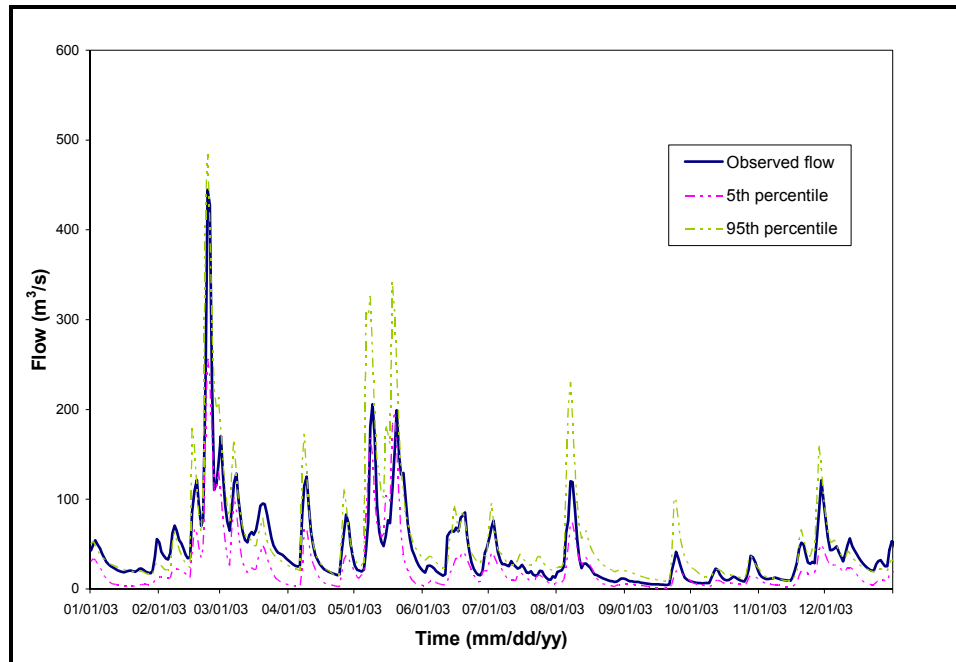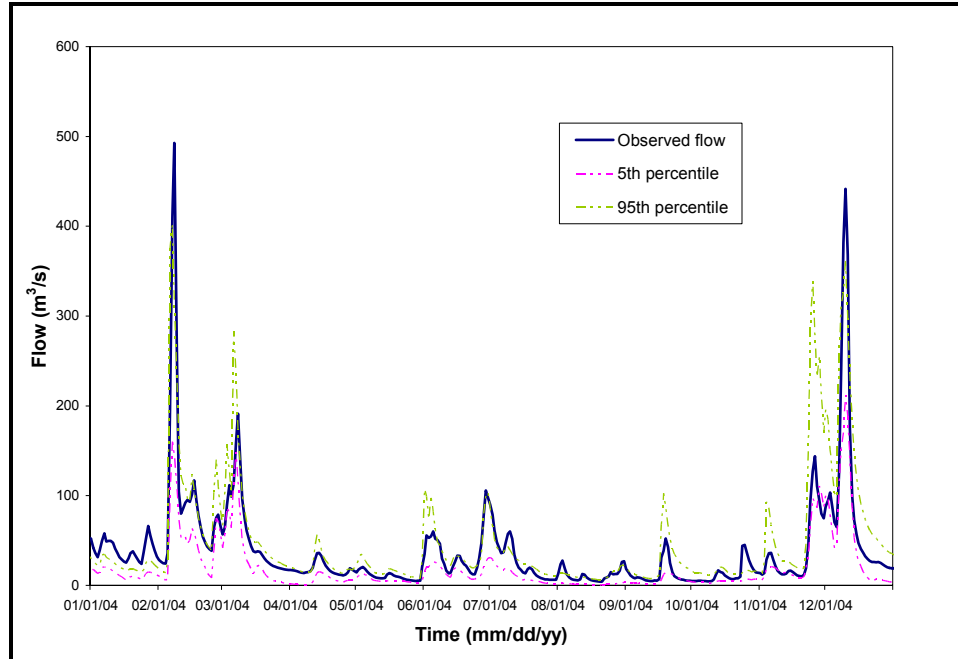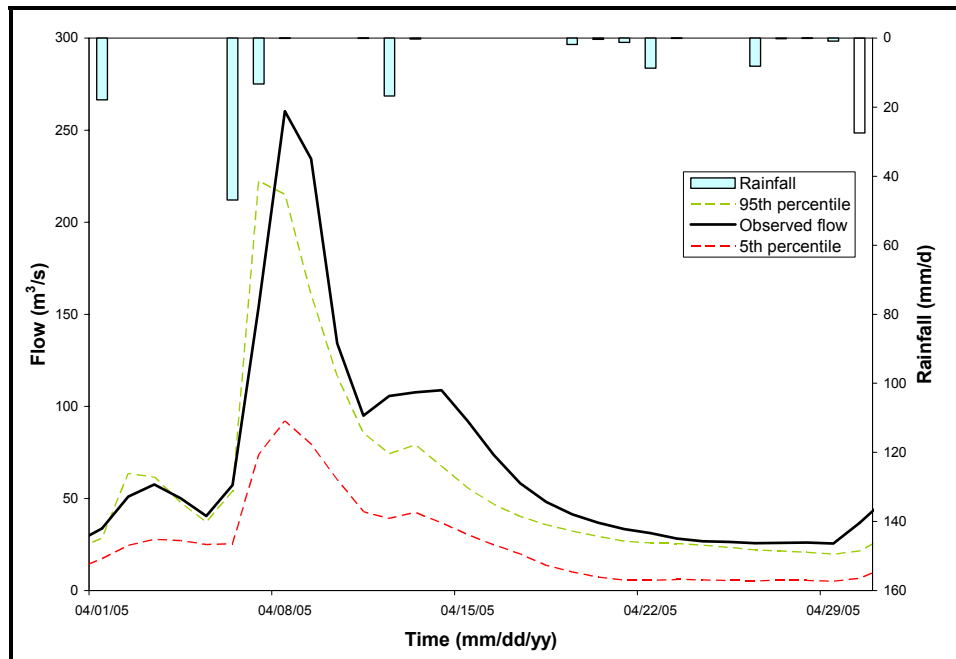

Figure 18.   Daily observed hydrographs and certainty bounds estimated by the MCS for April/2005

78
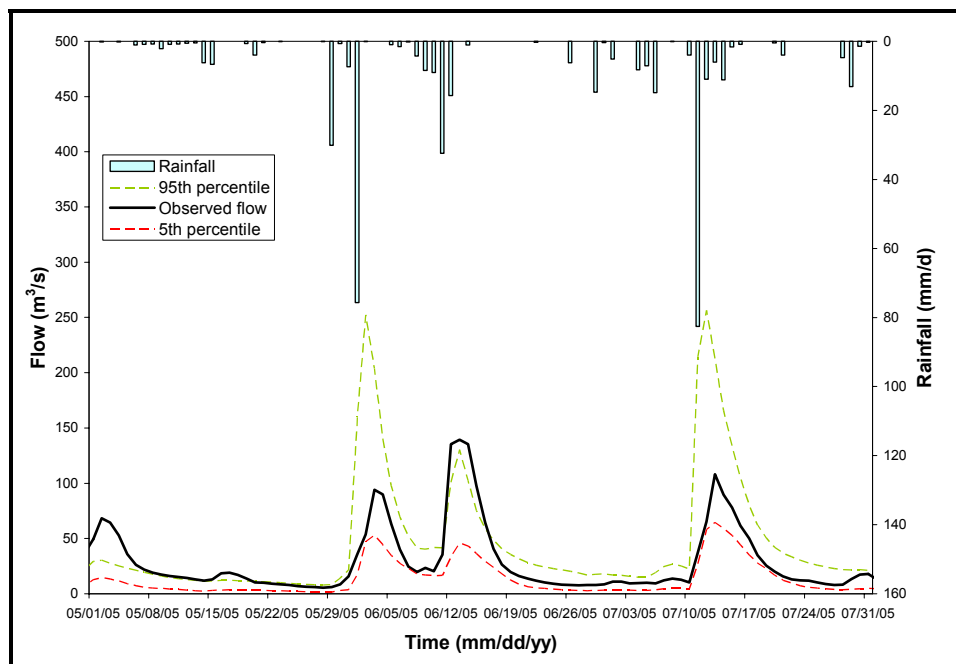
Figure 19.   Daily observed hydrographs and certainty bounds estimated by the MCS for May-July/2005

Table 24 depicts selected percentiles of the model *Sharpness* and observed flow. This table showed that the higher the observed flow, the higher the wide of certainty bounds (*Sharpness*). Additionally, the model *Sharpness* results were in the same order of magnitude as the observed data.

Table 24.   Selected percentiles of the model *Sharpness* and observed flows

Percentile	Model *Sharpness* (m^3/s)	Observed flow (m^3/s)
Minimum	4.8	4.2
25th	10.8	11.4
50th	16.2	23.2
75th	27.0	45.3
Maximum	336.7	492.7

79

4.1.2 Hydraulic Property Variability of the Main Channel

This scenario evaluated the RF1 FTABLE database rather than the USGS FTABLE database used in the baseline scenario (see Table 9 in methodology). Model *Reliability* resulting from both FTABLE databases are presented in Table 25. Relative error analysis of Table 25 showed underestimation of observed flows within the 90% certainty bounds by 6.0% when the RF1 FTABLE database was used.

Table 25.   Model *Reliability* results using the baseline and RF1 FTABLE scenarios (2003-2005)

Baseline scenario (%)	RF1 FTABLE scenario (%)	Relative error (%)
65.4	61.5	-6.0

Model *Reliability* results using the baseline and RF1 FTABLE scenarios by selected observed flow percentiles are shown in Table 26. The HSPF model results, using the RF1 FTABLE database, consistently underestimated observed flows within the 90% certainty bounds. The lowest and highest relative errors (see equation 10 in methodology) were -0.8% and -23.4%, respectively. Both scenarios calculated close results for normal and below normal flows. A large difference was calculated for above normal flows.

80

Table 26.   Model *Reliability* results using the baseline and RF1 FTABLE
            scenarios by selected observed flow percentiles (2003-2005)

Observed flow percentiles	Baseline scenario (%)	RF1 FTABLE scenario (%)	Relative error (%)
<25th	92.3	91.6	-0.8
25th-75th	60.2	58.4	-3.0
>75th	48.2	36.9	-23.4

Figures 20-25 show comparisons of certainty bounds using the baseline
and RF1 FTABLE scenarios for selected storms. The certainty bounds calculated
by both scenarios differ considerably from one another. All of the certainty
bounds of peak flows using the RF1 FTABLE database were higher than those of
estimated with the baseline scenario. Most of the certainty bounds of storm
events estimated with the RF1 FTABLE database were behind the baseline
scenario results by at least one day.

81
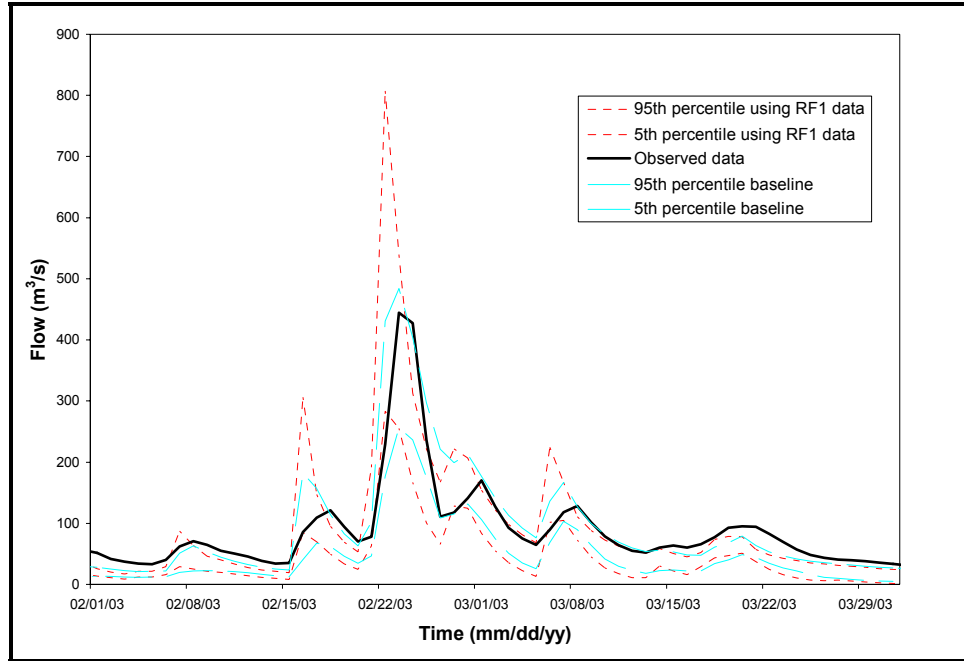
Figure 20.   Daily observed hydrographs and certainty bounds estimated by the baseline scenario and RF1 FTABLE scenario for February-March/2003
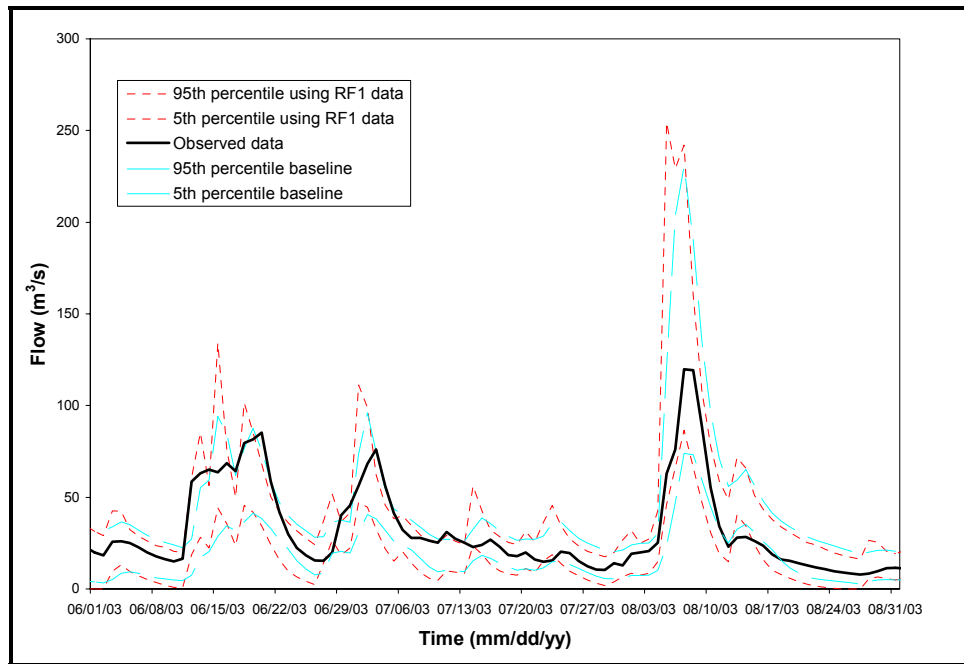
Figure 21.   Daily observed hydrographs and certainty bounds estimated by the baseline scenario and RF1 FTABLE scenario for June-August/2003

82
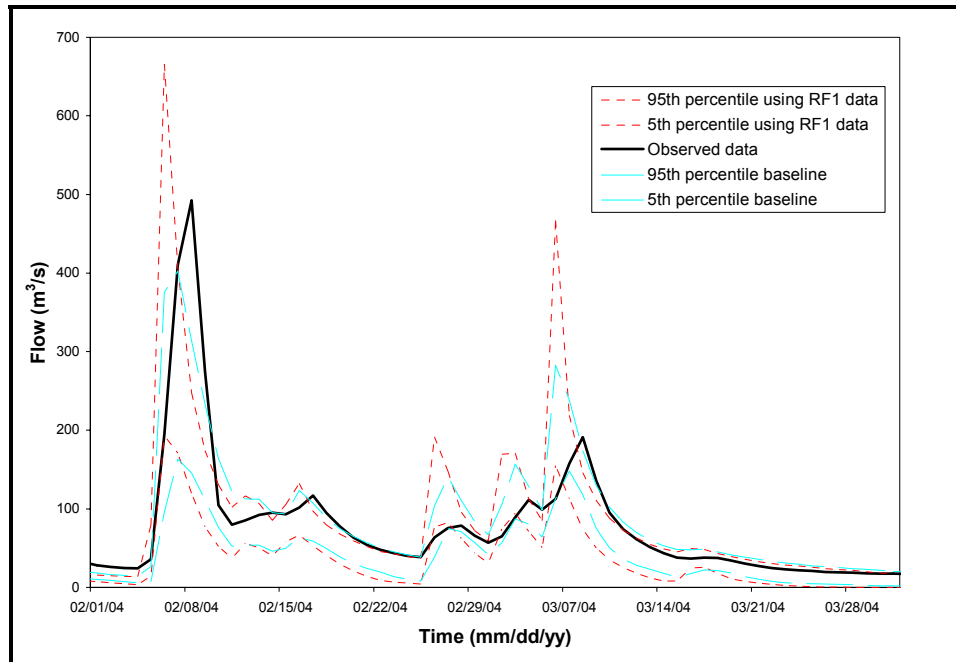
Figure 22. Daily observed hydrographs and certainty bounds estimated by the baseline scenario and RF1 FTABLE scenario for February-March/2004
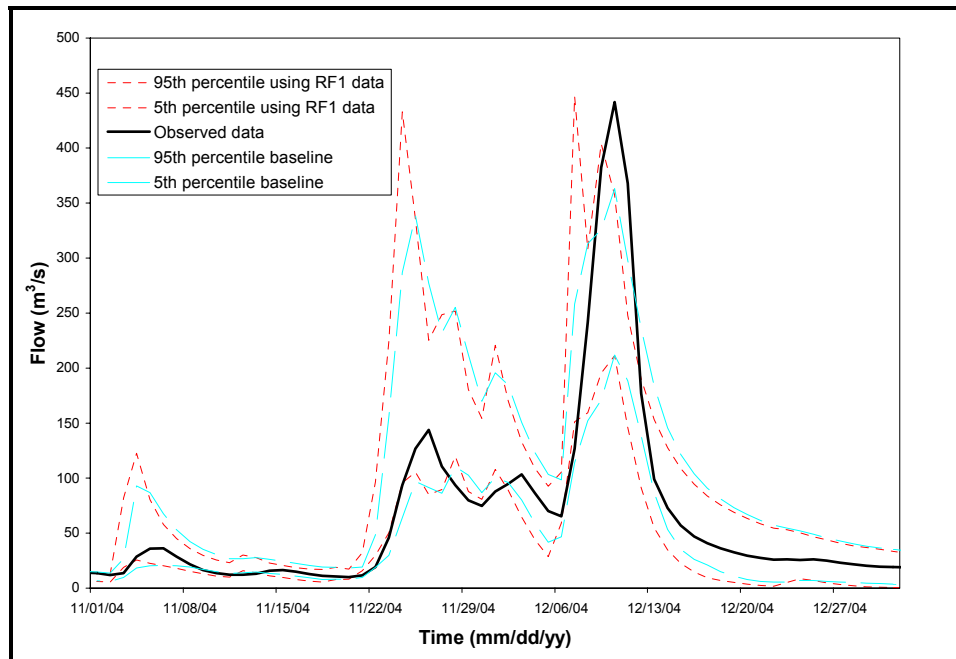
Figure 23. Daily observed hydrographs and certainty bounds estimated by the baseline scenario and RF1 FTABLE scenario for November-December/2004

83
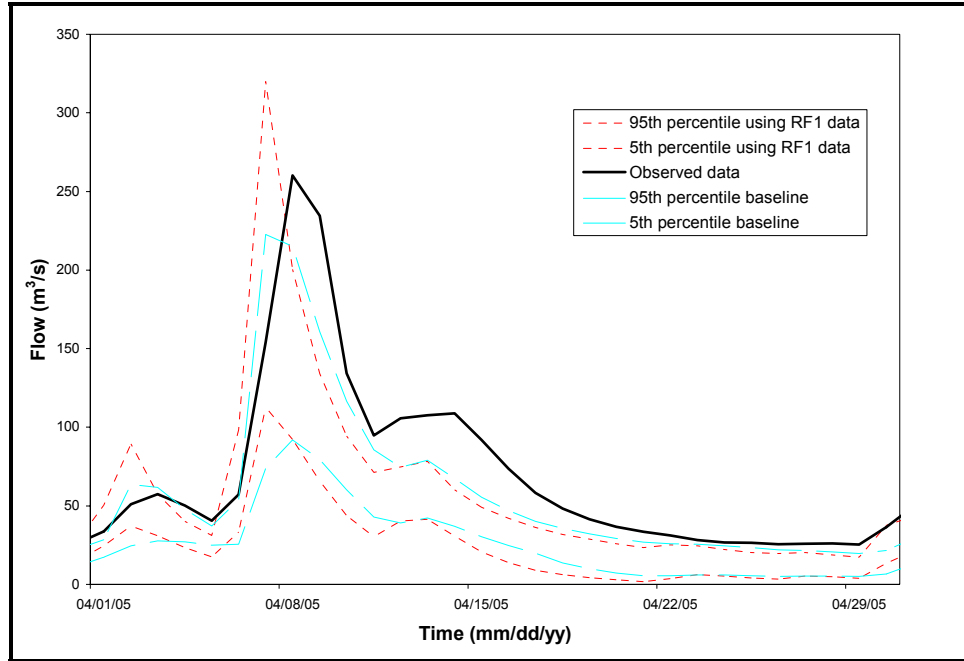
Figure 24.   Daily observed hydrographs and certainty bounds estimated by the
baseline scenario and RF1 FTABLE scenario for April/2005
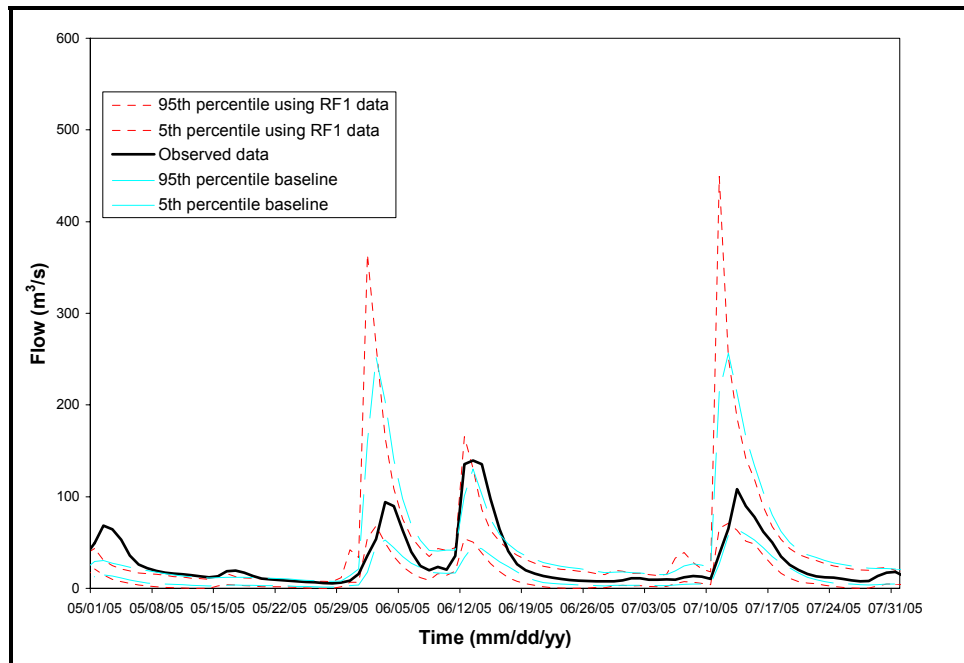
Figure 25.   Daily observed hydrographs and certainty bounds estimated by the
baseline scenario and RF1 FTABLE scenario for May-July/2005

84

Table 27 depicts selected percentiles of the model *Sharpness* (width of the 90% certainty bounds) using the baseline and RF1 FTABLE scenarios. The RF1 FTABLE scenario overestimated the model *Sharpness* for most of the percentiles. When both time series (1,096 days) of the model *Sharpness* were compared, the minimum, median, and maximum relative errors (see equation 11 in methodology) were -29.3%, 3.7%, and 373.1%, respectively. These results showed a large range of relative errors, but the median relative error was close to zero (Figure 26). Figure 27 shows relative error of model *Sharpness* versus observed flows. In this Figure, most of the values were clustered between -25% and 25% of relative errors and observed flows lower than 100 m^3/s. In general, any tendency was found when the model *Sharpness* using both scenarios was compared. However, high differences in some selected days (overpredicted flows using RF1 FTABLE in observed normal flows) were found.

Table 27.   Selected percentiles of the model *Sharpness* using the baseline and RF1 FTABLE scenarios

Percentile	Baseline scenario (m^3/s)	RF1 FTABLE scenario (m^3/s)
Minimum	4.8	4.3
25th	10.8	11.6
50th	16.2	17.3
75th	27.0	29.3
Maximum	336.7	627.6

85
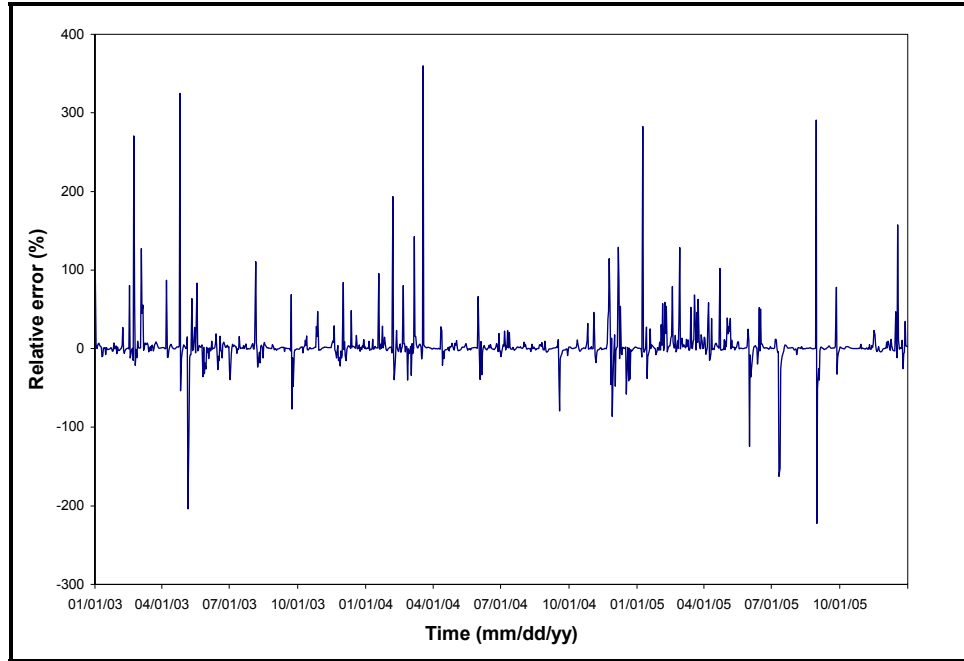
Figure 26.   Relative error of model *Sharpness* using the baseline and RF1
              FTABLE scenarios
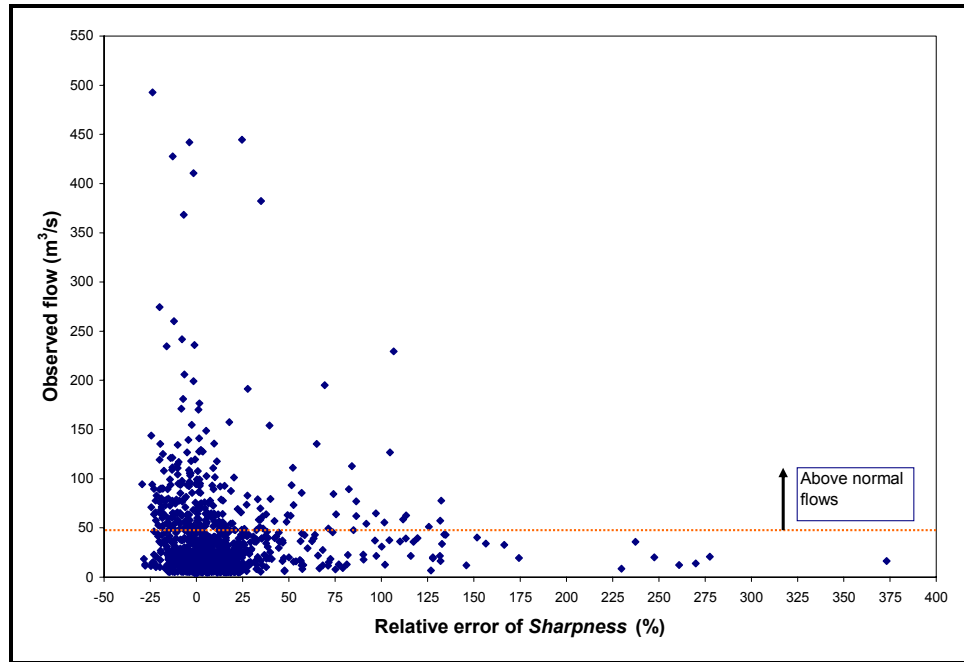
Figure 27.   Relative error of model *Sharpness* using the baseline and RF1
              FTABLE scenarios versus observed flow

86

In summary, the model *Sharpness* using the baseline scenario and RF1 scenario differ significantly from one another (most of relative errors were calculated between -25% and 25%). Model *Reliability* differences were more marked for above normal flows than for normal and below normal flows. Flow peak certainty bounds calculated using the RF1 scenario were consistently higher than the baseline scenario results. The baseline scenario certainty bounds showed higher water retention times than the RF1 FTABLE scenario results. Most of the certainty bounds of storm events estimated by the RF1 FTABLE database were behind of the baseline scenario results by at least one day.

4.1.3 Spatial Rainfall Variability

This section evaluated the spatial rainfall variability on the Luxapallila Creek watershed and its propagation on model results. NEXRAD rainfall data from 01/01/2003 to 12/31/2005 were used in this study.

4.1.3.1 Analysis of NEXRAD Data

Spatial rainfall variability was studied using seven different sets of grid points of NEXRAD data (115, 109, 86, 58, 29, 6, and 2 grid points). NEXRAD rainfall data were recorded for 386 out of 1096 days between 01/01/2003 and 12/31/2005, so analysis of rainfall spatial variability focused on these 386 days. The coefficient of variation of daily rainfall values by selected percentiles is showed in Table 28. There was a large range of coefficient of variation for the daily rainfall values among NEXRAD grid point sets (1.3% to 454.5%). The

87

baseline set of NEXRAD data (115 grid points) showed a high range of rainfall spatial variability among percentiles in the Luxapallila Creek watershed. There was no consistent pattern of variation from 115 grid points through 29 grid points; however, the coefficient of variation decreased for 6 grid points and 2 grid points. The 2 NEXRAD grid points showed the lowest spatial rainfall variation of the system.

Table 28.   Coefficient of variation (%) for daily rainfall values by selected percentiles, 2003-2005

Percentile	115 grid points	109 grid points	86 grid points	58 grid points	29 grid points	6 grid points	2 grid points
0th	10.5	10.4	10.0	9.8	10.5	7.7	1.3
5th	18.5	18.0	18.2	17.8	18.7	14.6	7.0
25th	36.5	36.1	36.5	36.0	36.0	33.3	21.4
50th	66.3	67.2	68.1	66.7	66.4	59.3	47.1
75th	121.8	123.9	123.6	123.0	126.8	108.3	105.7
95th	200.4	200.3	197.5	202.3	222.4	189.2	141.4
100th	295.9	296.3	301.4	359.7	454.5	244.9	141.4

Table 29 depicts selected percentiles of relative errors of daily NEXRAD rainfall coefficient of variation between 115 grid points and selected grid point sets (RE_{CV}). Negative RE_{CV} indicated lower spatial rainfall variability of the NEXRAD set evaluated (see equation 8 in methodology). Median RE_{CV} values were close to zero when 115 NEXRAD grid points were compared to 109, 86, 58, and 29 NEXRAD grid points. RE_{CV} values were greater when the number of NEXRAD grid points being evaluated was lower. The largest RE_{CV} values were calculated using 2 NEXRAD grid points. In general, rainfall percentiles lower than

50th showed decreased rainfall spatial variability with a decreasing number of NEXRAD grid points. However, for rainfall percentiles higher than 50th, the tendency was increased spatial rainfall variability due to a decreasing number of NEXRAD grid points.

Table 29.   Relative errors of daily NEXRAD rainfall coefficient of variation between 115 grid points and the remaining sets (%)

Percentiles	109 grid points	86 grid points	58 grid points	29 grid points	6 grid points	2 grid points
0th	-17.9	-14.8	-26.7	-40.0	-71.0	-97.4
5th	-4.0	-7.0	-14.0	-18.6	-50.9	-85.0
25th	-1.6	-1.5	-6.0	-6.9	-27.3	-54.7
50th	-0.1	1.2	-0.7	1.1	-6.0	-24.2
75th	1.3	3.7	3.8	9.4	14.0	6.5
95th	2.6	7.3	12.3	27.3	41.0	70.5
100th	4.7	15.1	25.1	60.5	86.1	155.0

4.1.3.2 Propagation of Spatial Rainfall Variability on Model Results

Again, the percentile analysis of model *Reliability* showed a decreasing trend with increasing observed flows (Table 30). There was no consistent pattern of variation among sets of rainfall grid points. The set of 2 NEXRAD grid points showed the poorest performance for below normal and normal flows. The set of 6 NEXRAD grid points showed the poorest performance for above normal flows.

Table 30. Flow percentile analysis of model *Reliability* due to spatial rainfall variability (%)

Flow percentiles	115 grid points	109 grid points	86 grid points	58 grid points	29 grid points	6 grid points	2 grid points
<25th	92.3	92.3	92.7	92.3	91.2	90.1	84.3
25th-75th	60.2	60.6	60.0	60.4	58.8	56.4	54.0
>75th	48.2	47.8	47.8	47.8	46.0	42.3	45.6

Table 31 shows percentile analysis of model Sharpness due to spatial rainfall variability. The model *Sharpness* results using only 2 NEXRAD grid points were markedly different from those results using the remaining NEXRAD data sets (115, 109, 86, 58, 29, and 6 grid points). Minimum, median, and maximum relative errors between 115 grid points and 2 NEXRAD grid points were -87.2%, -9.0%, and 132.8%, respectively. A negative relative error means lower model *Sharpness* using 2 rather than 115 NEXRAD grid points.

Table 31. Percentile analysis of model *Sharpness* due to spatial rainfall variability (%)

Percentiles	115 grid points	109 grid points	86 grid points	58 grid points	29 grid points	6 grid points	2 grid points
Minimum	4.8	4.8	4.8	4.8	4.8	4.9	4.4
25th	10.8	10.7	10.7	10.9	10.6	11.0	9.0
50th	16.2	16.1	16.1	16.2	15.9	16.4	14.4
75th	27.0	27.0	26.9	27.5	26.7	27.5	25.3
Maximum	336.7	330.4	330.2	360.4	346.2	391.5	307.3

Figures 28 and 29 show scatterplots of the 5th flow percentiles using 115 grid points versus 109, 86, 58, and 29 grid points and versus 6 and 2 grid points, respectively, for the 2003-2005 period. The points clustered along the 1:1 line

90

are shown in Figure 28. It was clear from Figure 29 that the flow points clustered along a 1:1 line for values lower than 50 m^3/s, but they were not clustered for flow values greater than 50 m^3/s. In addition, flows estimated using 2 and 6 grid points presented a tendency of underestimating and overestimating flows greater than 50m^3/s, respectively. Figures 30 and 31 show scatterplots of the 95th flow percentiles using 115 grid points versus 109, 86, 58, and 29 grid points and versus 6 and 2 grid points, respectively, for the 2003-2005 period. These graphs showed the same trends as Figures 28 and 29.
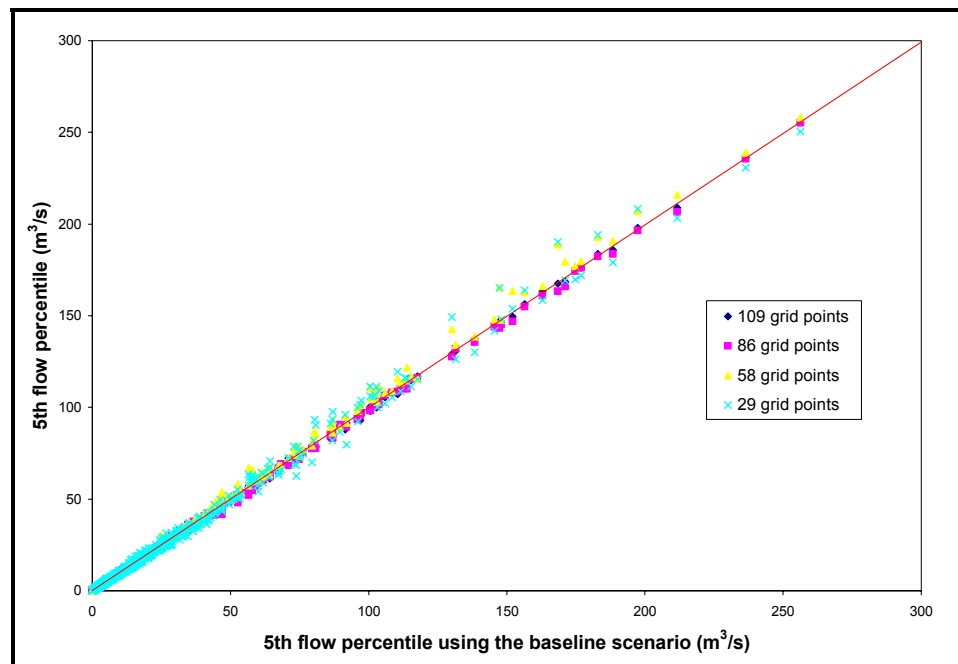
Figure 28.   Scatterplot of 5th flow percentiles using 115 grid points versus 109, 86, 58, and 29 grid points (2003-2005)

91
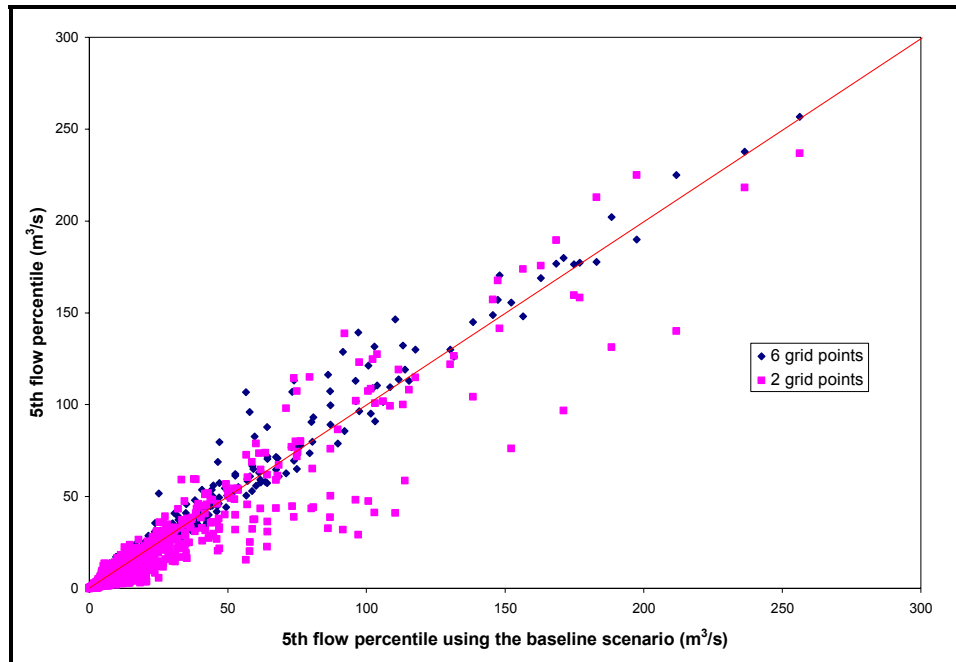
Figure 29. Scatterplot of 5th flow percentiles using 115 grid points versus 6 and 2 grid points (2003-2005)
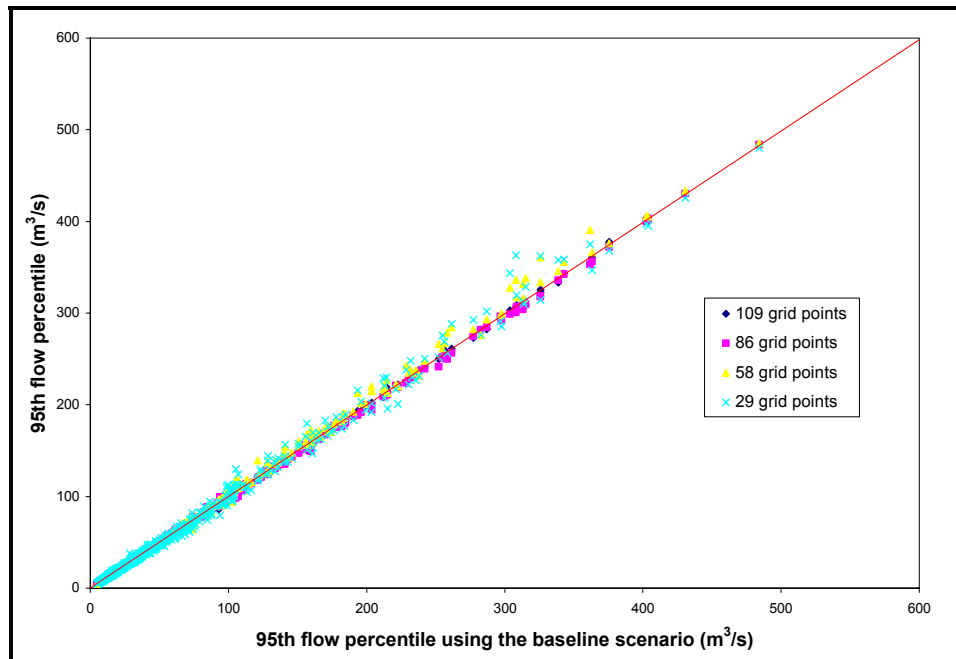
Figure 30. Scatterplot of 95th flow percentiles using 115 grid points versus 109, 86, 58, and 29 grid points (2003-2005)

92
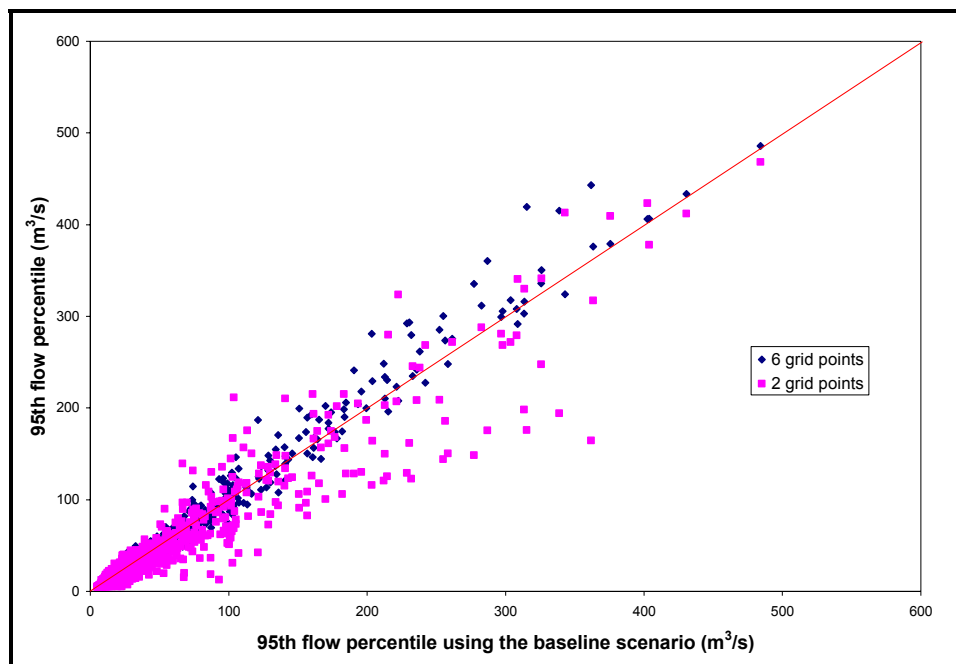
Figure 31.   Scatterplot of 95th flow percentiles using 115 grid points versus 6 and 2 grid points (2003-2005)

In summary, large variations in rainfall spatial variability were found when decreasing the number of NEXRAD grid points in the Luxapallila Creek watershed model especially when 6 and 2 NEXRAD grid points were evaluated. The model *Sharpness* results using 2 NEXRAD grid points were markedly different from those results using the baseline scenario. The model *Reliability* results using 109, 86, 58, and 29 NEXRAD grid points were close to those results using the baseline scenario (115 NEXRAD grid points).

4.2 Uncertainty Methods

Results of parameter uncertainty propagation on HSPF model outputs using the Harr method are shown in this section. Additionally, the Harr results

93

were compared to the baseline scenario results (see section 4.1.1.2 Parameter Uncertainty).

4.2.1 Harr Method

The Harr method results were computed for the same timescales and components as were presented for the baseline scenario results. The Harr method used 24 simulations (two times the number of HSPF parameters) to solve the system, and normal distributions were used for the selected HSPF parameters.

Model *Reliability* results using the Monte Carlo and Harr methods are presented in Table 32. Relative error analysis in Table 32 shows overestimation of observed flows within 90% of certainty bounds around 11% when the Harr method was used.

Table 32.　Model *Reliability* results using MCS and Harr method (2003-2005)

MCS (%)	Harr (%)	Relative error (%)
65.4	72.7	11.2

Relative errors of model *Reliability* results by observed flow percentiles from the Monte Carlo and Harr methods are shown in Table 33. The lowest and highest relative errors were -0.8% and 18.6%, respectively. Both uncertainty methods calculated close results for below normal flows. The Harr method

94

consistently overestimated observed flows within the 90% certainty bounds for normal and above normal flows.

Table 33.   Relative errors of model *Reliability* results by observed flow percentiles due to the Monte Carlo and Harr methods (2003-2005)

Observed flow percentiles	MCS (%)	Harr (%)	Relative error (%)
<25th	92.3	91.6	-0.8
25th-75th	60.2	71.4	18.6
>75th	48.2	55.8	15.9

Figure 32 displays 5th flow percentiles by the MCS and Harr methods. High variability and a markedly high overestimation were shown by the Harr results. Figure 33 illustrates 95th flow percentiles by the MCS and Harr methods in which a markedly high overestimation and high variability were shown by the Harr results.

95
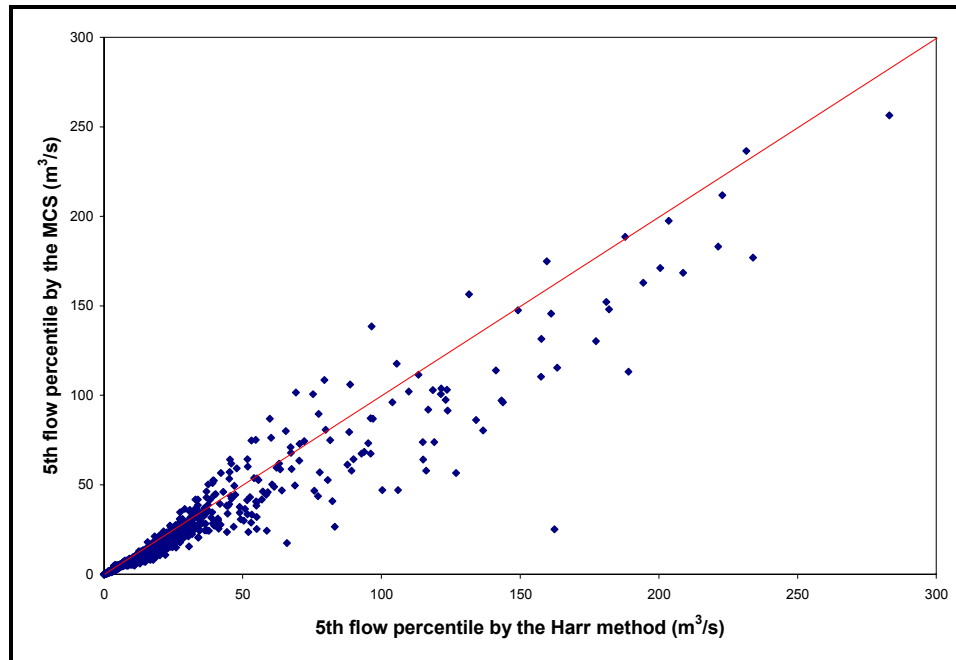
Figure 32.   Scatterplot of 5th flow percentile by the MCS and Harr methods (2003‑2005)
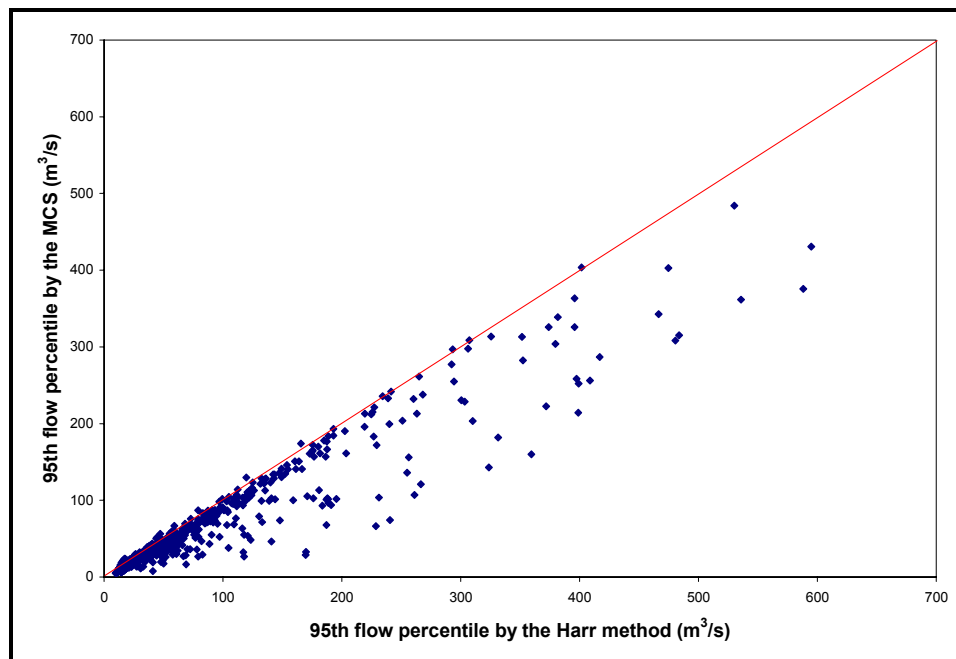
Figure 33.   Scatterplot of 95th flow percentiles by the MCS and Harr methods (2003‑2005)

96

Figures 34-39 show comparisons of certainty bounds generated by the MCS and Harr methods for selected storms. The certainty bounds calculated by both methods significantly differ from one another. All of the certainty bounds for peak flows by the Harr method were wider and higher than those yielded by the MCS.
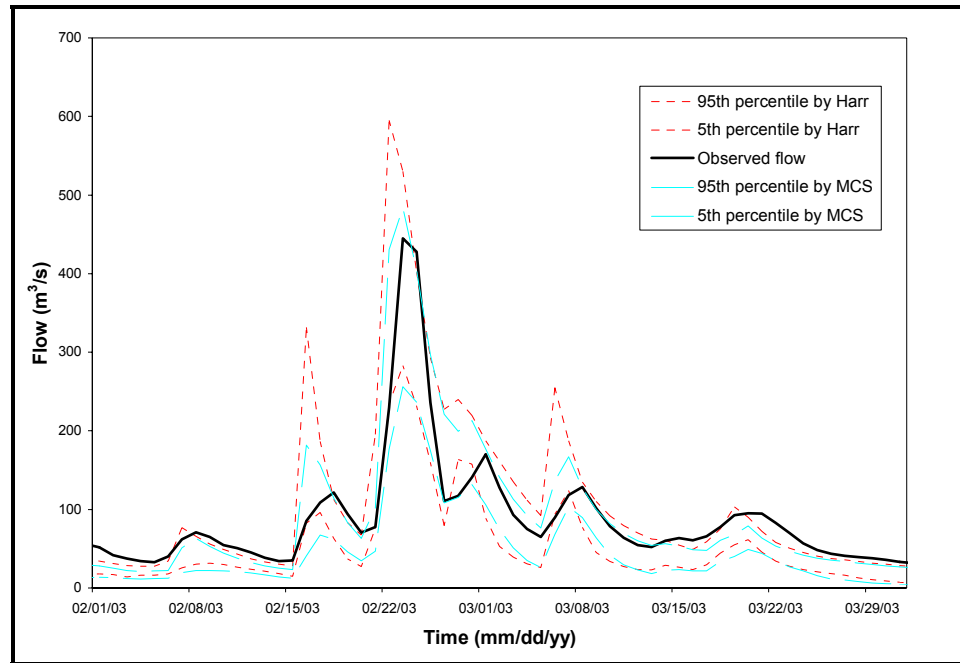
Figure 34.   Daily observed hydrographs and certainty bounds estimated by the MCS and Harr methods for February-March/2003

97
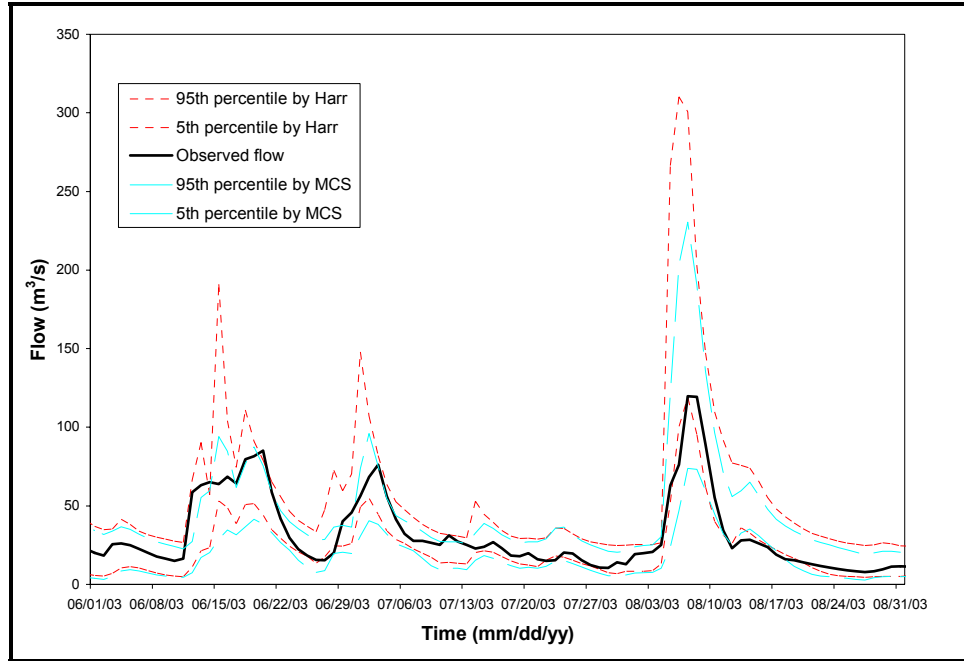
Figure 35.   Daily observed hydrographs and certainty bounds estimated by the
MCS and Harr methods for June-August/2003
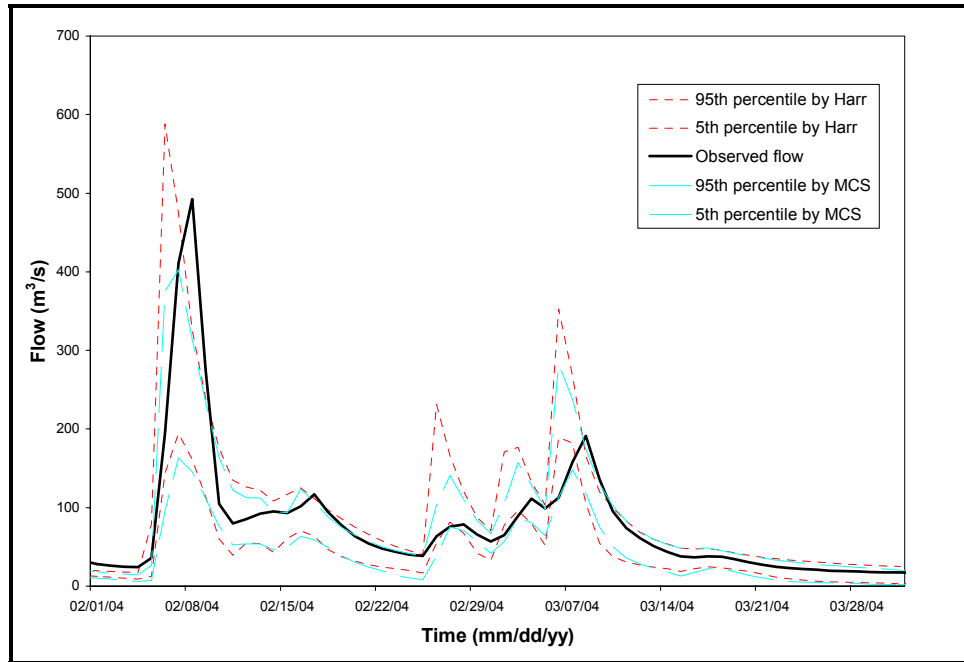
Figure 36.   Daily observed hydrographs and certainty bounds estimated by the
MCS and Harr methods for February-March/2004

98
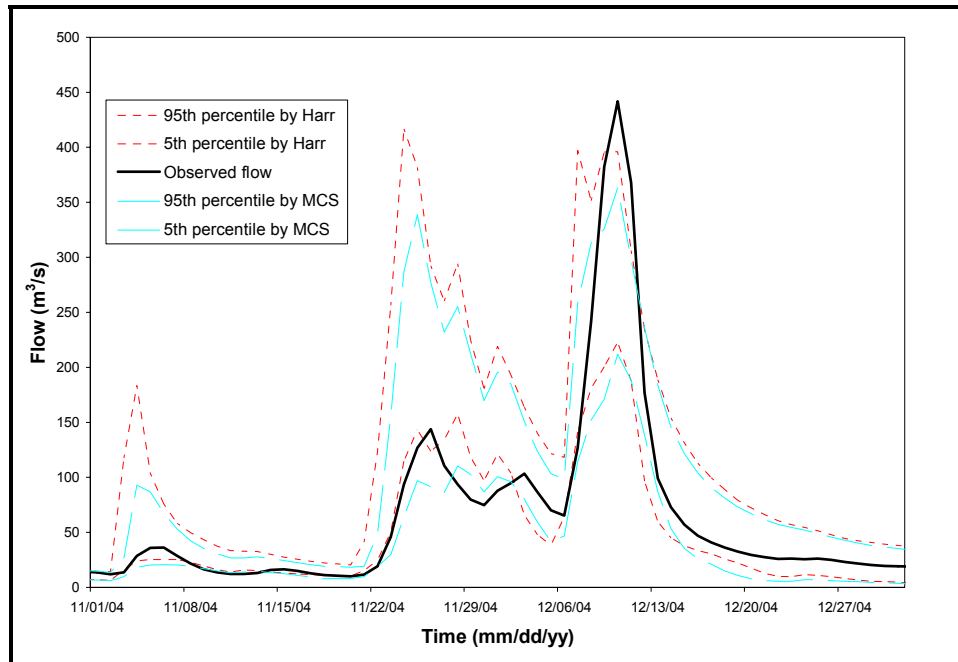
Figure 37.   Daily observed hydrographs and certainty bounds estimated by the MCS and Harr methods for November-December/2004
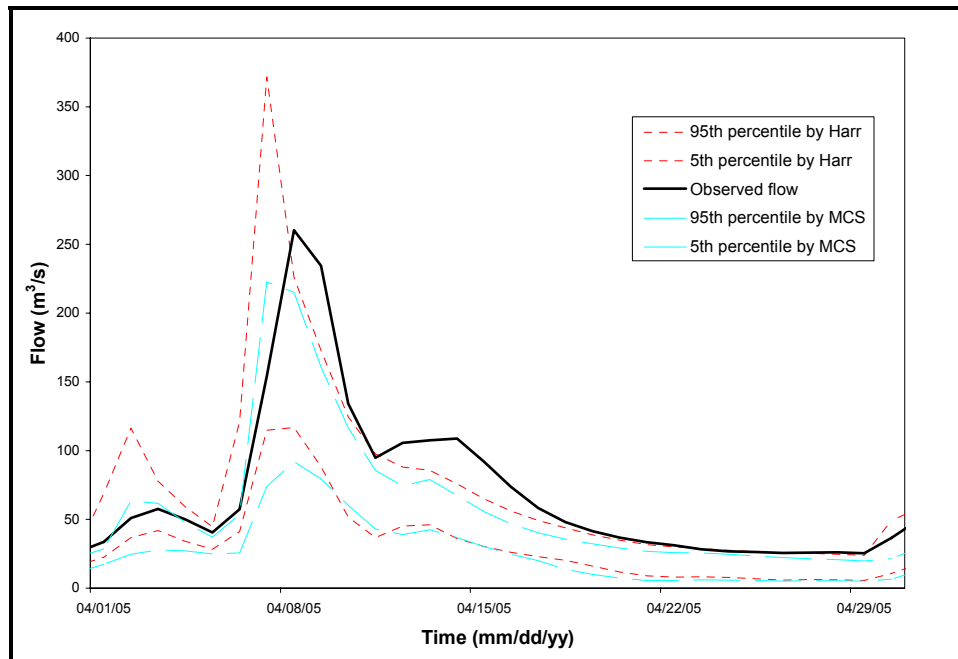
Figure 38.   Daily observed hydrographs and certainty bounds estimated by the MCS and Harr methods for April/2005

99
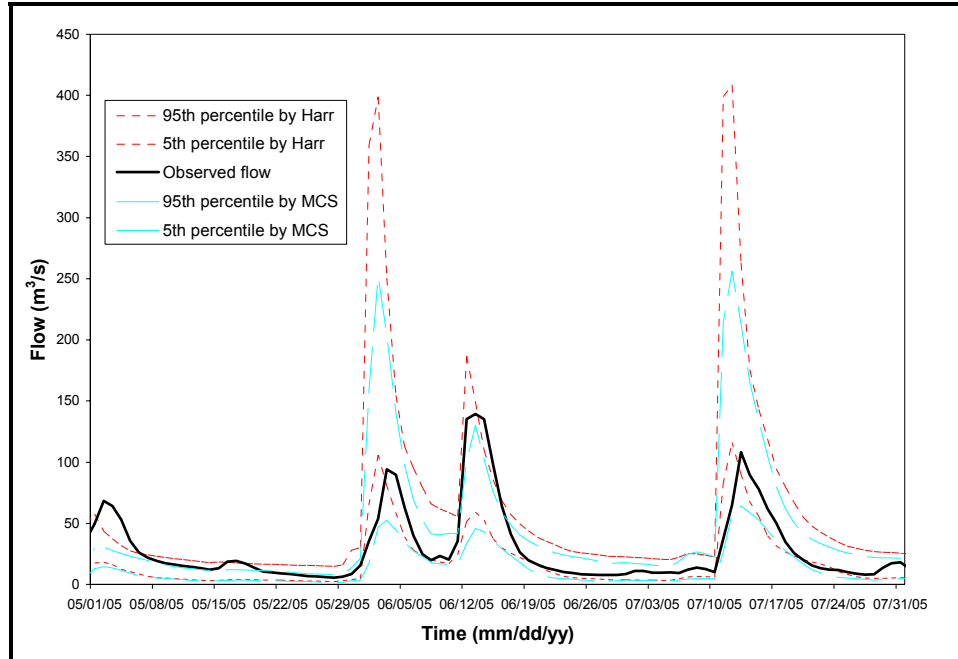
Figure 39.   Daily observed hydrographs and certainty bounds estimated by the MCS and Harr methods for May-July/2005

Table 34 depicts selected percentiles of the model *Sharpness* calculated using the Monte Carlo and Harr methods. Clearly, the Harr method results overestimated the width of the 90% certainty bounds (model *Sharpness*) for each percentile. The minimum, median, and maximum relative errors of *Sharpness* criteria values between the MCS and Harr methods were -43.6%, 20.7%, and 563.6%, respectively. The higher model *Sharpness* calculated using the Harr method may be explained by the use of just 24 Harr runs rather than the 5,000 Monte Carlo runs. Additionally, the Harr method selected the parameter values using normal distributions of the evaluated parameters rather than the triangular distributions used by the Monte Carlo method.

100

Table 34.   Selected percentiles of the range of the model *Sharpness* using
the Monte Carlo and Harr methods

Percentile	MCS (m^3/s)	Harr (m^3/s)
Minimum	4.8	7.1
25th	10.8	13.4
50th	16.2	19.1
75th	27.0	34.9
Maximum	336.7	444.4

A drawback of the Harr method was the use of several parameter limit values rather than the calculated values to stay within the pre-established range of the HSPF parameters.   Detailed definition of the 12 HSPF hydrology parameters used in this study is found in USEPA (2000). Table 35 shows the number of HSPF parameter values calculated out range using the Harr method. In general, 16% of the parameter values calculated by the Harr method were changed. HSPF parameters related to storm events, INTFW and IRC, yielded 20.8% and 16.7% respectively of values out of range. All of the new INTFW values were relocated to the lowest limit and, therefore, peak flows were expected to increase. IRC and AGWRC parameters control the rate at which interflow and groundwater, respectively, are discharged from storage. The KVARY parameter is used to describe non-linear groundwater recession rate. All of the new IRC and AGWRC values were changed to the highest limit and thus, slow flow rates in the recession limbs were estimated. The new KVARY values were relocated to the lowest limit and consequently, no seasonal variability of the groundwater flow was expected. DEEPFR, BASETP, AGWETP, CEPSC, and

101

LZETP parameters control loss of water from the system and were replaced to the lowest value; therefore, streamflows were expected to increase.

Table 35.   Number of parameter values calculated out of range by the Harr method

Parameter	Relocation of the coordinates		Number of parameter values out of the range	Percentage of total
	Lowest	Highest		
LZSN	1		1	4.2
INFILT			0	0.0
KVARY	4		4	16.7
AGWRC		2	2	8.3
DEEPFR	9		9	37.5
BASETP	5		5	20.8
AGWETP	7		7	29.2
CEPSC	5		5	20.8
UZSN	1		1	4.2
INTFW	5		5	20.8
IRC		4	4	16.7
LZETP	3	1	4	16.7

In summary, the rearrangement of the Harr coordinates yielded more streamflow in the system and, therefore, the Harr model *Sharpness* was higher than the Monte Carlo results (baseline scenario). Christian and Baecher (2002) analyzed the problem of coordinate relocation in the Harr method for bounded parameters. They pointed out that "*there seem to be no simple, elegant ways out of this dilemma.*" The use of other uncertainty methods (e.g., Rosenblueth's method or the Monte Carlo method) or reducing the number of random variables was recommended by the authors.

102

4.3 Comparison between the Baseline Scenario and the Remaining Scenarios

Table 36 depicts the analysis of the model *Reliability* (%) among evaluated scenarios. Below normal flow values (flow values lower than 25th percentile) yielded close results for all the scenarios, except the one using 2 NEXRAD grid points. Table 37 shows relative errors of the model *Reliability* ($RE_{reliability}$) between the baseline scenario and the remaining scenarios (see equation 10 in methodology). The range of $RE_{reliability}$ values for below normal flows was between -8.7% and 0.4. The scenario that used 2 NEXRAD grid points yielded the highest underestimation (-8.7%) of observed flows between the 90% certainty bounds for below normal flows. The range of $RE_{reliability}$ values for normal flows (flow values between 25th and 75th percentiles) was between -10.3% and 18.6%. The scenarios that applied the Harr method and 2 NEXRAD grid points showed the highest opposite results. The range of $RE_{reliability}$ values for above normal flows (flow values greater than 75th percentile) was between -23.4% and 15.8%. The scenarios that utilized the Harr method and RF1 FTABLE database yielded the highest overestimation and underestimation, respectively, of observed flows between the 90% certainty bounds.

103

Table 36. Flow percentile analysis of the model *Reliability* (%) among evaluated scenarios

Scenario		<25th	25th-75th	>75th
Baseline		92.3	60.2	48.2
Probabilistic point estimate method (Harr's method)		91.6	71.4	55.8
Hydraulic property variability of the main channel (RF1 FTABLE database)		91.6	58.4	36.9
	109	92.3	60.6	47.8
	86	92.7	60.0	47.8
Spatial rainfall variability	58	92.3	60.4	47.8
(number of NEXRAD grid points)	29	91.2	58.8	46.0
	6	90.1	56.4	42.3
	2	84.3	54.0	45.6

Table 37. Relative errors of the model *Reliability* ($RE_{reliability}$) between the baseline scenario and the remaining scenarios

Scenario		<25th	25th-75th	>75th
Probabilistic point estimate method (Harr's method)		-0.8	18.6	15.8
Hydraulic property variability of the main channel (RF1 FTABLE database)		-0.8	-3.0	-23.4
	109	0.0	0.7	-0.8
	86	0.4	-0.3	-0.8
Spatial rainfall variability	58	0.0	0.3	-0.8
(number of NEXRAD grid points)	29	-1.2	-2.3	-4.6
	6	-2.4	-6.3	-12.2
	2	-8.7	-10.3	-5.4

Table 38 depicts the model *Sharpness* results among evaluated scenarios. Below normal flow simulations yielded model *Sharpness* values between 9.0 and 13.4 m³/s. Normal flow simulations showed model *Sharpness* results between 14.4 and 19.1 m³/s. Above normal flow simulations yielded model *Sharpness* figures between 25.3 and 34.9 m³/s. Table 39 shows relative errors of the model *Sharpness* ($RE_{Sharpness}$) calculated between the baseline

104

scenario and the remaining scenarios. The range of $RE_{Sharpness}$ for below normal flows was between -16.7% and 24.1%. The scenarios that utilized the Harr method and 2 NEXRAD grid points yielded the highest overestimation and underestimation, respectively, of the model *Sharpness* for below normal flows. The range of $RE_{Sharpness}$ for normal flows was between –11.1% and 17.9%. Again, the scenarios that applied the Harr method and 2 NEXRAD grid points showed the highest opposite results. The range of $RE_{Sharpness}$ for above normal flows was between -6.3% and 29.3%. As showed for below and normal flows, the scenarios that utilized the Harr method and the 2 NEXRAD grid points yielded the highest overestimation and underestimation, respectively, of the model *Sharpness*,.

Table 38.   Selected percentiles of the model *Sharpness* (m^3/s) among evaluated scenarios

Scenario		<25th	25th-75th	>75th
Baseline		10.8	16.2	27.0
Probabilistic point estimate method (Harr's method)		13.4	19.1	34.9
Hydraulic property variability of the main channel (RF1 FTABLE database)		11.6	17.3	29.3
	109	10.7	16.1	27.0
	86	10.7	16.1	26.9
Spatial rainfall variability	58	10.9	16.2	27.5
(number of NEXRAD grid points)	29	10.6	15.9	26.7
	6	11.0	16.4	27.5
	2	9.0	14.4	25.3

Table 39.   Relative errors of the model *Sharpness* ($RE_{Sharpness}$) calculated
between the baseline scenario and the remaining scenarios (%)

Scenario		<25th	25th-75th	>75th
Probabilistic point estimate method (Harr's method)		24.1	17.9	29.3
Hydraulic property variability of the main channel (RF1 FTABLE database)		7.4	6.8	8.5
	109	-0.9	-0.6	0.0
	86	-0.9	-0.6	-0.4
Spatial rainfall variability	58	0.9	0.0	1.9
(number of NEXRAD grid points)	29	-1.9	-1.9	-1.1
	6	1.9	1.2	1.9
	2	-16.7	-11.1	-6.3

In summary, the impact between the baseline scenario and the remaining scenarios in the Luxapallila Creek HSPF watershed model was evaluated using two criteria: the model *Reliability* (number or percentage of observed flows within the HSPF 90% certainty bounds) and the model *Sharpness* (width of the HSPF 90% certainty bounds).

The 2 NEXRAD grid point scenario yielded the highest discrepancy in model *Reliability* when flows below normal were evaluated. The Harr scenario for normal flows depicted the largest difference when model *Reliability* was evaluated. The RF1 FTABLE scenario yielded the largest underestimation of observed flows within the HSPF 90% certainty bounds when flows above normal were evaluated.

The Harr scenario showed the largest difference for all three flow groups when HSPF *Sharpness* was evaluated. The Harr and RF1 FTABLE scenarios consistently overestimated the width of the 90% certainty bounds. The scenario

106

using 2 NEXRAD grid points showed the largest underestimation of HSPF model

Sharpness, for below normal, normal, and above normal flows.

CHAPTER V

SUMMARY AND CONCLUSIONS

The evaluation of three uncertainty sources (parameter uncertainty, channel hydraulic variability, and rainfall spatial variability) provided information about the sources and degree of the Hydrologic Simulation Program – FORTRAN (HSPF) streamflow uncertainty, which is essential for model applications and decision making. This study evaluated characteristics of uncertainty in each of these scenarios using two systematic approaches: the Monte Carlo method, considered the baseline scenario and the Harr method, a probabilistic point estimate method. This study used meteorological, topographic, land use, and streamflow data from the Luxapallila Creek watershed, Mississippi/Alabama. Daily observed streamflow data from 01/01/2003 to 12/31/2005 at the watershed outlet (USGS station 2443500) were used to assess the 90% certainty bounds of streamflow simulations for each scenario. Daily observed streamflow data were clustered into three groups to assess the model performance by each class: below normal (<11.4 m^3/s), normal (11.4 m^3/s and 45.3 m^3/s), and above normal flows (>45.3 m^3/s). The difference between the baseline scenario and the remaining scenarios applied to the HSPF Luxapallila Creek watershed model was evaluated using two criteria: the number or

108

percentage of observed flows within the HSPF 90% certainty bounds (*Reliability*) and the width of the HSPF 90% certainty bounds (*Sharpness*).

The first question addressed in this study was, "How uncertainty in model parameters, rainfall spatial data, and channel hydraulic properties propagates through flow simulations of a lumped watershed model?"

- Analysis of parameter uncertainty propagation on streamflow simulations from 12 HSPF parameters was accomplished using 5,000 random samples from triangular distributions for each parameter and 115 NEXRAD grid point data from 01/01/2003 to 12/31/2005. The parameter uncertainty propagation results revealed that the HSPF model *Reliability* was higher for below normal flows than normal and above normal flows. Additionally, the model *Sharpness* results were higher for above normal flows than normal and below normal flows, respectively. Thus, the higher the model *Sharpness,* the lower the model *Reliability*. Observed flows out of the 90% certainty bounds were near the bounds, especially for the 5th percentile bound (11.4% of discrepancy). Assumptions of this modeling exercise that may affect model *Reliability* and *Sharpness* results were as follows: one cross section of data collected at the outlet represented the entire system (the main channel is 70 km length); wetland areas (100 km^2) were simulated as a pervious area assuming no interaction with the water table (see HSPF manual v12, section: water budget pervious, high water table, low gradient); riparian areas could be affecting the hydraulic properties of the channel (such as water storage-release relationships);

109

the Luxapallila model did not have any interaction with groundwater flow; the model was segmented by one basin (1,801 km^2); the HSPF model algorithms did not account for interaction among hydrologic respond units (HRUs) (HRUs were simulated separately one from each other), but interaction between HRUs and the main channel was done (surface runoff, interflow, and baseflow volumes go directly to the main channel); HSPF model *Reliability* was evaluated using observed deterministic data at the outlet of the watershed (observed data were assumed "exactly" known); and, model parameters were perturbed in a lumped fashion (no distinction among pervious areas). Most of the previous assumptions were due to the lack of observed data, and/or limitations of the HSPF algorithms.

• The effect of spatial rainfall variability was studied using six sets of random NEXRAD grid points (109, 86, 58, 29, 6, and 2 grid points) from the 115 available NEXRAD grid points. Large variations in rainfall spatial variability were found by decreasing the number of NEXRAD grid points in the Luxapallila Creek watershed model, especially when 6 and 2 NEXRAD grid points were evaluated. The model *Sharpness* results using 2 NEXRAD grid points were markedly different from those results using the remaining NEXRAD data sets. For instance, the median relative error of coefficient of variation between 115 NEXRAD data and 2 NEXRAD data was -24.2%; this error yielded a median relative error of -9.0% for model *Sharpness* between the same scenarios. The model *Reliability* results

110

using 109, 86, 58, and 29 NEXRAD grid points were close to those results using the baseline scenario (115 NEXRAD grid points).

- Uncertainty in channel hydraulic properties was assessed by comparing the baseline scenario (USGS FTABLE) versus the RF1 FTABLE scenario. The results suggested that hydraulic property variability of the main channel affected storm event paths at the watershed outlet, especially the time to peak flow and recessing limbs of storm events. The uncertainty analysis also revealed that a better physical characterization of the system gave better results and that FTABLE data development is a critical issue in the HSPF Luxapallila model.

The second question addressed herein was "How consistent is the Harr method (probabilistic point estimate method) in estimating the 90% certainty bounds of streamflow simulations?"

- Variability of 12 HSPF hydrology parameters was propagated through the model to compute the 90% certainty bounds of daily streamflow simulations. The Harr method calculated 11% more observed flows within the 90% certainty bounds than the Monte Carlo results. Computational efficiency was improved, using 24 runs (two minutes) with Harr's method to estimate the HSPF 90% certainty bounds versus 5,000 runs (12 hours) using the Monte Carlo method. A drawback of the Harr method was the use of several parameter limit values instead of the calculated value to keep the pre-established range of the HSPF parameters. In some parameters around 30% of values were changed and the rearrangement

111

of the Harr coordinates yielded more streamflow in the system. Therefore, the model *Sharpness* was wider with the Harr results than with the Monte Carlo results (median relative errors around 20% were calculated for model *Sharpness*). Model *Sharpness* was wider with the Harr method because it forced extreme values of each parameter to be sampled with the same or higher frequency as the central values, thus exploring a broader range of HSPF outputs than those generated using the Monte Carlo method (triangular distributions). The Harr method *Sharpness* bias was fairly constant throughout the different flows (below normal, normal, and above normal); however, the model *Reliability* results were variable throughout the different flows, with relative errors of -0.8%, 18.6%, and 15.8% for below normal, normal, and above normal flows, respectively. The comparison showed that Harr's method could be an appropriate initial indicator of parameter uncertainty propagation on streamflow simulations, in particular on hydrology models with several parameters.

The third question raised in this study was: "Where do researchers need to put resources in terms of data collection so uncertainty in streamflow simulations may be lowered?"

- The relative errors of model *Sharpness* for below normal, normal, and above normal flows were lower than 100% (between -16.7% and 8.5%) when rainfall spatial variability and channel hydraulic variability were evaluated. Model *Reliability* showed a bias tendency of decreasing when using both sources of uncertainty (rainfall spatial variability and channel

112

hydraulic variability), with relative error values as low as -23.4%. The storm paths (time to peak flow and slope of recessing limbs) changed dramatically when hydraulic property variability was analyzed, with a relative error of -23.4% for model *Reliability* between the baseline scenario and RF1 FTABLE scenario was for above normal flows). Finally, parameter uncertainty was still more important than other sources of uncertainty analyzed in this study because all of the median relative errors of HSPF model *Reliability* and *Sharpness* were lower than +/- 100%.

CHAPTER VI

RECOMMENDATIONS AND FUTURE RESEARCH

The focus of this study was on the quantification of uncertainty from three different sources in the Hydrologic Simulation Program – FORTRAN (HSPF) streamflow results: parameter uncertainty, channel hydraulic variability, and rainfall spatial variability. However, it must be noted that other sources of uncertainty exist and propagate in a similar fashion on the model outputs. Other sources of uncertainties can arise from land use/land cover inputs and discretization; watershed topographic delineation or digital elevation model resolution; reach network discretization; potential evapotranspiration and evaporation data; rainfall inputs; and model structure. Further research is required to quantify the error propagation from these areas on model simulations. Additionally, this study focused on evaluating Harr's method, a probabilistic point method. For hydrology models with several parameters (this study used 12 HSPF parameters), the Harr method technique could be an appropriate initial indicator of parameter error propagation on streamflow simulations. More work should be devoted to better calculating the probability density function and certainty bounds of model parameters. Finally, parameter sensitivity analysis is

114

required to find the most important parameters that affect the HSPF certainty bounds.

BIBLIOGRAPHY

Al-Abed, N.A., and H.R. Whiteley, 2002. Calibration of the Hydrological Simulation Program Fortran (HSPF) Model Using Automatic Calibration and Geographical Information Systems. *Hydrological Process* 16:3169-3188.

Albek, M., Ü.B. Öğütveren, and E. Albek, 2004. Hydrological Modeling of Seydi Suyu Watershed (Turkey) with HSPF. *Journal of Hydrology* 285:260-271.

Anagnostou, E.N., and W.F. Krajewski, 1999. Uncertainty Quantification of Mean-Areal Radar-Rainfall Estimates. *Journal of Atmospheric and Oceanic Technology* 16:206-215.

Andreassian, V., C. Perrin, C. Michel, I. Usart-Sanchez, and J. Lavabre, 2001. Impact of Imperfect Rainfall Knowledge on the Efficiency and the Parameters of Watershed Models. *Journal of Hydrology* 250:206-223.

Aronica, G., G. Freni, and E. Oliveri, 2005. Uncertainty Analysis of the Influence of Rainfall Time Resolution in the Modelling of Urban Drainage Systems. *Hydrological Processes* 19:1055-1071.

Beach, R.B., J.S Clough, P.M. Craig, A.S. Donigian, R.A. McGrath, R.A. Park, A. Stoddard, S.C. Svirsky, and C.M. Wallen, 2000. Quality Assurance Project Plan: Modeling Study of PCB Contamination in the Housatonic River. Prepared under USACE Contract No. DACW33-00-D-0006, Task Order 0003 with Roy F. Weston, Inc. and EPA Contract No. 68-C-98-010, with AQUA TERRA Consultants. Prepared for U.S. Army Corps of Engineers New England District Concord, Massachusetts and U.S. Environmental Protection Agency Region 1 Boston, Massachusetts.

Benaman, J., and C.A. Shoemaker, 2004. Methodology for Analyzing Ranges of Uncertain Model Parameters and Their Impact on Total Maximum Daily Load Process. *Journal of Environmental Engineering* 130(6):648-656.

Bergman, M. J., W. Green, and L.J. Donnangelo, 2002. Calibration of Storm loads in the South Prong Watershed, Florida, Using BASINS/HSPF. *Journal of the American Water Resources Association* 38(5): 1423-1436.

Beven, K.J., 2001. Rainfall-Runoff Modelling: The Primer. John Wiley & Sons, Ltd.

Beven, K., and A. Binley, 1992. The Future of Distributed Models: Model Calibration and Uncertainty Prediction. *Hydrological Processes* 6:279-298.

Beven, K., and J. Freer, 2001. Equifinality, Data Assimilation, and Uncertainty Estimation in Mechanistic Modelling of Complex Environmental Systems Using the GLUE Methodology. *Journal of Hydrology* 249:11-29.

Bicknell, B.R., J.C. Imnoff, Jr., T.H. Jobes, and A.S. Donigian, 2001. Hydrological Simulation Program – Fortran (HSPF) version 12, User's Manual. Prepared for AQUA TERRA Consultants Mountain View, California, in cooperation with Water Resources Discipline U.S. Geological Survey Reston, Virginia , and U.S. Environmental Protection Agency Athens, Georgia.

Bingner, R.L., F.D. Theurer, R.G. Cronshey, and R.W. Darden, 2001. AGNPS 2001 Web Site. [Online]. Available at:
http://www.ars.usda.gov/Research/docs.htm?docid=5199 March 9 2007.

Binley, A.M., K.J. Beven, A. Calver, and L.G. Watts, 1991. Changing Responses in Hydrology: Assessing the Uncertainty in Physically Based Model Predictions. *Water Resources Research* 27(6):1253-1261.

Bronstert, A., and A. Bardossy, 2003. Uncertainty of Runoff Modelling at the Hillslope Scale Due to Temporal Variations of Rainfall Intensity. *Physics and Chemistry of the Earth* 28:283-288.

117

Burnash, R.J.C., 1995. Chapter 10: The NWS River Forecast System – Catchment Modeling. In: V. P. Sigh (Editor), Computer Models of Watershed Hydrology. Water Resources Publications, Littleton, CO, pp. 311-366.

Butts, M.B., J.T. Payne, M. Kristensen, and H. Madsen, 2004. An Evaluation of the Impact of Model Structure on Hydrological Modelling Uncertainty for Streamflow Simulation. *Journal of Hydrology* 298:242-266.

Carpenter, T.M., and K.P. Georgakakos, 2004. Impacts of Parametric and Radar Rainfall Uncertainty on the Ensemble Streamflow Simulations of a Distributed Hydrologic Model. *Journal of Hydrology* 298:202-221.

Carrubba, L., 2000. Hydrologic Modeling at the Watershed Scale Using NPSM. *Journal of the American Water Resources Association* 36(6):1237-1246.

Chew, C.R., L.W. Moore, and R.H. Smiths, 1991. Hydrological Simulation of Tennessee's North Reelfoot Creek Watershed. *Research Journal of the Water Pollution Control Federation* 63(10):10-16.

Christiaens, K., and J. Feyen, 2002. Use of Sensitivity and Uncertainty Measures in Distributed Hydrological Modeling with and Application to the MIKE SHE Model. *Water Resources Research* 38(9), 1169, doi:10.1029/2001WR000478.

Christian, J.T., and G.B. Baecher, 2002. The Point-Estimate Method with Large Numbers of Variables. *Int. J. Numer. Anal. Meth. Geomech*., 26:1515-1529, doi:10.1002/nag.256.

Chu, T.W., 2003. Modeling Hydrologic and Water Quality Response of a Mixed Land Use Watershed in Piedmont Physiographic Region. Ph.D. dissertation, University of Maryland.

Danish Hydraulic Institute (DHI), 1998. MIKE SHE Water Movement User Guide and Technical Reference Manual.

Dawdy, D.R., and T. O'Donnell, 1965. Mathematical Models of Catchment Behavior. *Journal of the Hydraulics Division* 91(HY4):123-137.

Diaz, J.N., 2004. Modeling Sediment Export Potential of the Rio Caonillas Watershed. M.S. Thesis, University of Puerto Rico.

Diaz, J.N., V. Alarcon, Z. Duan, M.L. Tagert, W. H. McAnally, J. L. Martin, and C.G. O'Hara, 2007. Sensitivity of Modeled Hydrology and Sediments to Land Use/Land Cover Data for the Luxapallila Creek Watershed, Alabama/Mississippi. Submitted to *Hydrological Processes*.

Doherty, J., and J.M. Johnston, 2003. Methodologies for Calibration and Predictive Analysis of a Watershed Model. *Journal of the American Water Resources Association* 39(2):251-265.

Donigian, A.S., 2000. HSPF Training Workshop Handbook and CD. Lecture #19. Calibration and Verification Issues, Slide #L19-22. EPA Headquarters, Washington Information Center, 10-14 January, 2000. Presented and prepared for U.S. EPA, Office of Water, Office of Science and Technology, Washington, D.C.

Donigian, A.S., B.R. Bicknell, and J.C. Imhoff, 1995. Chapter 12: Hydrological Simulation Program – FORTRAN (HSPF). In: V. P. Sigh (Editor), Computer Models of Watershed Hydrology. Water Resources Publications, Littleton, CO, pp. 395-442.

Draper, D., 1995. Assessment and Propagation of Model Uncertainty. *Journal of the Royal Statistical Society B* 57(1):45-97.

Draper, N.R., and H. Smith, 1998. Applied Regression Analysis. John Wiley & Sons.

Engelmann, C.J.K., A.D. Ward, A.D. Christy, and E.S. Bair, 2002. Application of the BASINS Database and NPSM Model on a Small Ohio Watershed. *Journal of the American Water Resources Association* 38(1):289-300

Environmental Modeling Systems, Inc – EMS-I, 2002. Watershed Modeling System – WMS, version 6.1, Reference/Tutorial Manual. South Jordan, UT.

119

Farajalla, N.S., 1995. Error Propagation in Distributed Hydrologic Modeling. Ph.D. dissertation, The University of Oklahoma.

Fontaine, T.A., and V.M.F. Jacomino, 1997. Sensitivity Analysis of Simulated Contaminated Sediment Transport. *Journal of the American Water Resources Association* 33(2): 313-326.

Garen, D.C., and S.J. Burges, 1981. Approximate Error Bounds for Simulated Hydrographs. *Journal of the Hydraulics Division* 107(HY11):1519-1534.

Georgakakos, K.P., D.-J. Seo, H.Gupta, J. Schaake, and M.B. Butts, 2004. Towards the Characterization of Streamflow Simulation Uncertainty through Multimodel Ensembles. *Journal of Hydrology* 298:222-241.

Gourley, J.J., and B.E. Vieux, 2003. The Effects of Radar-Derived Rainfall Uncertainties of Forecasts from a Distributed Hydrological Model. In: Weather Radar Information and Distributed Hydrological Modelling, Y. Tachikawa, B.E. Vieux, K.P. Georgakakos, and E. Nakakita (Editors). IAHS Publ. no. 282, pp. 130-137.

Gupta, H.V., K.J. Beven, and T. Wagener, 2005. Model Calibration and Uncertainty Estimation. In: Encyclopedia of Hydrological Sciences, M. Anderson (Editor). John Wiley & Sons Ltd.

Haan, C.T., 2002. Statistical Methods in Hydrology. 2nd ed., Iowa State Press.

Haan, C.T., B. Allred, D.E. Storm, G.J. Sabbagh, and S. Prabhu, 1995. Statistical Procedure for Evaluating Hydrologic/Water Quality Models. *Transactions of the ASAE* 38(3):725-733.

Haan, P.K., and R.W. Skaggs, 2003. Effect of Parameter Uncertainty on DRAINMOD Predictions: I. Hydrology and Yield. *Transactions of the ASAE* 46(4):1061-1067.

Harr, M.E., 1989. Probabilistic Estimates for Multivariate Analysis. *Applied Mathematical Modelling* 13:313-318.

Hasofer, A.M., and N.C. Lind, 1974. An Exact and Invariant First Order Reliability Format. *Journal of Engineering Mechanics,* ASCE, 100(EM-1):111-121.

Hayashi, S., S. Murakami, M. Watanabe, and X. Bao-Hua, 2004. HSPF Simulation of Runoff and Sediment Loads in the Upper Changjiang River Basin, China. *Journal of Environmental Engineering*, 130(7):801-815.

Hromadka II, T.V., and R.H. McCuen, 1989. An Approximate Analysis of Surface Runoff Model Uncertainty. *Journal of Hydrology* 111:321-360.

Im, S., K.M. Brannan, S. Mostaghimi, and J. Cho, 2004. Simulating Fecal Coliform Bacteria Loading from an Urbanizing Watershed. *Journal of Environmental Science and Health*, A39(3):663-679.

Jacomino, V.M.F., and D.E. Fields, 1997. A Critical Approach to the Calibration of a Watershed Model. *Journal of the American Water Resources Association* 33(1): 143-154.

James, L.D., and S.J. Burges, 1982. Chapter 11: Selection, Calibration, and Testing of Hydrologic Models. In: Hydrologic Modeling of Small Watersheds. ASAE, Monograph Number 5. C.T. Haan, H.P. Johnson, and D.L. Brakensiek, (Editors). American Society of Agricultural Engineers, St Joseph, MI. pp 437-472.

Jia, Y., 2004. Robust Optimization for Total Maximum Daily Load Allocations. Ph.D. dissertation, University of Virginia.

Johnson, D., M. Smith, V. Koren, and B. Finnerty, 1999. Comparing Mean Areal Precipitation Estimates from NEXRAD and Rain Gauge Networks. *Journal of Hydrologic Engineering* 4(2):117-124.

Johnson, M.S., W.F. Coon, V.K. Mehta, T.S. Steenhuis, E.S. Brooks, and J. Boll, 2003. Application of Two Hydrologic Models with Different Runoff Mechanisms to a Hillslope Dominated Watershed in the Northeastern US: a Comparison of HSPF and SMR. *Journal of Hydrology* 284:57-76.

Laroche, A., J. Gallichand, R. Lagacé, and A. Pesant, 1996. Simulating Atrazine Transport with HSPF in an Agricultural Watershed. *Journal of Environmental Engineering* 122(7):622-630.

Legates, D.R., and G.J. McCabe, 1999. Evaluating the Use of "Goodness-of-Fit" Measures in Hydrologic and Hydroclimatic Model Validation. *Water Resources Research* 35(1):233-241.

Linsley, R.K., M.A. Kohler, and J.L.H. Paulhus, 1988. Hydrology for Engineers. McGraw-Hill.

Lopez, V., F. Napolitano, and F. Russo, 2005. Calibration of a Rainfall-Runoff Model Using Radar and Raingague Data. *Advances in Geosciences* 2:41-46.

Manache, G., and C.S. Melching, 2004. Sensitivity Analysis of a Water-Quality Model Using Latin Hypercube Sampling. *Journal of Water Resources Planning and Management* 130(3):232-242.

McAnally, W.H., J.L. Martin, J.N. Diaz, Z. Duan, C.A. Mancilla, M.L. Tagert, C. O'Hara, and J.A. Ballweber, 2006. Assimilating Remotely Sensed Data into Hydrologic Decision Support Systems: BASINS Evaluation. Department of Civil Engineering and GeoResources Institute, Mississippi State University, MS.

McKay, M.D., R.J. Beckman, and W.J. Conover, 1979. A Comparison of Three Methods for Selecting Values of Input Variables in the Analysis of Output from a Computer Code. *Technometrics* 21(2):239-245.

Melching, C.S., 1992. An Improved First-Order Reliability Approach for Assessing Uncertainties in Hydrologic Modeling. *Journal of Hydrology* 132:157-177.

Melching, C.S., 1995. Chapter 3: Reliability Estimation. In: Computer Models of Watershed Hydrology, V.P. Sigh (Editor). Water Resources Publications, Littleton, CO, pp. 69-118.

Melching, C.S., and W. Bauwens, 2001. Uncertainty in Coupled Nonpoint Source and Stream Water-Quality Models. *Journal of Water Resources Planning and Management* 127(6):403-413.

Metropolis, N., and S. Ulam, 1949. The Monte Carlo Method. *Journal of the American Statistical Association* 44(247):335-341.

Moon, J., R. Srinivasan, and J.H. Jacobs, 2004. Stream Flow Estimation Using Spatially Distributed Rainfall in the Trinity River Basin, Texas. *Transactions of the ASAE* 47(5):1445-1451.

Moore, L.W., H. Matheny, T. Tyree, D. Sabatini, and S.J. Klaine, 1988. Agricultural Runoff Modeling in a Small West Tennessee Watershed. *Research Journal of the Water Pollution Control Federation* 60(2):242-249.

Morgan, M.G., and M. Henrion, 1990. Uncertainty: A Guide to Dealing with Uncertainty in Quantitative Risk and Policy Analysis. Cambridge University Press.

Nash, J.E., and J.V. Sutcliffe, 1970. River Flow Forecasting through Conceptual Models, Part I – a Discussion of Principles. *Journal of Hydrology* 10, 282-290.

National Oceanic & Atmospheric Administration (NOAA)/National Climatic Data Center (NCDC), 2007. NCDC Radar Resources. [Online]. Available: http://lwf.ncdc.noaa.gov/oa/radar/radarresources.html March 6, 2007.

Neary, V.S, E. Habib, and M. Fleming, 2004. Hydrologic Modeling with NEXRAD Precipitation in Middle Tennessee. *Journal of Hydrologic Engineering* 9(5):339-349.

Neitsch, S.L., J.G. Arnold, J.R. Kiniry, and J.R. Williams, 2005. Soil and Water Assessment Tool Theoretical Documentation Version 2005. GSWRL-Agricultural Research Service and BRC-Texas Agricultural Experiment Station, Temple, TX.

Osborn, H.B, and L.J. Lane, 1982. Chapter 3: Precipitation. In: Hydrologic Modeling of Small Watsheds, C.T. Haan, H.P. Johnson, and D.L. Brakensiek (Editors). American Society of Agricultural Engineers, pp. 81-118.

Paul, S., 2003. Bacterial Total Maximum Daily Load (TMDL): Development and Evaluation of a New Classification Scheme for Impaired Waterbodies of Texas. Ph.D. dissertation, Texas A&M University.

Ponce, V.M., 1989. Engineering Hydrology: principles and practices. Prentice Hall.

Rogers, C.C.M., K.J. Beven, E.M. Morris, and M.G. Anderson, 1985. Sensitivity Analysis, Calibration and Predictive Uncertainty of the Institute of Hydrology Distributed Model. *Journal of Hydrology* 81:179-191.

Ronen, Y., 1988. The Role of Uncertainties. In: Uncertainty Analysis, Y. Ronen (Editor). CRC Press, Inc.

Rosenblueth, E., 1975. Point Estimates for Probability Moments. *Proc. Nat. Acad. Sci. USA* 72(10):3812-3814.

Rosenblueth, E., 1981. Two-point Estimates in Probabilities. *Applied Mathematical Modelling* 5:329-335.

Rossman, L.A., 2005. Storm Water Management Model User's Manual Version 5.0. National Risk Management Research Laboratory, Office of Research and Development, USEPA, Cincinnati, OH. EPA/600/R-05/040.

Senarath, S.U.S., 2000. On Evaluating the Validity of Continuous, Distributed Hydrologic Model Predictions in Spatially Heterogeneous Hortonian Watersheds. Ph.D. dissertation, The University of Connecticut.

Sharif, H.O., F.L. Ogden, W.F. Krajewski, and M. Xue, 2004. Statistical Analysis of Radar Rainfall Error Propagation. *Journal of Hydrometeorology* 5:199-212.

Sieber, A., and S. Uhlenbrook, 2005. Sensitivity Analyses of a Distributed Catchment Model to Verify the Model Structure. *Journal of Hydrology* 310:216-235.

Singh, V.P. (Editor), 1995. Computer Models of Watershed Hydrology. Water Resources Publications.

Singh, V.P., and D.A. Woolhiser, 2002. Mathematical Modeling of Watershed Hydrology. *Journal of Hydrology Engineering* 7(4):270-292.

Singh, V.P., and D.K. Frevert (Editors), 2002a. Mathematical Models of Large Watershed Hydrology. Water Resources Publications.

Singh, V.P., and D.K. Frevert, 2002b. Mathematical Modeling of Watershed Hydrology. In: Mathematical Models of Large Watershed Hydrology, V.P. Singh, and D.K. Frevert (Editors). Water Resources Publications, pp. 1-22.

Singh, V.P., D.K. Frevert, J.D. Rieker, V. Leverson, S. Meyer, and S. Meyer, 2006. Hydrologic Modeling Inventory: Cooperative Research Effort. *Journal of irrigation and Drainage Engineering*, 132(2):98-103.

Sobol', I.M., 1994. A Primer for the Monte Carlo Method. CRC Press, Inc.

Souid, M.A., 1999. Reliability of Rainfall-Runoff Models. Ph.D. dissertation, State University of New York.

Steiner, M., J.A. Smith, S.J. Burges, C.V. Alonso, and R.W. Darden, 1999. Effect of Bias Adjustment and Rain Gauge Data Quality Control on Radar Rainfall Estimation. *Water Resources Research* 35(8):2487-2503.

Thomann, R.V., 1982. Verification of Water Quality Models. *Journal of the Environmental Engineering Division*, Proceedings of the American Society of Civil Engineering, 108 (EE5), 923-940

Todini, E., 2007. Hydrological Catchment Modelling: Past, Present and Future. *Hydrol. Earth Syst. Sci.*, 11(1), 468-482.

Tung, Y.K., 1996. Uncertainty and Reliability Analysis. In: Water Resources Handbook, L.W. Mays (Editor). McGraw-Hill, pp. 7.1-7.65.

Tung, Y.K., and B.C. Yen, 2005. Hydrosystems Engineering Uncertainty Analysis. McGraw-Hill.

U.S. Army Corps of Engineers (USACE), 2001. Hydrologic Modeling System HEC-HMS User's Manual (Version 2.1). Hydrologic Engineering Center, Davis, CA.

U.S. Environmental Protection Agency (USEPA), 2000. BASINS Technical Note 6: Estimating Hydrology and Hydraulic Parameters for HSPF. [Online]. Available: http://www.epa.gov/waterscience/BASINS/tecnote6.pdf November 9, 2006.

U.S. Environmental Protection Agency (USEPA), 2001. Better Assessment Science Integrating Point and Nonpoint Sources, BASINS Version 3.0, User's Manual. EPA-823-B-01-001. U.S. Environmental Protection Agency, Office of Water, Washington, D.C.

U.S. Environmental Protection Agency (USEPA), 2002. Draft Guidance on the Development, Evaluation, and Application of Regulatory Environmental Models. [Online]. Available:
http://www.epa.gov/ord/crem/library/CREM%20Guidance%20Draft%2012_03.pdf March 9, 2007.

U.S. Environmental Protection Agency (USEPA), 2006a. HSPFParm version 1.3 beta July 2002. [Online]. Available:
http://www.epa.gov/OST/ftp/basins/HSPFParm/ April 7, 2006.

U.S. Environmental Protection Agency (USEPA), 2006b. Flow Calibration Tutorial: Calibration Scenarios. [Online]. Available:
http://www.epa.gov/waterscience/ftp/basins/training/tutorial/scenario.htm   June 13, 2006.

U.S. Environmental Protection Agency (USEPA), 2007. U.S. EPA Reach File (RF1) for the Conterminous United States in BASINS. [Online]. Available: http://www.epa.gov/waterscience/basins/metadata/rf1.htm March 29, 2007.

Vieux, B.E., 2002. Radar Rainfall Applications in Hydrology. In: P.B. Bedient and W.C. Huber (Editors), Hydrology and Floodplain Analysis. Prentice Hall, pp. 648-681.

Wagener, T., 2003. Evaluation of Catchment Models. *Hydrological Processes* 17:3375-3378.

Wagener, T., N. McIntyre, M.J. Lees, H.S. Wheater, and H.V. Gupta, 2003. Towards Reduced Uncertainty in Conceptual Rainfall-Runoff Modelling: Dynamic Identifiability Analysis. *Hydrological Processes* 17:455-476.

Wagener, T., H.S. Wheater, and H.V. Gupta, 2004. Rainfall-Runoff Modelling in Gauged and Ungauged Catchments. Imperial College Press, London, UK.

Willmott, C.J., and K. Matsuura, 2005. Advantages of the Mean Absolute Error (MAE) over the Root Mean Square Error (RMSE) in Assessing Average Model Performance. *Climate Research* 30:79-82.

Wood, E.F., 1976. An Analysis of the Effects of Parameter Uncertainty in Deterministic Hydrologic Models. *Water Resources Research* 12(5):925-932.

Wu, J., 2004. Water-Quality-Based BMP Design Approach and Uncertainty Analysis for Integrated Watershed Management. Ph.D. dissertation, University of Virginia.

Young, C.B., 2000. Evaluation of NEXRAD Precipitation Estimates and Their Potential Use for Nonpoint Source Pollution Modeling. Ph.D. dissertation, The University of Iowa.

Yu, P.S., T.C. Yang, and S.J. Chen, 2001. Comparison of Uncertainty Analysis Methods for a Distributed Rainfall-Runoff Model. *Journal of Hydrology* 244:43-59.

Zhang, H.X., 2001.   The Critical Flow-Storm Approach and Uncertainty Analysis for the TMDL Development Process. Ph.D. dissertation, University of Virginia.